

**DISSOLUTION BEHAVIOURS OF STRUCTURED  
PARTICLES**

CHANGDONG LI

Submitted in accordance with the requirements for the degree of Doctor of  
Philosophy

University of Leeds

Institute of Particle Science and Engineering

School of Chemical and Process Engineering

July 2014

The candidate confirms that the work submitted is his own and that appropriate credit has been given where reference has been made to the work of others.

This copy has been supplied on the understanding that it is copyright material and that no quotation from the thesis may be published without proper acknowledgement.

The right of Changdong Li to be identified as Author of this work has been asserted by him in accordance with the Copyright, Designs and Patents Act 1988.

© 2014 The University of Leeds and Changdong Li

## **ACKNOWLEDGEMENTS**

The research has been carried out by myself that has been fully and explicitly indicated in the thesis. Furthermore, I would like to thank the Institute of Particle and Science Engineering and Procter & Gamble Newcastle Innovation Centre for partially funding my research work. And also I would also like to thank Prof. Yulong Ding as my supervisor and Dr. Carlos Amador for providing many helps and guides on my research and my thesis revision.

## ABSTRACT

The work presented in this thesis aims at the fundamental understanding and investigation of dissolution behaviors of structured particles. This topic is relevant to numerous industrial applications including detergent, pharmaceutical, agrochemical and energy products. Both experimental works and theoretical analyses were carried out in this work. The particles of several different materials including sodium carbonate and polymers with specific characteristic and structure were used into the experimental works in this thesis. Polymers used in this thesis included carboxymethyl cellulose, croscarmellose sodium and crospovidone. The studies on characteristics of these particles included the determination of particle size, shape and structure with several measurement techniques.

The dissolution process was measured with experimental methods under different solution conditions including temperature, stirring speed and pH. Based on these measured data, the dissolution kinetics such as dissolution rate constant were quantified with mathematical models and analyzed with theoretical studies. In this way, the dissolution behaviors of different structured particles could be finally identified and analyzed with the quantified data of dissolution process and dissolution kinetics. Additionally according to the quantification process, the effects of these solution conditions on dissolution kinetics could also be determined and identified that how these conditions impact dissolution kinetics. Main conclusions of my work on dissolution experiments in this thesis were simply summarized as the following that:

- An increasing in the temperature and stirring speed leads to the increases of dissolution rate and dissolution rate constant of sodium carbonate particles in all

cases.

- The dissolution rate and the rate constant decreases with the increasing of pH value of solution.
- Carboxymethyl cellulose and crospovidone show a clear effect to enhance the dissolution rate and the rate constant of sodium carbonate-polymer composite tablets.
- Crospovidone also has a stronger effect to enhance the dissolution process and kinetics than carboxymethyl cellulose
- Croscarmellose sodium shows a clear effect to weaken the dissolution rate and the rate constant of sodium carbonate-polymer composite tablet.

## TABLE OF CONTENTS

<b>ACKNOWLEDGEMENTS.....</b>	<b>I</b>
<b>ABSTRACT.....</b>	<b>II</b>
<b>TABLE OF CONTENTS.....</b>	<b>IV</b>
<b>LIST OF FIGURES .....</b>	<b>VI</b>
<b>LIST OF TABLES .....</b>	<b>XII</b>
<b>LIST OF SYMBOLS .....</b>	<b>XIV</b>
<b>CHAPTER 1. INTRODUCTION .....</b>	<b>1</b>
<b>CHAPTER 2. LITERATURAL REVIEW .....</b>	<b>5</b>
2.1 Particle Size and Shape .....	5
2.1.1 Particle Size Characterization.....	5
2.1.2 Particle Shape characterization.....	8
2.2 Structure of Particle.....	14
2.2.1 Introduction.....	14
2.2.2 Measurement Methodologies of Particle Structure .....	14
2.3 Solubility of Particles .....	22
2.3.1 Introduction.....	22
2.3.2 Measurements and Applications.....	24
2.4 Diffusion of Particles in Liquid.....	25
2.4.1 Concepts of Diffusion.....	25
2.4.2 Quantifications and Applications.....	26
2.5 Dissolution of Particles .....	29
2.5.1 Dissolution Process.....	29
2.5.2 Dissolution Models and Theories .....	30
2.5.3 Mathematical Models of Particle Dissolution .....	33
2.5.4 Research on Dissolution of Particles .....	40
2.6 Conclusions of Literature Review .....	41
<b>CHAPTER 3. DISSOLUTION OF SINGLE SPHERICAL SODIUM CARBONATE PARTICLE .....</b>	<b>43</b>
3.1 Introduction .....	43
3.2 Experimental Methodology.....	43
3.3 Mathematical Model.....	48
3.4 Results and Discussions .....	50
3.5 Conclusions .....	69

<b>CHAPTER 4. DISSOLUTION OF SODIUM CARBONATE TABLETS .....</b>	<b>71</b>
4.1 Introduction .....	71
4.2 Experimental Methodology .....	71
4.3 Results and Discussions .....	76
4.3.1 Structure of sodium carbonate tablet .....	76
4.3.2 Data Analysis Method of Dissolution Experiment of Sodium Carbonate Tablet under Temperature and Stirring speed.....	79
4.3.3 Dissolution Kinetics of Sodium Carbonate Tablet under Temperatures and Stirring speeds.....	87
4.4 Conclusions .....	100
<b>CHAPTER 5. DISSOLUTION OF TABLETS CONTAINING SODIUM CARBONATE AND POLYMERS.....</b>	<b>102</b>
5.1 Introduction .....	102
5.2 Material and Preparation .....	105
5.2.1 Materials .....	105
5.2.2 Preparation of Materials.....	108
5.3 Experimental Methodology .....	110
5.4 Mathematical Model.....	112
5.5 Results and Discussions .....	112
5.5.1 Dissolution Kinetics of Sodium Carbonate- Carboxymethyl Cellulose Composite Tablet.....	113
5.5.2 Dissolution Kinetics of Sodium Carbonate-Croscarmellose Sodium Composite Tablet.....	130
5.5.3 Dissolution Kinetics of Sodium Carbonate-Crospovidone Composite Tablet .....	148
5.5.4 Comparison of Dissolution Rate Constant of Sodium carbonate-Polymer Composite Tablet.....	165
5.6 Conclusions .....	166
<b>CHAPTER 6. CONCLUSIONS OF RESEARCH WORK AND SCOPE FOR FUTURE WORK .....</b>	<b>168</b>
6.1 Conclusions of Research .....	168
6.2 Scope of future research .....	169
<b>REFERENCES.....</b>	<b>170</b>

## LIST OF FIGURES

Figure 2.1. Zingg's classification of particle shape. ....	10
Figure 2.2 A typical schematic diagram of SEM set-up.....	15
Figure 2.3 IUPAC classification of adsorption isotherms.....	18
Figure 2.4 A schematic diagram of a typical XRD measurement.....	20
Figure 2.5 Description of diffusion layer theory.....	32
Figure 2.6 Description of interfacial barrier model. ....	32
Figure 2.7 Description of Danckwerts model. ....	33
Figure 3.1 XRD patterns of $\text{Na}_2\text{CO}_3$ and $\text{Na}_2\text{CO}_3 \cdot \text{H}_2\text{O}$ .....	44
Figure 3.2 Pre-preparation scheme of single sodium carbonate particle .....	45
Figure 3.3 Nikon Eclipse Ti Microscopy .....	45
Figure 3.4 Capture of Single spherical sodium carbonate particle used in dissolution experiments with Nikon Eclipse Ti Microscope .....	46
Figure 3.5 A typical dissolution experiment process scheme for single spherical sodium carbonate particle.....	47
Figure 3.6. SEM images of one single Sodium carbonate particle with zoom-in scale of (a) $100\mu\text{m}$ , (b) $10\mu\text{m}$ , (c) $2\mu\text{m}$ .....	52
Figure 3.7 Adsorption and desorption isotherm log plot of sodium carbonate particles .....	53
Figure 3.8 BET surface area plot of sodium carbonate particles .....	53
Figure 3.9 BET isotherm plot of sodium carbonate particles .....	54
Figure 3.10 BET test report of sodium carbonate particles .....	54
Figure 3.11 A dissolution process of one single sodium carbonate particle under $30^\circ\text{C}$ from high speed camera .....	56
Figure 3.12 Measurement of particle diameter under $30^\circ\text{C}$ at different time .....	57



Figure 3.13 Fitting of measured concentration of sodium carbonate under 30oC with Equation (5 .....	59
Figure 3.14 Diameter of single sodium carbonate particle as function of time under different temperature .....	60
Figure 3.15 Diameter of single sodium carbonate particle as function of time under different pH .....	60
Figure 3.16 Concentration of dissolved sodium carbonate as function of dissolution time under different temperature .....	61
Figure 3.17 Concentration of dissolved sodium carbonate as function of dissolution time under different pH .....	61
Figure 3.18 Fitting of measured experiment concentration with equation (5) under (a) 30°C; (b) 40°C; (c) 50°C; (d) 60°C; (e) 70°C .....	64
Figure 3.19 Fitting of measured experiment concentration with equation (5) under (a) pH 4; (b) pH 7; (c) pH 8; (d) pH 9; (e) pH 10 .....	66
Figure 3.20 The dissolution rate constant of single spherical sodium carbonate particle under different temperature .....	67
Figure 3.21 The dissolution rate constant of single spherical sodium carbonate particle under different pH .....	67
Figure 4.1 Compressed sodium carbonate tablet .....	72
Figure 4.2 Set-up process of typical dissolution experiment .....	73
Figure 4.3 Stirring hotplate used for dissolution experiment.....	74
Figure 4.4 Temperature controller of stirring hot plate.....	75
Figure 4.5 XRD measurement of sodium carbonate tablets comparing with initial sodium carbonate particles .....	77
Figure 4.6 SEM images of Sodium carbonate tablet with scale of (a) 100µm and (b)	

2 $\mu$ m.....	79
Figure 4.7 Calibration of conductivity values with dissolved amount of sodium carbonate .....	81
Figure 4.8 Ratio of dissolved sodium carbonate as function of time under 60°C and 300RPM.....	84
Figure 4.9 Fitting of dissolution experiment with Hixson-Crowell model under 60°C and 300RPM.....	86
Figure 4.10. Ratio of dissolved sodium carbonate under 300RPM. ....	89
Figure 4.11. Ratio of dissolved sodium carbonate under 500RPM. ....	89
Figure 4.12. Ratio of dissolved sodium carbonate under 700RPM. ....	90
Figure 4.13. Fitting with Hixson-Crowell model on dissolution experimental data of sodium carbonate tablet under 300RPM and (a) 20°C; (b) 30°C; (c) 40°C; (d) 50°C; (e) 60°C. ....	93
Figure 4.14. Fitting with Hixson-Crowell model on dissolution experimental data of sodium carbonate tablet under 500RPM and (a) 20°C; (b) 30°C; (c) 40°C; (d) 50°C; (e) 60°C. ....	96
Figure 4.15. Fitting with Hixson-Crowell model on dissolution experimental data of sodium carbonate tablet under 700RPM. ....	98
Figure 4.16. Dissolution rate constant of sodium carbonate tablet fitting with Hixson-Crowell model under different temperature and pH.....	99
Figure 5.1. Molecular structural formula of CMC [99] .....	103
Figure 5.2. SEM image of carboxymethyl cellulose.....	107
Figure 5.3. SEM image of croscarmellose sodium .....	107
Figure 5.4. SEM image of crospovidone .....	108
Figure 5.5 Set-up process of typical dissolution experiment of composite tablet ..	111

Figure 5.5. SEM image of tablet with mixture of sodium carbonate and carboxymethyl cellulose.....	114
Figure 5.8 Ratio of dissolved sodium carbonate from composite tablet containing 3% carboxymethyl cellulose under 30°C.....	117
Figure 5.9 Fitting of dissolution experiment for composite tablet containing 3% CMC under 30°C.....	119
Figure 5.10. Ratio of dissolved amount of sodium carbonate from pure sodium carbonate tablet, composite tablet containing 3% carboxymethyl cellulose and 5% carboxymethyl cellulose under (a) 20°C; (b) 30°C; (c) 40°C; (d) 50°C; (e) 60°C. .....	122
Figure 5.11 Linear fitting of dissolution limited range with Hixson-Crowell model for composite tablet containing 3% carboxymethyl cellulose under (a) 20°C; (b) 30°C; (c) 40°C; (d) 50°C; (e) 60°C.....	126
Figure 5.12 Linear fitting of dissolution limited range with Hixson-Crowell model for composite tablet containing 5% carboxymethyl cellulose under (a) 20°C; (b) 30°C; (c) 40°C; (d) 50°C; (e) 60°C.....	128
Figure 5.13 Dissolution rate constant for pure sodium carbonate tablet, composite tablet with 3% carboxymethyl cellulose 5% carboxymethyl cellulose.....	129
Figure 5.14. SEM image of sodium carbonate-croscarmellose sodium composite tablet.....	132
Figure 5.15 XRD test of composite tablet containing 3% croscarmellose sodium comparing with pure sodium carbonate tablet.....	132
Figure 5.16 XRD test of composite tablet containing 5% croscarmellose sodium comparing with pure sodium carbonate tablet.....	133
Figure 5.17 Ratio of dissolved sodium carbonate from composite tablet containing 3%	

croscarmellose sodium under 30°C .....	136
Figure 5.18 Fitting of dissolution experiment for composite tablet containing 3% croscarmellose sodium under 30°C .....	137
Figure 5.19 Ratio of dissolved amount of sodium carbonate under (a) 20°C; (b) 30°C; (c) 40°C; (d) 50°C; (e) 60°C .....	140
Figure 5.20 Linear fitting of dissolution limited range with Hixson-Crowell model for composite tablet containing 3% CCMC under (a) 20°C; (b) 30°C; (c) 40°C; (d) 50°C; (e) 60°C .....	144
Figure 5.21 Linear fitting of dissolution limited range with Hixson-Crowell model for composite tablet containing 5% CMCC under (a) 20°C; (b) 30°C; (c) 40°C; (d) 50°C; (e) 60°C .....	146
Figure 5.22 Dissolution rate constant for pure sodium carbonate tablet, composite tablet with 3% croscarmellose sodium and 5% croscarmellose sodium .....	147
Figure 5.23. SEM image of sodium carbonate-crospovidone composite tablet .....	149
Figure 5.24 XRD of sodium carbonate-crospovidone composite tablet containing 3% crospovidone comparing with pure sodium carbonate tablet .....	150
Figure 5.25 XRD of XRD of sodium carbonate-crospovidone composite tablet containing 5% crospovidone comparing with pure sodium carbonate tablet .....	150
Figure 5.26 Ratio of dissolved sodium carbonate from composite tablet containing 3% crospovidone under 30°C .....	153
Figure 5.27 Fitting of dissolution experiment for composite tablet containing 3% crospovidone under 30°C .....	154
Figure 5.28 Ratio of dissolved sodium carbonate from pure sodium carbonate, composite tablet containing with 3% crospovidone and 5% crospovidone under (a) 20°C; (b) 30°C; (c) 40°C; (d) 50°C; (e) 60°C. ....	157

Figure 5.29 Linear fitting of dissolution limited range with Hixson-Crowell model for composite tablet containing 3% PVPP under (a) 20°C; (b) 30°C; (c) 40°C; (d) 50°C; (e) 60°C .....	161
Figure 5.30 Linear fitting of dissolution limited range with Hixson-Crowell model for composite tablet containing 5% PVPP under (a) 20°C; (b) 30°C; (c) 40°C; (d) 50°C; (e) 60°C .....	163
Figure 5.31 Dissolution rate constant for pure sodium carbonate tablet, composite tablet with 3% crospovidone and 5% crospovidone .....	164
Figure 5.32. Dissolution rate constants of pure sodium carbonate tablet; composite tablet containing 3% carboxymethyl cellulose, 3% croscarmellose sodium and 3% crospovidone respectively. ....	165
Figure 5.33. Dissolution rate constants of pure sodium carbonate tablet; composite tablet containing 5% carboxymethyl cellulose, 5% croscarmellose sodium and 5% crospovidone respectively. ....	166

## LIST OF TABLES

Table 2.1. The measurements of particle roundness based on different definitions .	10
Table 2.2. Classification scheme for sphericity of particle with Riley's research ....	12
Table 2.3. Classification of degree of irregularity.....	13
Table 2.4. Mechanical process of dissolution .....	30
Table 2.5. Exponent of Korsmeyer-Peppas model.....	38
Table 3.1 Diameter of sodium carbonate particle as function of dissolution time under 30°C.....	57
Table 3.2 Remaining amount of undissolved sodium carbonate as function of time	58
Table 3.3 Concentration of sodium carbonate in solution as function of time under 30°C.....	58
Table 3.4 Viscosity of water from 30°C to 70°C .....	68
Table 4.1 Measured conductivity values with completely dissolved amount of sodium carbonate .....	80
Table 4.2 Conductivity of dissolution experiment under 60°C and 300 RPM.....	82
Table 4.3 Dissolved amount of sodium carbonate from experiment under 60°C and 300 RPM with calibration .....	82
Table 4.4 Concentration of sodium carbonate in solution as function of time under 60°C and 300 RPM .....	83
Table 4.5 Values of adjusted coefficient of determination from measurement data for dissolution models at different temperatures under the stirring speed of 300RPM. ....	85
Table 5.1 Conductivity values of composite tablet containing 3% carboxymethyl cellulose under 30°C .....	115
Table 5.2 Dissolved amount of sodium carbonate within composite tablet containing	

3% carboxymethyl cellulose under 30°C .....	116
Table 5.3 Concentration of sodium carbonate from composite tablet containing 3% carboxymethyl cellulose in solution under 30°C .....	117
Table 5.4 Conductivity values of composite tablet containing 3% croscarmellose sodium under 30°C.....	133
Table 5.5 Dissolved amount of sodium carbonate from composite tablet containing 3% croscarmellose sodium under 30°C.....	134
Table 5.6 Concentration of sodium carbonate from composite tablet containing 3% croscarmellose sodium in solution under 30°C.....	135
Table 5.7 Conductivity values of composite tablet containing 3% crospovidone under 30°C.....	151
Table 5.8 Dissolved amount of sodium carbonate from composite tablet containing 3% crospovidone under 30°C .....	151
Table 5.9 Concentration of sodium carbonate from composite tablet containing 3% crospovidone in solution under 30°C .....	152

## LIST OF SYMBOLS

$D_K$	Diameter of curvature of the sharpest corner
$L_W$	Longest diameter measured through the sharpest corner
$L$	Length of the grain, in projected plane
$I$	Width of the pebble, in the projected plane
$D_r$	Diameter of curvature of any corners
$D_i$	Diameter of the largest inscribed circle
$n$	Number of corners, including those whose diameters are zero
$I_{(2D)}$	Irregularity index of particle
$x$	Distance from the center of largest inscribed circle to the nearest point of concavity
$y$	Distance from the center of largest inscribed circle to the convex hull
$a, b$	Distance from center of largest inscribed circle to the tip of projections to side of concavity
$A, B$	Angles between $a$ and $x$ , $b$ and $x$ respectively
$\Delta N$	Transfer of quantity
$\vec{J}$	Vector of diffusion flux
$\Delta S$	Transfer area
$v$	Velocity
$\Delta t$	Transfer time
$J$	Diffusion flux
$D$	Diffusion coefficient
$\phi$	Concentration in the dimensions of [amount per unit volume]
$x$	Transfer length in dimensions
$\mu$	Mobility of particles
$k_B$	Boltzmann's constant
$T$	Absolute temperature
$\mu_q$	Electrical mobility of charged particles
$q$	Electrical charge of particles
$\eta$	Viscosity of medium
$r$	Radius of spherical particles
$\nabla$	Gradient operator
$M$	Dissolved mass



$t$	Dissolution time
$S$	Surface area of particle
$C_s$	Equilibrium solubility
$C_t$	Concentration in solution
$K$	Dissolution rate constant
$h$	Diffusion layer thickness
$v$	Volume of solution
$Q_t$	Dissolved amount of particle
$Q_0$	Initial amount of particle
$K_0$	Zero-order dissolution constant
$C_0$	Initial concentration
$K_H$	Higuchi dissolution rate constant
$K_f$	First-order dissolution rate constant
$w_0$	Initial amount of particle
$w_t$	Remaining amount of particle
$K_h$	Hixson-Crowell dissolution rate constant
$\frac{M_t}{M_\infty}$	Ratio of dissolved drug
$n$	Exponent
$M_0$	Initial amount of particle
$T$	Lag time from the measurement result of dissolution process
$a$	Scale parameter with time dependence
$b$	Shape parameter of dissolution process curve
$R$	Dissolution reference batch
$T$	Dissolution test batch
$n$	Number of time points
$A$	Surface area of particles
$A_0$	Initial surface area of particles
$\alpha$	Hydrodynamic radius of sucrose molecule

$\mu$	Viscosity of the medium
$\nu$	Kinematic viscosity of medium
$\omega$	Angular velocity

## CHAPTER 1. INTRODUCTION

Dissolution of solids has been studied for more than one century and has been well applied into many industrial fields on various chemical or physical applications for example food and pharmaceutical products. The fundamental findings on dissolution of solids are not only involved with the theoretical realization of dissolution, but also expanded into the applications with its scientific and regulatory properties. In many industrial fields based on these research. The research on dissolution of structured particles has the common relations with the characteristics of the particles themselves, physically or chemically. The physical characteristics of particles applied into dissolution studies are normally pointed as its objective properties. The notional name of physical properties of particles is most related to its size, shape, surface and structure. The research on physical properties has been greatly developed from the determination of size and shape of regular particles to the establishments of more precise measurement methods and techniques by computer in two or three dimensions for irregular particles. Therefore, the research on the aspects of physical properties of particles and its dissolution behaviours, and also a determined relation between both aspects are significant for practical industry and theoretical research development.

In this thesis, the research on the dissolution of structured particles contains the dissolution research of sodium carbonate and polymers with determined particle characteristics. As the important compositions of detergent with high proportion, the research on dissolution of sodium carbonate and polymers shows the significant impact on the quality of final detergent products that pertinent to Procter & Gamble applications. Although the importance of dissolution research on materials has been

deeply realized, few studies in the past years focus on the research of the dissolution behaviours of sodium carbonate and related polymer that are used as ingredients of detergent. From the view of industrial application, the final purpose of this research on the dissolution of sodium carbonate and polymers is to improve the using effect and product utility for example reducing dissolution time or dissolving more thoroughly under adverse conditions, and also provide useful ideas to the forms of final detergent products to achieve the increasingly improved utility requirements. From the view of development of theoretical research, because few research focus on the dissolution of sodium carbonate and its related industrial materials with different structures in the past years, the works in this thesis are expected to contribute to state the reliable conclusions to complete the research on area of dissolution of sodium carbonate and polymers. And what more important is to quantify the link between particle structures and experimental conditions with the dissolution behaviours with the accurate experimental methods and results.

The works in this thesis firstly starts from the research on the dissolution of one single spherical sodium carbonate particle and then steps into the research on the dissolution behaviors of sodium carbonate tablets that are made of sodium carbonate particles. Finally, three kinds of polymers are mixed with sodium carbonate respectively with different proportions to form sodium carbonate-polymer component tablets. The experimental works are carried out to investigate the dissolution behaviors of composite tablets with different polymers and the dissolution kinetics are quantified to examine the effect of these polymers. All the dissolution experiments are carried out at different solution environments. The influences of solution conditions are quantified accurately with the appropriate mathematical models that are selected by the comparison method. Following this

way, the relationships between the dissolution kinetics of experimental objects containing different structures with conditions are linked and the explanations on the relationships are further discussed. The findings of these relationships are expected to be crucially important for formulations and manufacturing processes detergent productions.

This thesis is divided into 6 chapters and the relevance to my work is clearly mentioned and discussed. Chapter 1 states a description of background, aims and intellectual contributions of my research in this thesis. Chapter 2 is the literature review part to review the relevant knowledge of my research topic in each section including the characteristics of particle size, shape and structure with theoretical development and measurement applications; solubility of solid particles in liquid on theoretical research and methodologies to measure the solubility; diffusion of particles in liquid by expressing the previous studies on quantification theories and applications; dissolution studies of particles in liquid including dissolution theories and models, mathematical models and main previous application and theoretical research on dissolution; finally the conclusions of literature review are expressed to relate previous research with my works in this thesis, point out the gaps with previous studies and highlight the knowledge that are used to support my statement of the novelty of my work. Chapter 3 states my research on dissolution of single spherical sodium carbonate particle under different temperatures and pH. The dissolution experiments are carried out with novel high speed image analysis method. The dissolution kinetics is quantified with shrinking sphere model and the effects of temperature and pH are examined in this Chapter. Chapter 4 represents my research on dissolution of sodium carbonate tablets. The dissolution experiments are carried out with conductivity method at different temperature and stirring speed, and

the dissolution kinetics are quantified with Hixson-Crowell model to examine the effect of temperature and stirring speed on dissolution kinetics. Chapter 5 states my research on dissolution kinetics of sodium carbonate-polymer composite tablet. The dissolution experiments are also carried out with conductivity method. The dissolution kinetics of composite tablet are quantified to examine the effect of different polymers on dissolution kinetics comparing with pure sodium carbonate tablet. In this way, the valuable results are obtained to discuss the application of these polymers into practical use with desired performance. Finally, Chapter 6 summarizes this thesis and then states comprehensive conclusions of my research. Furthermore, several potential scopes of future research work are introduced and discussed in this chapter.

## **CHAPTER 2. LITERATURAL REVIEW**

### **2.1 Particle Size and Shape**

#### **2.1.1 Particle Size Characterization**

With the first attempt to investigate the properties of different materials particles, the definitions of particles are usually taken into account of their size, shape and other morphologies such as size distribution and texture. Normally the basic definition of particle can be described as a small localized object with its own physical or chemical properties. The external forms of particles can perform as particles, pellets, tablets, crystals and aggregates. To research and present the correct properties and behaviors of particles, the effective data measurements and suitable data interpretations are very significant.

When the description of a particle property is mentioned, the first question usually is pointed as what is the meaning of the particle size. The definition of size is addressed as a dimensional parameter introduced into solid, liquid and gas particles. For the spherical particles, the size is uniquely defined by its diameter. For the regular particles such as cubes, the size is normally defined by the length of one single dimension and may be defined by more than one dimensions for some particles such as cones. But for a typical material particle in reality, the shape of particle is likely to be irregular. Therefore the definition of size of regular particles cannot be applied to these irregular particles and the particle size more depends on the particle measurement methods. The repeatable particle size measurement techniques are significant.

Previous research on particle size submitted a complete knowledge and

application system with analysis or measurement techniques on particle size and size distribution. With different measurement techniques and methods of particle size and size distribution, various previous research have been accomplished related to measurement and analysis of different materials. Gee and Bauder et al. [1] expressed the particle size analysis methods including pipette and hydrometer methods from sample preparation to implementation. Black [2] showed the measurements of fractionation and size analysis of soil particles. Allen [3] expressed the measurements methods of particle size on the aspects of surface area and pore size. Chantrell and Popplewell et al. [4] provided the measurement methods of particle size distribution factors in Ferro-fluid. Uchino and Sadanaga et al. [5] investigated the effect of particle size on crystal structures. Zhang et al. [6] presented a systematic study on the role of particle size in pure and doped nano-crystalline TiO<sub>2</sub> photo-catalysts.

When the particles are set as a group, the understanding of particle size of this group is not only related to the diameter of individual particles. The particle size distribution is used to define the relative amount of particles according to the size of each particle [7]. The particle size distribution is significant to understand the physical and chemical properties of group of particles. Through previous studies on particle size and size distribution, the measurement techniques applied into practical experiments and applications can be stated as sieving analysis, sedimentation analysis, imaging analysis, laser scattering and other techniques.

Sieving analysis is the technique used to measure particle size or size distribution of bulk particles. It is the basic measurement technique used into the basic measurement of particle size or distribution. The process of sieving normally is from the mechanical sensing. The method of sieving is applied to the bulk of particles



with the range from micro-meter to centimeter, and the data of particle size can be directly got from the measurement. It is worth of noting that the measurement of particle size distribution through this technique is very depended on the separation by sieves, for example the particles may be difficult to pass through the very fine sieves. Another notes of this technique is the amount of energy to sieve deeply affects the particle size distribution. Once the energy is over proper range, the particles may be damaged due to the friction of each particle. This technique is easy to be operated and applied for various kinds of material particles. However, the accuracy with sieving analysis of particle size and size distribution is not high.

Sedimentation analysis is a hydraulic sensing method to measure the hydraulic diameter of a particle. This method is applied to the bulk of particles with the range from 1 to 10 micrometer. The particle size can be obtained from the measured data by the sedimentation mathematical model. With this technique, the particle size measured with this technique is the derived diameter of particle such as equivalent spherical diameter. It is the technique based on the particles suspending in the viscous liquid. The sedimentation time lasts longer if the particle is smaller, thus this method is well applied for particles below 10 $\mu$ m. Because the samples must have to be dispersed in a liquid medium, the measurement performance significantly depends to the selection of liquid media. Therefore, the application of this technique is limited to practical research and studies.

Laser light scattering is an optical sensing method to measure the bulk of equivalent sphere particles with a wide range from nanometer to millimeter. The particles size is calculated by the measurement data by the mathematical model. The most widely used laser light scattering technique is laser diffraction equipment such as Mastersizer. This technique can be used into the measurement of dry or wet

particles.

Imaging analysis is the most widely used optical sensing technique to measure both individual particle and bulk of particles with the range from nanometer to kilometer. Usually the size with imaging analysis is regarded as projected diameter that can be measured directly from the measurement process with microscopy. It is a rapid and accurate method to measure the samples by taking the images and using software to analyze the size. The measurement equipment and software are well developed in currently applications. Therefore, in most cases, imaging analysis with microscopy is the first choice to determine particle size.





Beside above common techniques used into measurement of particle size and size distribution, there are also techniques that have been applied into the measurement of particle size and size distribution such as coulter analysis and air elutriation analysis. However, for a typical measurement of particle size and size distribution, sieving analysis and imaging analysis with microscopy are the two main techniques due to the combining of rapid operation and accurate performance for specific purpose.

### **2.1.2 Particle Shape characterization**

The shape of particle is usually used to describe the external geometrical expression. To define the shape of particle, there are four important aspects needed to be considered which are form, roundness, irregularity and sphericity [8]. Form is described as the tri-dimensional characteristic of particle through the definition of ratios of length, width and thickness. Roundness is related to the relative angularity of corners and edges. Irregularity is the deviation of three dimensional external expression of particle. Sphericity is defined as the degree of particle which is as a true sphere. The roundness and irregularity of particle is independent of form, but

sphericity of particle is dependent of both form and roundness.

Typically before the form of particle is determined, the quantification of length, width and thickness of particle is necessary to be determined. With the three dimensional measurement, length is the longest dimension of particle, width is the longest dimension perpendicular to length and thickness is the dimension perpendicular to both length and width. With the measurement of length, width and thickness, the degrees of flattening and elongation are the most important parameter to determine the shape of one particle. Wentworth [9] defined the flatness of particle by the formulation of  $(\text{length} + \text{width})/2\text{thickness}$ . Zingg [10] used the ratios of width to length and thickness to width to classify the basic four shapes. According to Zingg's expression, the classifications of particle shape are shown in Figure 2.1. Based on the classifications of Zingg, the names of shape were named as disc-shaped, spherical, bladed and rod-like by Pettijohn [11] and Krumbein [12]. In their definition, the ratio of thickness/length had been used to measure the flatness of particle and the ratio of width/length was used to measure the elongation of particle.

ZINGG CLASSES	$b/a < 2/3$	$b/a > 2/3$
$c/b < 2/3$	<b>BLADE</b> 	<b>DISC</b> 
$c/b > 2/3$	<b>ROD</b> 	<b>SPHERE</b> 

**Zingg classes**  
 $a > b > c$ : axis lengths of the ellipsoid

**Figure 2.1.** Zingg’s classification of particle shape. [11]

The measurement of roundness of particle is related to the sharpness of corners and edges of particle rather than the overall particle. Based on this definition, previous studies had stated many methods and models to measure and quantify the roundness of particle. These models developed by different researchers are shown in Table 2.1.

**Table 2.1.** The measurements of particle roundness based on different definitions

Formula	Range	Description
$\frac{D_K}{L_W}$ [13]	0-1	Ratio of diameter of curvature of sharpest corner to the long axis of grain
$\frac{D_K}{(L + I)/2}$ [14]	0-1	Ratio of diameter of curvature of sharpest corner to mean diameter
$\frac{\sum \frac{D_r}{D_i}}{n} = \frac{\sum D_r}{n D_i}$ [15]	0-1	Average ratio of diameter of curvature of all corners to diameter of largest inscribed circle

$\frac{n}{\sum \frac{D_i}{D_r}}$ [10]	0-1	Reciprocal of average ratio of diameter of largest inscribed circle to diameter of curvature of all corners
$\frac{D_K}{I}$ [16]	0-1	Ratio of diameter of curvature of sharpest corner to intermediate axis of grain
$\frac{D_K}{D_i}$ [17]	0-1	Ratio of diameter of curvature of sharpest corner to diameter of largest inscribed circle

Sphericity is the aspect that is depended on form and roundness of particles. Based on the previous studies, sphericity is the most important parameter to determine the degree of spheres. In this way, the determination of sphericity degree of one particle is important to examine and classify the spherical property of one particle. Typically, the sphericity of one particle is determined from its projection sphericity with imaging analysis by microscopy. The projection sphericity developed from previous researchers was usually determined by the ratio of diameter of a circle with the same area as the particle to the diameter of the smallest circumscribed circle. With this definition, many researchers such as Cox [18] and Rittenhouse [19] developed 2D measurement method with microscopy to investigate the sphericity of particles that were applied to sand size or gravel particles. However, some researchers such as Riley [20] developed 3D measurement method to measure the sphericity of particle. With Riley's research, the particle can be defined and classified with the limits of sphericity and the classification scheme for particles is represented in Table 2.2.

**Table 2.2.** Classification scheme for sphericity of particle with Riley's research

Definition	Very high sphericity	High sphericity	Moderate sphericity	Low sphericity	Very low sphericity
Class limits	0.894-1.000	0.775-0.894	0.632-0.775	0.447-0.632	0.000-0.447

For the regular shape particles, the measurements of form, sphericity and roundness with two or three dimensional methods are enough to investigate the shape of particles. However, if the particles are shown the clearly indentations and projections on the surface, these particles can be described as the irregular. To measure the irregular particles, a method has been developed by quantifying the number and magnitude of surface projections and indentations with two dimensional images. The irregularity index can be calculated as

$$I_{(2D)} = \sum \frac{y - x}{y}$$

Where  $x$  is the distance from the centre of largest inscribed circle to the nearest point of concavity,  $y$  is the distance from the centre of largest inscribed circle to the convex hull.

The total degree of profile irregularity can be calculated as

$$y = \frac{a \cos A + b \cos B}{2}$$

Where  $a$  and  $b$  are the distance from centre of largest inscribed circle to the tip of projections to side of concavity,  $A$  and  $B$  are the angles between  $a$  and  $x$ ,  $b$  and  $x$  respectively.

A simple classification of degree of irregularity is shown in Table 2.3.

**Table 2.3.** Classification of degree of irregularity

	Class limits	Geometric mid-point
Extremely irregular	> 2.0	/
Very irregular	1.0 – 2.0	1.414
Moderately irregular	0.5 – 1.0	0.707
Slightly irregular	0.0 – 0.5	0.250
Perfectly regular	0.0	/

Although shape is one of the fundamental properties of all particles, the quantification on the shape is kind of the most difficult aspect in the determination of structure of particle. Therefore, previous research are mainly related to the configuration of the definition and measurement of particle shape particle two or three-dimensionally. Based on these methodologies, the further studies on shape impact to many material applications are done by experimental or simulation methods. Winterbottom [21] expressed and developed a method to predict the equilibrated shapes of small particles on solid substrates. Champion and Katare et al. [22] showed that particle shape could be the new factor to affect the designing and final properties of drug carriers comparing with traditional factors. Cleary and Sawley [23] studied the effect of particle shape on hopper discharge by a simulation method for modelling the industrial granular flows. In many cases, the effects of particle shape are combined with the effect of particle size to be discussed. Mosharraf and Nystrom [24] studied the effect of particle shape and size on the dissolution rate of insoluble drugs including barium sulphate, oxazepam and glibenclamide. Cho and Dodds et al. [25] studied the effect of shape gathered with size of natural and crushed soil particles on the packing density, stiffness and strength.

## **2.2 Structure of Particle**

### **2.2.1 Introduction**

The structure of a particle is a key factor which determines the properties of particle. The description of particle structure can be expressed from the internal components properties to external properties such as size, shape and morphology. For the internal properties, the structure of each component of particle can be defined as the spatial arrangement. To quantify the internal structure, three aspects should be known including the amount of each component, the size of each phase, and the distribution of these phase. However, the quantification of these aspects is not related to the properties of external structure such as morphology and shape of particle. Therefore, to obtain the clear whole information of particle structure, both internal and external structure information are used to be combined to express the structure properties of a particle.

### **2.2.2 Measurement Methodologies of Particle Structure**

As the common and basic methods to measure the structure of particle, optical technologies are well applied to the internal and external structure either in two or three dimensional methods such as the measuring of amounts of phase volumes, sizes and homogeneity measurement. The most widely used techniques measuring particle structure include scanning electron microscopy, BET measurement technique, X-ray Diffraction, and other structure measurement techniques such as Infrared Spectroscopy.

#### ***Scanning Electron Microscopy (SEM)***

Scanning electron microscopy (SEM) is one important 2D technique to measurement the characteristics of particles with electron microscopy. With this



technique, the images of measured particles are produced by scanning the samples with a focused beam of electrons. These electrons will interact with the atoms of measured particles. After interaction of electrons with atoms, various signals are detected. These signals will contain and show the information of surface topography and composition of measured particle samples. When SEM starts to run, the electron beam is scanned a raster scan pattern. Then the position of beam is used produce the image of particle surface combing with detected signals. A typical schematic diagram of SEM set-up for measurement of samples is shown in Figure 2.2 [26].

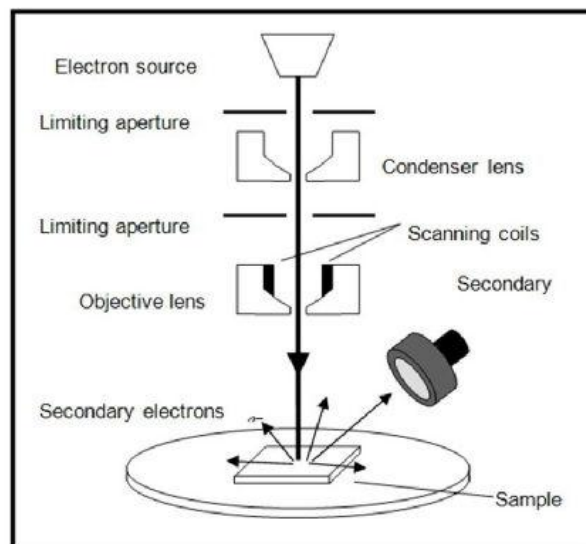


**Figure 2.2** A typical schematic diagram of SEM set-up.

With this technique, the resolution of SEM can reach better than 1 nm. The prepared samples can be measured and observed at various conditions including in high vacuum, low vacuum, or wet conditions which are normally used into environmental SEM. Also the measurement with SEM can be achieved under cryogenic or elevated temperatures. For a typical SEM test, the most common detection mode by SEM is achieved with the secondary electrons that are emitted by atoms exciting by electron beam. For the measured samples with the relevant flat

surface conditions, the plume of secondary electrons can be normally contained by the sample. However for the measured samples with tilted surface conditions, the plume of secondary electrons is partially exposed and more electrons are thus emitted. By detecting and collecting these secondary electrons that are emitted from the scanning of samples, the display and topography surface image of measured particles are produced. These images normally contain the surface information of samples with high resolution. These surface images and the information containing resolution and scale bar etc. can be used to understand and analyze the surface characteristics and structures of measure samples.

### ***BET measurement technique***

For the analysis of particle's structure, the information of surface area with pore properties is very important to understand the characteristics of measured particles. Among modern techniques, BET measurement with its equipment is the most common used technique to measure and analysis the surface properties containing porous information of sample particles. With this technique, the surface area analysis is achieved with BET theory, the pore size and volume analysis can be achieved with BJH theory.

Simply speaking, the BET method is developed based on adsorption of gas on the surface of samples. With the measurement of amount of gas adsorbed at a certain pressure, the surface area of samples is allowed to be determined. BET method is based on the BET adsorption theory. Brunauer-Emmett-Teller (BET) theory is developed to explain the physical adsorption of gas molecules on the surfaces of particles [27]. The equation BET theory can be expressed as

$$\frac{1}{W((P_0/P)-1)} = \frac{1}{W_m C} + \frac{C-1}{W_m C} \left(\frac{P}{P_0}\right)$$

Where W is the weight of adsorbed gas; P/P<sub>0</sub> is the relative pressure; W<sub>m</sub> is the weight of adsorbate as monolayer; and C is the BET constant.

This theory provides the basis for the analysis of measurement of specific surface area of samples. Normally, the specific surface area of samples are evaluated by BET analysis with nitrogen multilayer adsorption method as the function of relative pressure [28]. The experimental adsorption isotherm systems for gas-solid adsorption have various shapes. The common used classification of adsorption isotherms is expressed by IUPAC [29] which is shown in Figure 2.3. These shapes of adsorption isotherm curve also provide useful preliminary information and prediction of pore structure of measured samples. With this classification, types of II, IV, and VI normally can be measured and analyzed with BET method that shows the stronger interaction of adsorptive-adsorbent than adsorptive-adsorbate; Types III, and V of shows the weak interactions between gas and adsorbent.

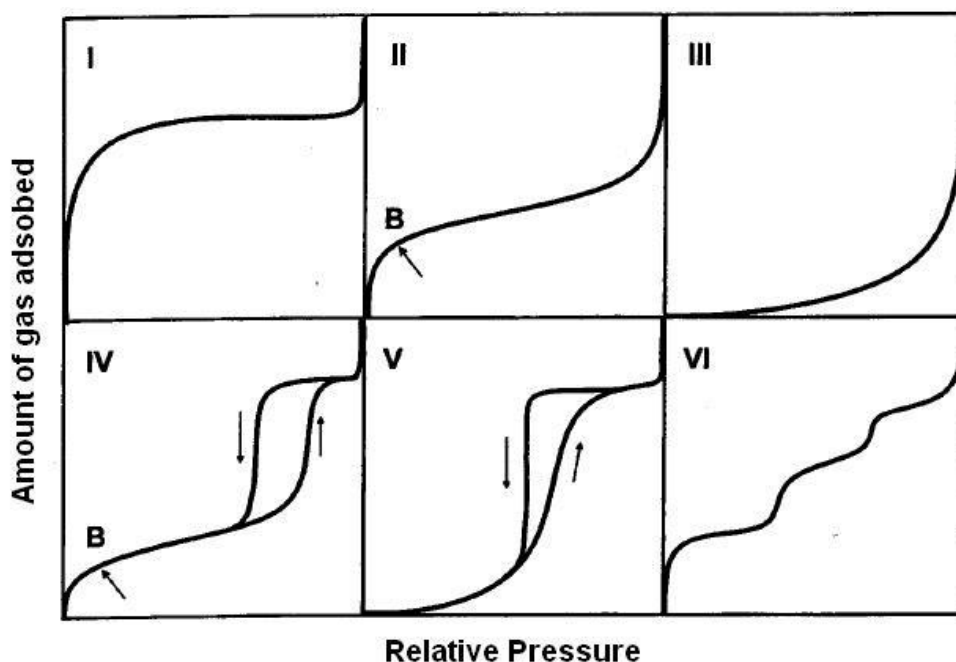


**Figure 2.3** IUPAC classification of adsorption isotherms

BJH method is based on the Barrett-Joyner-Halenda (BJH) theory. BJH theory was proposed in 1951. This theory was initially used to the analysis the relatively wide-pore adsorbents with a wide pore size distribution [30]. It is now also used to determine the pore area and specific pore volume with adsorption and desorption techniques. Pore volume and pore area distribution can be analyzed in the mesopore and macropore ranges [31] that classified by IUPAC with BJH theory with a full complement of adsorbate thickness models [32]. Also the average pore diameter can be determined with the BJH adsorption and desorption isotherms measurements.

### ***X-ray Diffraction (XRD)***

X-ray diffraction, normally known as XRD, is a nondestructive technique that is normally used to identify the crystalline phases and orientations of sample particles. Usually, this technique is an important tool to identify the atomic and molecular structure of a crystal since the crystalline atoms make the beam of incident X-rays to diffract into many specific directions. With the measured angles and intensities of

diffracted beams, a 3D image of electron density within crystals can be produced. With this electron density, the mean positions of atoms within crystals can be determined. Now the application of XRD can be usually introduced as measuring the average spacing between layers or rows of atoms, determining the orientation of a single crystal or grain, evaluating the crystal structures of unknown materials and measure the size shape and internal stress of small crystalline regions.

XRD technique can be thought to be based on Bragg's Law with the equation shown as [33]:

$$n\lambda = 2d \sin \theta$$

This equation expresses the cleavage faces of crystals appear to reflect X-ray beams at different angles of incidence theta where d is the distance between two layers within a crystal;  $\lambda$  is the wavelength of incident X-ray beam; n is one integer.

With a typical measurement with XRD technique, a schematic diagram is shown in Figure 2.4 [34].

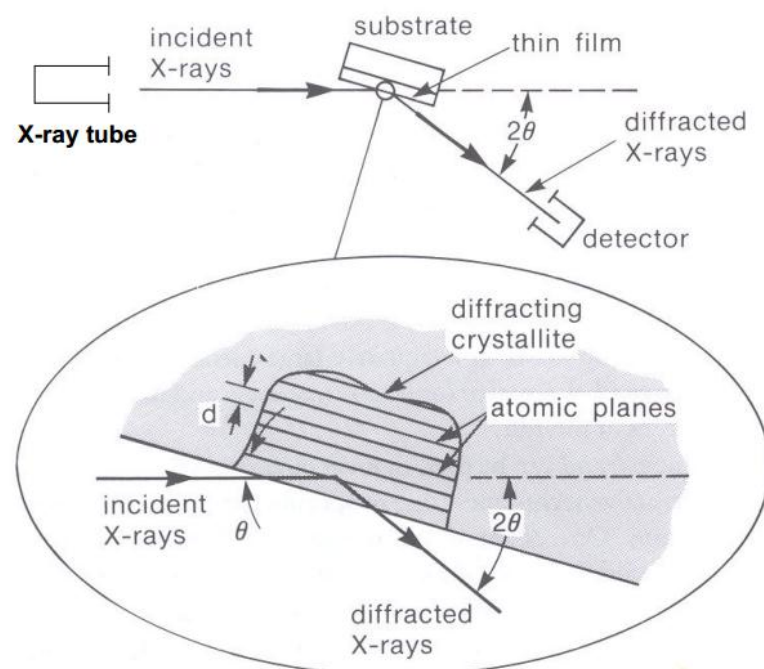


**Figure 2.4** A schematic diagram of a typical XRD measurement

For the analysis with measurement of XRD for the phase identification, a typical process can be thought as obtaining XRD pattern at first. Then the d-spacing is measured with measurement, and the integrated intensities are obtained. At last, the measured data are compared with known standards in the JCPDS files to determine the information of measured samples. Before the measurement starts, the samples should normally be prepared as powders with the size between 0.1 $\mu\text{m}$  to 40 $\mu\text{m}$ . The bulks of sample powders should obtain smooth surface after polishing. With the measurement data, the shapes of peak including peak position, width and intensity are significant for the analysis of XRD data, as well as XRD pattern. With the measured data, the structure of crystals also can be determine such as lattice parameters, strain and grain size.

### ***Infrared Microscopy (IR)***

IR spectroscopy is a widely used type of spectroscopy for analytical testing of gemological information of samples. This technique is based on the absorption spectroscopy and applies the infrared light that owns a longer wavelength and lower frequency than visible light to deal with the infrared region of electromagnetic spectrum. For a typical measurement with IR spectroscopy, the measured samples could be with the form of solid, liquid or gaseous. The instrument of infrared spectrometer is used to produce the infrared spectrum. A typical IR spectrum should be a figure of infrared light absorbance on the vertical axis as function of frequency or wavelength on the horizontal axis. A common experimental instrument of IR spectrometer used widely is the Fourier Transform Infrared Spectrometer (FTIR).

Normally, all infrared instruments are applied with- mid or near-infrared optics

with the frequency of 500-7000  $\text{cm}^{-1}$ . Within this frequency range, the spatial resolution of IR spectroscopy could be reached to micrometer-scale. For the far-infrared spectroscopy with the frequency of 50-400  $\text{cm}^{-1}$ , it is normally used to measure the lattice vibration of samples. However, it is not usually used into the gemological testing with far-infrared range.

When the infrared microscopy is not used into the measurement, two types of accessories are usually used into the direction and focusing the infrared beam to samples including beam-condensing optics [35] and diffuse-reflectance infrared Fourier transform (DRIFT) [36]. Beam-condensing optics are usually used into the measurement of transmission or absorption spectroscopy, and DRIFT optics are usually used for the measurement of reflection or absorption spectroscopy. Both optical methods are applied for macro-scale samples larger than millimeters. However, it is still lack of the spatial resolution to analyze the sub-millimeter microscopic samples.

Based on these advanced techniques, huge amount of previous studies and research had been carried out to measure the structure of particles of various different materials. Carlson [37] studied the structure of alpha particles by microscopic method with interaction models. Flagan and Lunden [38] developed the condensation method to synthesize the nanostructured particles from vapor phase in the carrier gas. Lemb and Oei et al. [39] examined the structure and size distribution of technegas particles by TEM and MS methods. Furthermore, the effects of particle shape on different functions also have been investigated in many cases. Palovic and Lvanovic [40] examined the effect of particle shape on determining the apparent density of electrolytic copper powders by sieve analysis and SEM analysis methods. Han and Miranda [41] studied the effect of surface structure of nanoparticles of Pt

on the chemisorption energy of OH and O. Bown [42] examined the particle structure of paper fillers and studied the effect of this structure on the paper properties.

## **2.3 Solubility of Particles**

### **2.3.1 Introduction**

For practical applications, solubility is one of the fundamental properties to investigate the characteristic properties of one substance. It can be used to describe the substance, indicate the polarity and distinguish from other different substances.

Solubility is the subject that solute (solid, liquid or gaseous) dissolve in the solvent (solid, liquid or gaseous solvent) to form the homogeneous solution. The property of solubility fundamentally depends on the physical and chemical properties of solute and solvent. Due to the process of dissolution may be related to the chemical reaction in solution, the solubility is not only the description of ability of solute of dissolving or liquefying. The measurement of solubility of a substance in solvent is usually with the saturation concentration, and under some certain conditions the equilibrium solubility can be exceeded to as the so called supersaturated solution [43].

From the view of molecular aspects to solubility, the solubility happens under dynamic equilibrium. That means the solubility is happening along with the processes of dissolution and phase joining. Thus the equilibrium solubility is at when these two processes proceed with a rate.

The solubility is mainly determined by the balance of intermolecular forces between the solute and solvent, and the entropy change. During the dissolution process, the entropy change usually involves two steps. During the process of



forming hydrated ions within dissolution process, a hydration layer is formed around the ions due to the strong electric charge effects of ions. With this hydration process, the degree of disorder within dissolution system becomes smaller. At the same time, the cluster structures of water molecules are destroyed due to the hydration of ions. It leads to the greater freedom of water molecules and the entropy of hydration becomes higher with the increasing degree of disorder of this dissolution system. Therefore, the change of entropy during dissolution process is determined by these two steps.

The dissolution process also can be described as three steps including breaking solute-solute attractions such as lattice energy, breaking solvent-solvent attractions such as hydrogen bonding and forming solvent-solute attractions in solvation. Lattice energy is usually defined for the crystalline solid to describe the energy of formation of the crystal from infinitely-separated ions, molecules or atoms, and invariably negative which was developed originally for the rocksalt-structured or sphalerite-structured compounds where the ions occupy high-symmetry crystal lattice sites. The value of enthalpy of solution is the sum of these three steps, and the energy will be released.

The intermolecular forces between solute-solute molecules and solvent-solvent molecules are significant to be considered. The process of bond breaking and bond forming happen simultaneously. If the solute-solvent force is bigger than the solute-solute and solvent-solvent force, the dissolution will happen.

The factors that affect this balance also affect the solubility such as temperature and pH. Besides these factors, solubility also depends on the presence of other species dissolved in solvent, the potential which the solid remains the

thermodynamically stable phase, and also the physical size of the crystal or droplet solute.

The solubility is usually described as a concentration that the maximum equilibrium amount of solute dissolving in unit solvent. This concentration is also related to different specified conditions. With this description, the solubility can be expressed simply. However, this expression is hardly depended on the presence of species in solvent.

### **2.3.2 Measurements and Applications**

Williamson [44] expressed a popular method to predicate the solubility that was similar with predicating dissolving properties. With this method, it describes the dissolving of one solute will express the best performance in the solvent which has the similar chemical structure with the solute. Therefore, the capacity of solvation of the solvent is strongly depended on the polarity of itself. Furthermore, the solubility of substance is much related to the entropy of mixing and more depended on the enthalpy of dissolution and hydrophobic effect.

The solubility constant also can be applied to describe the saturated solutions of low solubility. This constant is used as a special equilibrium constant to express the balance between dissolved ions and undissolved. Therefore this constant is sure to apply on the reverse of dissolving reactions. Similar with other equilibrium constants, the solubility constant is strongly affected by temperature. However, different with solubility, the solubility constant is independent of the presence of other components in solvent. For the polymers solubility, the Flory-Huggins solution theory [45] is usually to describe the solubility of polymer as a theoretical model. Besides the theoretical model, the Hansen solubility parameter [46] and Hildebrand

solubility parameter [47] are also used to predicate the solubility of polymers as the empirical model. Furthermore, this empirical model can be applied to predicate the solubility from physical constants such as enthalpy of fusion. Under the condition of hydrophobic solvent and hydrophilic solvent, the partition coefficient is usually used to measure the solubility of different components.

## **2.4 Diffusion of Particles in Liquid**

### **2.4.1 Concepts of Diffusion**

Diffusion is one of phenomena which happen everywhere in nature and practical life. Simply speaking, diffusion is the way leading to mixing or mass transport. From the theoretical views, Philibert [48] represented the description of diffusion from two ways:

- Diffusion is a phenomenological approach with the explanation of Fick laws of diffusion and their mathematical models.
- Diffusion also can be considered as the physical and atomistic description with the explanation of the random walk of diffusion particles.

From the view of phenomenological approaching, the diffusion flux is proportional to the negative gradient of concentrations according to Fick's laws. Generally this approach goes from the higher concentration area to the lower concentration area. From the view of physical and atomistic description, diffusion can be regarded due to the random move of diffusing particles. Based on the diffusion of molecular, the movements of molecular are self-propelled and random due to the thermal energy. This phenomenon was first discovered by Robert Brown to be named as Brownian motion [49]. Then the theories of Brownian motion and atomistic diffusion were developed by Albert Einstein [50].

### 2.4.2 Quantifications and Applications

To quantify the process of diffusion, some basic mathematic models are developed. Basically speaking, these mathematic models are built to express the diffusion flux over the concentrations. The diffusion flux can be described as the transfer of unit quantity through a unit area with velocity per time. The equation is shown as:

$$\Delta N = (\vec{J}, v)\Delta S\Delta t + o(\Delta S\Delta t)$$

Where  $\vec{J}$  is the vector of diffusion flux;  $\Delta N$  is the transfer of quantity;  $\Delta S$  is the transfer area;  $v$  is the velocity and  $\Delta t$  is the transfer time. With the replacement of vector transfer area  $\Delta \vec{S} = v\Delta S$ , this equation can be transformed into

$$\Delta N = (\vec{J}, \Delta \vec{S})\Delta t + o(\Delta \vec{S}\Delta t)$$

It is worth noting that for the definition of transfer quantity, it can be regarded or described as the particle's number, mass, energy or electric charge.

Furthermore, the most widely used mathematical model to be applied into diffusion is Fick's law of diffusion which was first expressed by Adolf Fick [51]. Normally speaking, Fick's law is used to describe and solve the diffusion and its coefficient. There have Fick's first law and Fick's second law to be well developed and built into applications.

Fick's first law is expressed as to relate the diffusion flux with concentration under the condition of the assumption of steady state. This law assumes that the diffusion flux travels from the area of high concentration to the area of low concentration with a proportional magnitude to concentration gradient. The equation of Fick's first law for one dimension can be expressed as:

$$J = -D \frac{\partial \phi}{\partial x}$$

Where  $J$  is the diffusion flux (amount per unit area per time) which is used to describe the transfer of amount through an area during a short time;  $D$  is the diffusion coefficient;  $\phi$  is the concentration in the dimensions of [amount per unit volume], and  $x$  is transfer length in dimensions.

The Fick's first law is usually used into practical applications by previous researchers. Lavery and Oldham et al. [52] used the Fick's first law to predict the pore-water nutrient fluxes. Denny and Kamaruddin et al. [53] studied the applications of Fick's first law to separate membrane from multicomponent mixtures.

The quantification of diffusion coefficient can be done by Stokes-Einstein equation [54]. Firstly, the initial diffusion coefficient can be expressed as:

$$D = \mu k_B T$$

Where  $D$  is the diffusion coefficient;  $\mu$  is the mobility of particles;  $k_B$  is the Boltzmann's constant and  $T$  is the absolute temperature.

There are two most widely application with this equation: Electrical mobility equation and Stokes-Einstein equation. Electrical mobility equation [55] can be expressed as

$$D = \frac{\mu_q k_B T}{q}$$

Where  $\mu_q$  is the electrical mobility of charged particles and  $q$  is the electrical charge of particles.

Stokes-Einstein equation can be expressed as

$$D = \frac{k_B T}{6\pi\eta r}$$

Where  $\eta$  is the viscosity of medium and  $r$  is the radius of spherical particles.

For two or more dimensions, the diffusion flux can be related to the gradient operator  $\nabla$  which is shown as

$$J = -D\nabla\phi$$

For one dimension diffusion, the driving for this diffusion is the amount of concentration gradient under ideal condition. However under the practical conditions especially with mixture chemical solutions, the driving force can be the gradient of chemical potential of each component.

The definition of Fick's second law can be described as the process that how diffusion leads to the changing of concentration with time. The equation can be expressed as:

$$\frac{\partial\phi}{\partial t} = D \frac{\partial^2\phi}{\partial x^2}$$

For the condition of two or more dimensions, the Fick's second law can be transformed into:

$$\frac{\partial\phi}{\partial t} = D\nabla^2\phi$$

Basically, it is assumed that the diffusion coefficient in Fick's second law is a constant. However, if the diffusion coefficient is not the constant, the Fick's second law becomes into:

$$\frac{\partial \phi}{\partial t} = \nabla \cdot (D \nabla \phi)$$

Based on Fick's second law, many applications were studied by previous researchers. Azuara and Cortes et al. [56] related the kinetics model of osmotic dehydration with Fick's second law. Ding and Petuskey [57] studied the solutions to solve issues of diffusion of Fick's second law by Laplace transformation method.

Besides the Fick's law of diffusion, many diffusion mathematical models and theories have been developed on many different applications. Avraham and Havlin [58] studied the anomalous diffusion model in porous medium. Weiss [59] developed the random walk model to study and investigate the aspects of diffusion.

## **2.5 Dissolution of Particles**

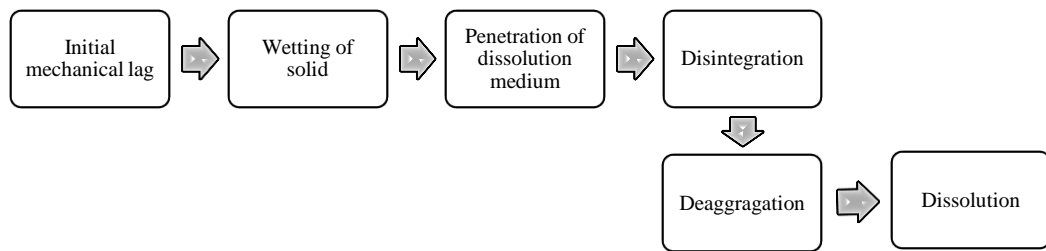
### **2.5.1 Dissolution Process**

Dissolution can be described as the process of which the solute forms into solution with a given solvent and conditions. For the solid solute, the solid itself will be disintegrated into separate ions, atoms or molecules forms. This dissolution process and its outcomes such as solubility can be obtained by the internal thermodynamic energy for example heat or entropy of solution. However, the kinetic process of dissolution is not involved as its dissolution process. Thus the free energies are the key to lead the occurring of dissolution, however in turn these free energies are controlled by the interactions of different chemical bonds in the solvent.

The process of dissolution can be regarded as the process of disintegration from the initial solid into final ions, atoms or molecules. During this process, dissolution also can be thought as the process from very limited dissolution to limited dissolution and finally into well dissolution. But the description of dissolution of

mechanism is another way. Thus the process of mechanism dissolution can be expressed in Table 2.4.

**Table 2.4.** Mechanical process of dissolution



### 2.5.2 Dissolution Models and Theories

In the research of dissolution, Higuchi [60] provided fundamental contributions to the development of dissolution theories. According to his research, there are three models alone or in combination to describe the dissolution process and mechanisms. These three models include: diffusion layer model, interfacial barrier model and Danckwerts model.

The diffusion layer model was simply used for a crystal solid to describe the dissolution process in the pure solvent without any reactive actions. This model was once expressed by Nernst [61]. According to his studies, it was assumed that there was a layer around the solid surface and the equilibrium conditions occurred on the surface. Then the dissolution process was driven by the diffusion movement of molecules in this layer. Therefore the dissolution process can be expressed that the first step of solid forming interface in solvent is very quick. And it leads to the formation of saturated stagnant layer around the surface. Then a slow diffusion



occurs from the surface into bulk through the diffusion layer. This process of diffusion layer model can be imaged in Figure 2.5.

The interfacial barrier model assumed that there was a high activation free energy to promote the interfacial transport process [62]. According to this model, the surface of solid is continually exposed to the solvent and the equilibrium is assumed at solute-solvent interface. Then the solute diffuses and is carried into the solvent by the packets under the agitating condition. Therefore there is no layer around the surface and the surface is continually replaced by the solvent medium. The process of interfacial barrier model can be imaged in Figure 2.6.

The Danckwerts model is assumed that the macroscopic packets of solvent reach the solute-solvent interface firstly by the eddy diffusion [63]. And then these packets at the interface can absorb into solute. This process continually occurs and the surface is continually replaced by the new packets. Therefore the surface renewal process can be related to the solute transport process. The process of this model can be imaged in Figure 2.7.

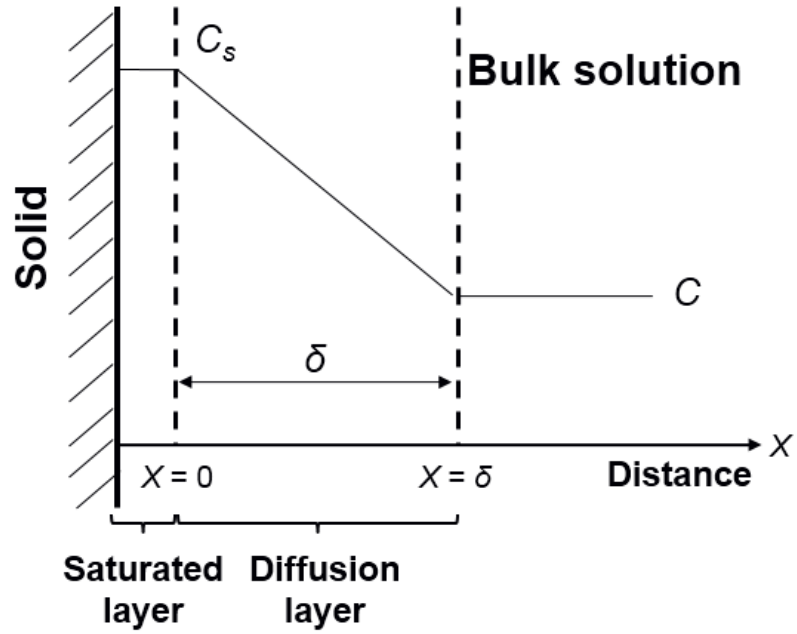


**Figure 2.5** Description of diffusion layer theory. [51]

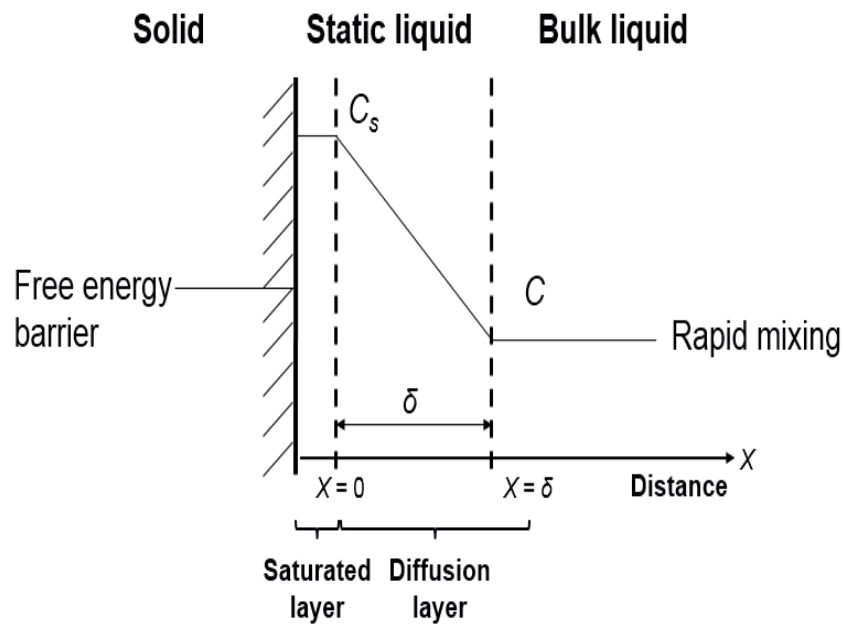


**Figure 2.6** Description of interfacial barrier model. [51]

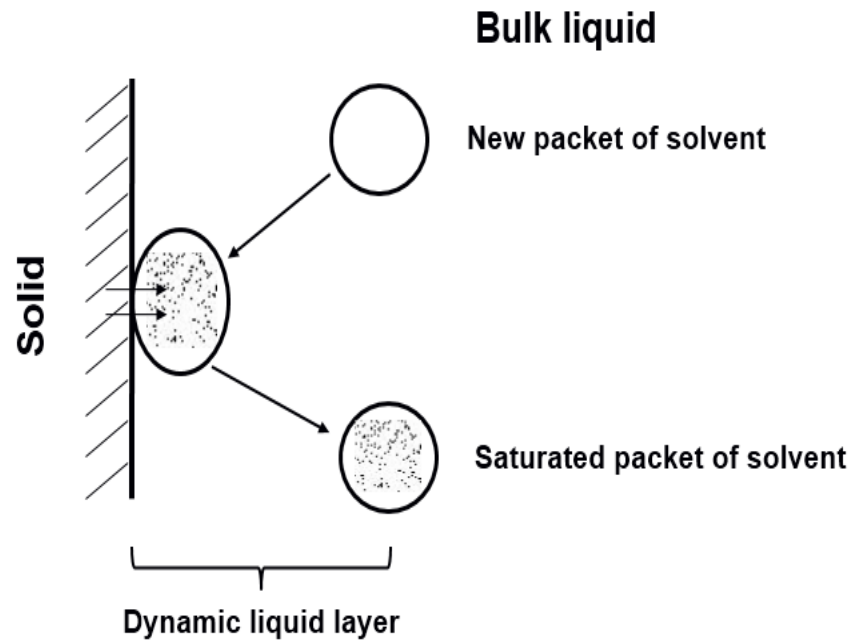


**Figure 2.7** Description of Danckwerts model. [51]

### 2.5.3 Mathematical Models of Particle Dissolution

The mathematical models on dissolution kinetics are greatly developed and expanded from medical sciences other industries. The initial aim of developing more and more mathematical models is to build effective productions. And in turn with using the mathematical models, the dissolution system can be predicted and realized before the system goes out. Furthermore, the development of mathematical model provides the methods to measure the parameters related to the dissolution system by fitting the model with experimental data. Therefore, the models can be thought as the mathematical method to identify the dissolution process and its parameters affecting dissolution kinetics.

There are many fundamental mathematical models based on Noyes-Whitney equation and Nernst-Brunner film theory on dissolution kinetics which can be expressed as statistical methods including exploratory data analysis method, repeated measures design and multivariate approach; model dependent methods

including zero-order model, first-order model, Higuchi model, Hixson-Crowell model, Baker-Lonsdale model, Korsmeyer-Peppas model and Weibull model; model independent method including difference factor and similarity factor.

The first principle to quantify the dissolution kinetics was described by Noyes and Whitney in 1897 [64] with the equation

$$\frac{dM}{dt} = KS(C_s - C_t)$$

where  $M$  is the dissolved mass,  $t$  is the dissolution time,  $S$  is the surface area of particles,  $C_s$  is the equilibrium solubility at the temperature,  $C_t$  is the concentration in solution at time and  $K$  is the dissolution rate constant.

This Noyes-Whitney law was developed from the dissolution observation of two different materials dissolving in water by Noyes and Whitney. With this equation, the dissolution could be assumed to be driven by the difference between the concentrations at particle surface which can be regarded as the equilibrium solubility with the concentration in the bulk. Therefore the dissolution process was controlled by the mass transfer from surface of particle to bulk.

Then, the dissolution mathematical model was greatly developed by Brunner and Nernst. With their studies, a relationship between diffusion coefficient and the concentration in bulk was stated. The equation to describe this theory is expressed by Nernst and Brunner [65] as

$$K = \frac{DS}{hv}$$

where  $D$  is the diffusion coefficient,  $h$  is the diffusion layer thickness and  $V$  is the volume of solution.

With this model, Nernst and Brunner stated that the dissolution process could be proposed into two steps. They assumed that the fluid in diffusion layer was stagnant. Furthermore, this theory also assumed that the dissolution process at the surface of particle is much faster than the mass transfer process and a linear concentration gradient happens in the particle surface layer. However, this ideal condition assumption may never achieve because the surface area of particle changes permanently with the dissolution process.

### **2.5.3.1 Statistical models**

#### ***Exploratory data analysis***

This method is used to understand and compare the dissolution data with a controlled dissolution process [66]. The comparison can be achieved with dissolution data in graphical and numerical method. The dissolution data can be plotted for every formulation with one or two error bars at each dissolution time point. Therefore the dissolution data can be summarized numerically and the differences between every dissolution data profile can be compared at each dissolution time point.

#### ***Multivariate approach***

This statistical method is based on the repeated measurements designs where the percent of dissolved is depended with the repeated factor of time. With the repeated measurements, the factors are measured repeatedly with more than two levels.

### **2.5.3.2 Model dependent methods**

These methods are based on different mathematical models which are used to describe the dissolution profiles. Once the appropriate model is determined, the dissolution process and profile are studied depending on the parameters from the

mathematical model. Therefore, the determination of appropriate mathematical model before used is necessary and the common method is the adjust coefficient of determination.

### ***Zero-order model [67]***

Zero-order model assumes that dissolution is independent of concentration in bulk, and only changing with dissolution time. In this way, the application of this model is limited with the only consideration of dissolution proportional to time. This model states that dissolution from particle will not disaggregate and the process is slow. This model is expressed as

$$Q_t = Q_0 + K_0 t$$

where  $Q_t$  is the dissolved amount of particle at time  $t$ ,  $Q_0$  is the initial amount of particle and  $K_0$  is the zero-order dissolution constant.

Yang and Fassihi [68] used this model to describe the dissolution of several types of particles especially for the matrix tablets of low soluble in coated forms.

### ***First-order model [69]***

This method is usually used to describe the adsorption or elimination of solid particles. However, the mechanism of dissolution process with this model is difficult to be conceptualized from a theoretical context. The first order kinetics can be represented as

$$-\frac{dC}{dt} = K_f c$$

where  $K_f$  is the first-order dissolution rate constant.

This equation can be transformed into

$$\log C = \log C_0 - Kt / 2.303 \quad \text{Or} \quad C_t = C_0 e^{-Kt}$$

Silvina and Bravo et al [70] expressed the application of this model for the drug dissolving in porous matrices.

### ***Higuchi model***

This model was firstly expressed by Higuchi [71] for planar, porous and geometrics systems [72] of matrix tablets with water soluble drugs. The assumption of this model can be described that the initial concentration should be higher than solubility, and the diffusion occurs only in one dimension with the constant coefficient in the sink bulk conditions. The model can be expressed as

$$f_t = Q = A\sqrt{D(2C_0 - C_s)C_s t}$$

where  $Q$  is the amount of dissolved particles in area  $A$  at time  $t$ ,  $C_0$  is the initial concentration,  $C_s$  is the solubility of particles and  $D$  is the diffusion coefficient of particle molecules. The common application of this equation is the simplified equation

$$f_t = Q = K_H t^{1/2}$$

where is the  $K_H$  Higuchi dissolution rate constant.

### ***Hixson-Crowell model***

This mathematical model was first expressed by Hixson and Crowell [73] as the regular area of particle is proportional to the cube root of volume. The equation can be described as

$$w_0^{1/3} - w_t^{1/3} = K_h t$$

where  $w_0$  is the initial amount of particle,  $w_t$  is the remaining amount of particle in solution at time  $t$  and  $K_h$  is the Hixson-Crowell dissolution rate constant.

This model is assumed that the surface of tablet is allowed to change with time and its geometrical shape diminished proportionally with time. Hixson and Crowell [74] expressed that the dissolution rate was controlled by the particles dissolution rate rather than the diffusion speed through the diffusion layer.

***Korsmeyer-Peppas model***

This model was expressed by Korsmeyer et al [75] in 1983 as a simple relationship to describe the drug dissolution from a polymeric system.

$$\frac{M_t}{M_\infty} = K t^n$$

where  $\frac{M_t}{M_\infty}$  is the ratio of dissolved drug at time  $t$ ,  $K$  is the dissolution rate constant and  $n$  is the exponent. It is noticed that the value of  $n$  is used to define different dissolution types for cylindrical shaped matrices.

The exponent in this model is represented in Table 2.5 to characterize the mechanism of particles by Riger [76] and Siepmann [77] for tablets.

**Table 2.5.** Exponent of Korsmeyer-Peppas model

Exponent (n)	Dissolution mechanism	Rate as a function of time
0.5	Fickian diffusion	$t^{-0.5}$
$0.45 < n \leq 0.89$	Non-Fickian transport	$t^{n-1}$



0.89	Case II transport	Zero-order model
> 0.89	Super case II transport	$t^{n-1}$

### **Weibull model**

This model is usually used to describe many different dissolution processes and compare the profiles of matrix in drug delivery. Furthermore, other applications are also carried out by previous researchers. Boekel [78] examined this model to study the thermal inactivation of vegetative cells.

The equation was expressed by Weibull which is shown as

$$M = M_0 \left[ 1 - e^{-\frac{(t-T)^b}{a}} \right]$$

where  $M$  is the amount of particle at time  $t$ ,  $M_0$  is the initial amount of particle,  $T$  is the lag time from the measurement result of dissolution process.  $a$  is a scale parameter with time dependence and  $b$  is the shape parameter of dissolution process curve. If  $b=1$ , the shape of dissolution curve corresponds to the shape of an exponential with  $k = 1/a$

$$M = M_0 (1 - e^{-k(t-T)})$$

If  $b$  is bigger than 1, the shape of dissolution curve has sigmoidal with a turning point, but if  $b$  is smaller than 1, the shape has a steeper increase than the shape when  $b$  equals 1.

### **2.5.3.3 Model independent with a difference and similarity factor method**

This method is used to compare the dissolution profiles with a simple model independent with a difference and similarity factor. Costa [79] evaluated the similarity factor to compare two dissolution profiles; Moore and Flanner [80]

expressed the detail of this method and Koester et al [81] investigated the release kinetics of CBZ mixed with  $\beta$ CD from HPMC matrix tablets with this method and mathematical equation. This method is appropriate for the comparison of the dissolution profiles with more than three dissolution time points.

The difference factor can be expressed as

$$f_1 = \left\{ \left[ \sum_{t=1}^n (R_t - T_t) \right] / \left[ \sum_{t=1}^n R_t \right] \right\} \times 100$$

where  $R$  is the dissolution reference batch at time  $t$ ,  $T$  is the dissolution test batch at time  $t$  and  $n$  is the number of time points.

The similarity factor is the measurement of similarity between two percent dissolution curves. The value of this factor is the logarithmic reciprocal square root transformation of the sum of squared error.

#### **2.5.4 Research on Dissolution of Particles**

The research on dissolution of particles can be regarded to be started from Noyes and Whitney in 1897 from the first dissolution experiment. Through their studies [64], the dissolution experiments on benzoic acid and lead chloride were carried out to provide the information of dissolution rate, surface change and the diffusion layer. Brunner [82] expressed his studies to show the dissolution rate related to the surface, temperature and revised the dissolution model to a new equation. Cooperated with Nernst [83], they developed the Brunner-Nernst dissolution equation. Then Hixson and Crowell [74] introduced their studies on dissolution equation to be related to the cubic-root law of weight. All these studies on dissolution can be thought as the expression of dissolution based on the diffusion layer theory. Then from 1950s, Higuchi [62] introduced another dissolution model, interfacial barrier model. And

Danckwert [63] expressed the third dissolution model in his research, Danckwert model.

After the development on dissolution models, the research on dissolution of particles started into the main area of pharmaceutical industry from 1950s. A link between dissolution researches with bioavailability was developed. The bioavailability showed the requirements on dissolution of tablets or capsules. The studies covered the studies on the factors that affected the dissolution rate. Wurster and Polli [84] studied that the dissolution rate was depended on solubility of particles. Levy [85] expressed the studies on the effect of particle size on dissolution rate. Swarbrick and Ma [86] studied the effect of pH on the dissolution of dapsone. Wurster and Taylor [87] expressed the dissolution studies for several particle physical conditions. Mosharraf [88] studied the effect of particle size and shape on the dissolution rate of micro-sized drugs. Hintz [89] studied the relationship between particle size distributions with the theoretical dissolution rate of a polydisperse powder by a computer simulation method. Haverkamp [90] studied the dissolution behaviors of alumina powder in cryolite that showed a relationship between the dissolution rate and temperature and stirring speed Niebergall [91] investigated the dissolution kinetics of three different compounds under different stirring speeds and they found that the dissolution rate was affected significantly by the flow velocity and surface dimension size in opposition.

## **2.6 Conclusions of Literature Review**

According to the literature review, the aspects related to the topic of this thesis are described and summarized systematically including the knowledge of particle size, shape, and internal structure, solubility of particles, diffusion and dissolution.

Linked to the research contents in this thesis, the shape of particles is determined by the two-dimensional image analysis and the size is measured by the measurement method for the particles with regular shape including spherical and cylindrical shape. To determine the internal structure of particles used in this thesis, the recommended measurement methods are SEM due to my research feasibility of the measurement equipment and the better measurement duration and quality with SEM. Applied into my experimental work in this thesis, the dissolution process is well understood theoretically with the diffusion layer theory and the explanation of the dissolution process is related to the properties of solubility and diffusion of particles. The dissolution process and kinetics can be quantified by several mathematical models, therefore the selection of appropriate mathematical model is necessary before quantification.

## **CHAPTER 3. DISSOLUTION OF SINGLE SPHERICAL SODIUM CARBONATE PARTICLE**

### **3.1 Introduction**

In this chapter, the work aims to investigate the dissolution process and quantify the dissolution kinetics of single spherical sodium carbonate particle under the conditions of temperature and pH. The spherical sodium carbonate particles are prepared through few steps before the dissolution experiment that are expressed in the section of methodology. The structure of spherical sodium carbonate particles are tested by SEM, and the surface and porosity information are test by BET. The dissolution experiments are carried out under different temperature and pH. In this way, the dissolution process and dissolution kinetics can be linked with temperature and pH. The effects of temperature and pH are therefore determined by quantifiing on the dissolution rate and dissolution rate constant.

To test the dissolution process of particles, the common method is to carry out the dissolution experiments by using U.S. Pharmacopeia (USP) dissolution apparatus [92]. However, because the size of one sodium carbonate particle is quite small with the range of millimetres, the normal dissolution apparatus measurements are not apply in my work. In this scenario, the dissolution experiments in my work are developed to analyse the dissolution process of single sodium carbonate particle by using high speed camera as test tool.

### **3.2 Experimental Methodology**

Sodium carbonate particles used in this work are provided by Procter & Gamble Newcastle Innovation Center. It is anhydrous sodium carbonate with the purity of 99.9%. GCAS of sodium carbonate particles is 10092603NM-014.

To identify and confirm the compound of sodium carbonate particles used in this work, the measurement with X-ray diffraction facility is carried out. The X-ray diffraction facility used in this work is P'Analytical XPert MPD with data analysis suit of Xpert Highscore Plus. With XRD measurement, the patterns are compared with ICDD PDF2/PDF4 reference databases shown in Figure 3.1. According to the results in Figure 3.1, the compound of particles used in this work is identified as anhydrous sodium carbonate with a very small amount of sodium carbonate hydrate. The chemical formula of anhydrous sodium carbonate is  $\text{Na}_2\text{CO}_3$  according to the reference database with the reference code of 05-001-0022. The chemical formula of sodium carbonate hydrate is  $\text{Na}_2\text{CO}_3 \cdot \text{H}_2\text{O}$  according to the reference database with the reference code of 00-008-0448.

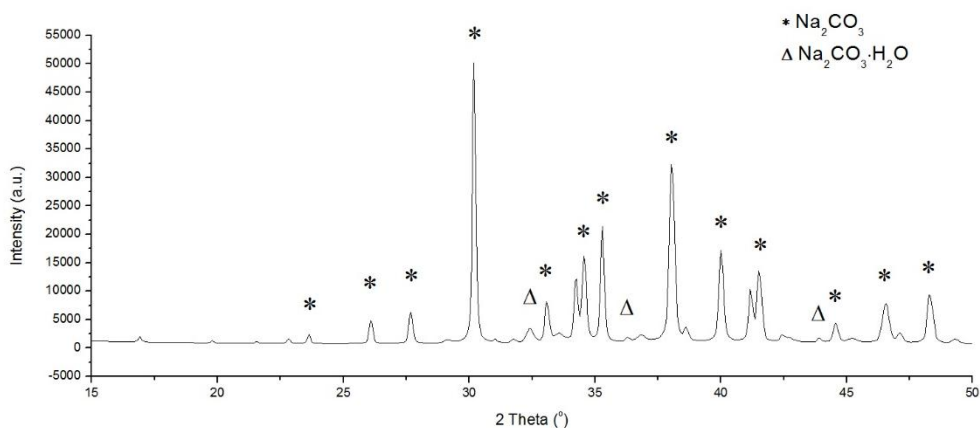


**Figure 3.1** XRD patterns of  $\text{Na}_2\text{CO}_3$  and  $\text{Na}_2\text{CO}_3 \cdot \text{H}_2\text{O}$

The sodium carbonate particles are pre-prepared before dissolution experiments and the characteristics of sodium carbonate particles used in this work are measured as following method shown in Figure 3.2.

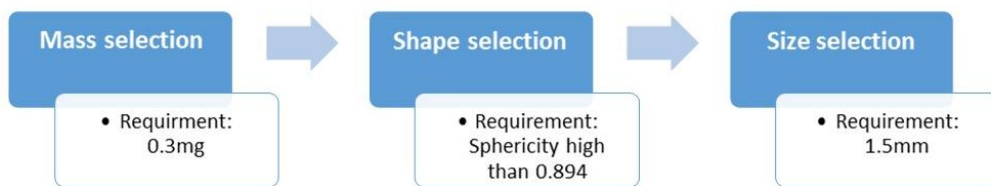


**Figure 3.2** Pre-preparation scheme of single sodium carbonate particle

Specifically speaking, the weight of one single sodium carbonate particle is measured firstly and only the particles with the same weight of 0.3mg are selected into next preparation. Then the shape of these sodium carbonate particles with same weight is measured and determined with imaging analysis method. With the classification scheme shown in literature review by Reily to definite spherical sodium carbonate particles, sphericity is the most important index to be examined and determined with the calculation of sphericity of measured particles. For the so called spherical sodium carbonate particles used in this work, only the particles with sphericity higher than 0.894 are used as spherical sodium carbonate particles. In this way, these sodium carbonate particles with same weight are measured with 2D microscopy measurement method by Nikon Eclipse Ti which is shown in Figure 3.3.

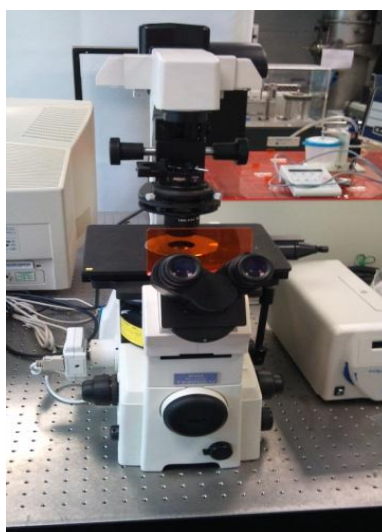


**Figure 3.3** Nikon Eclipse Ti Microscopy

The sphericity that is measured as the ratio of diameter of a circle with the same area as the particle to the diameter of the smallest circumscribed circle of measured particles are determined. Only for the measured particles with the sphericity higher than 0.894 are selected as the spherical particles. Next, the diameter of these spherical particles with the same weight is also measured by imaging analysis method with the same microscopy. With the images from microscopy, only the spherical particle with the same diameter of 1.5mm that is measured as the projection diameter from microscopy image is finally selected and used into dissolution experiment. In this way, the spherical sodium carbonate particles used in this work can be determined with the same weight of 0.3mg and the same diameter of 1.5mm. One example of final selected single spherical sodium carbonate particle from microscopy image is shown in Figure 3.4. This capture of this example of single spherical sodium carbonate particle is shot by Nikon Eclipse Ti Microscope with the lens of CFI 10X and the resolution can reach to 1 $\mu$ m.

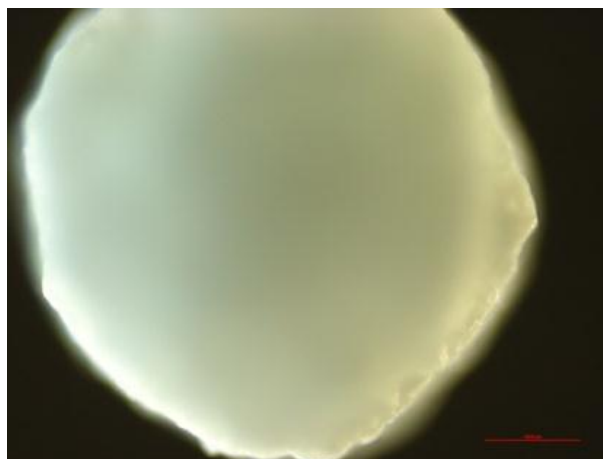


**Figure 3.4** Capture of Single spherical sodium carbonate particle used in dissolution experiments with Nikon Eclipse Ti Microscope.

To measure and quantify the dissolution process of one single spherical sodium carbonate particle at different conditions, a novel high speed image analysis method is developed and applied by using high speed camera to record the dissolution



process of one single spherical sodium carbonate particles. A typical dissolution experiment process scheme is shown in Figure 3.5.

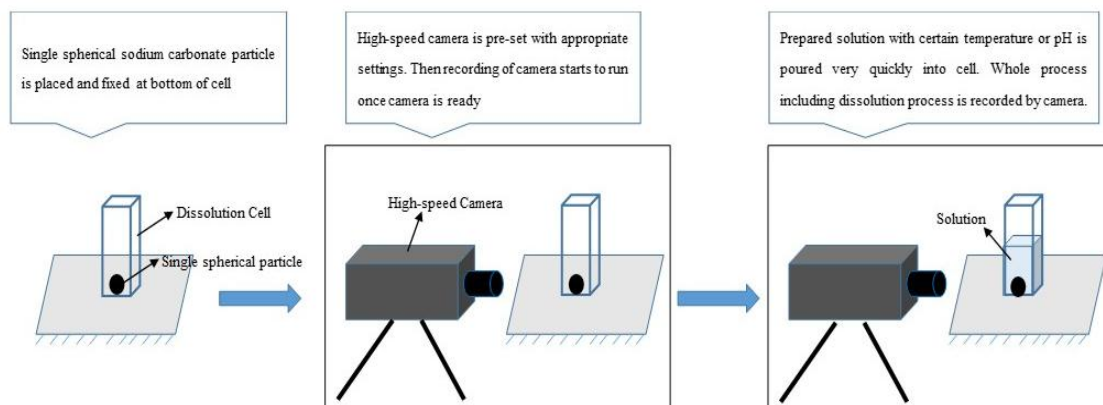


**Figure 3.5** A typical dissolution experiment process scheme for single spherical sodium carbonate particle.

With this method, one single particle is carefully placed and fixed at the bottom of a transparent 12mm square glass cell for each case. The transparent 12mm square glass cells used in this work are 12mm Glass cell (PCS1115) bought from Malvern. Once the high-speed camera of Photron Fastcam SA5 is well pre-set with recording frames of 50 fps and starts to record, the cell is immediately filled with 0.2ml distilled water. With the recording from high speed camera, the whole dissolution process of this particle from the beginning of particle contacting with water to the end of dissolution when this spherical particle disappears in this camera is completely recorded. The resolution of dissolution process images recorded by high speed camera is 640 x 640 with FPS of 50.

With the analysis of this recorded dissolution process, the diameter of this spherical sodium carbonate particle can be determined and measured as function of time. With the assumption of dissolution process, the density of one particle keeps as a constant and the diameter of measured particle only diminishes as function of time.

In this way, the weight of undissolved particle can be calculated. And then the dissolution process is determined and quantified into the dissolution profile.

The dissolution experiments are carried out at different temperatures of 30°C, 40°C, 50°C, 60°C and 70°C, and pH of 4, 7, 8, 9 and 10. Before every specific dissolution experiment starts, the distilled water is prepared before filled into cell to contain the certain condition. For the dissolution experiments at different temperatures, the distilled water is pre-heated to reach the specific temperature and then filled into the cell. Because the dissolution process is very short, the loss of temperature during the dissolution process can be minimized. For the dissolution experiments under different pH, the distilled water is prepared using standard pH buffers to reach the specific pH condition. The standard pH buffer solutions used in this work is the PHA-4 and PHA-10 solutions from OMEGA. For the conditions of pH 4 and 10, the pH buffer solutions are used directly as filling into the cell. For the conditions of other pH, the buffer solutions are blended with distilled water to reach the required pH. Then the solution with prepared pH is then filled into the cell.

### **3.3 Mathematical Model**

With the measured dissolution data of each case, the dissolution kinetics can be quantified with the shrinking sphere model applied for spherical particles. Shrinking sphere model [93] introduces that the dissolution rate is proportional to the surface area of particle. It takes into account the dissolution process and behaviours at the surface of particle as the driving force instead of mass transport controlled. Although the material particle may be porous, it also assumes that there is no exchange of electrolyte from pores into bulk electrolyte.

With this shrinking sphere model, the dissolution rate can be presented as

$$\frac{dC}{dt}V = KA \quad (1)$$

where  $K$  is the rate constant,  $A$  is the surface area of spherical particle,  $C$  is the concentration of dissolved sodium carbonate in bulk.

The surface area of spherical sodium carbonate particle decreases with the undissolved weight of particle by the equation that

$$A = A_0 \left( \frac{M}{M_0} \right)^{2/3} \quad (2)$$

where  $A_0$  is the initial surface area of granule,  $M_0$  is the initial mass of particle and  $M$  is the amount of undissolved particle.

The undissolved weight of particle can be related to the concentration of sodium carbonate in bulk by the equation that

$$M = M_0 - (C - C_0)V \quad (3)$$

where  $C_0$  is the initial concentration of sodium carbonate in bulk which equals to 0 in this study and  $V$  is the volume of distilled water used as solvent.

The surface area can be related to the weight of particle if equation (2) and (3) are combined, so equation (1) can be transformed as

$$\frac{dC}{dt}V = KA_0 \left( 1 - \frac{V}{M_0}C \right)^{2/3} \quad (4)$$

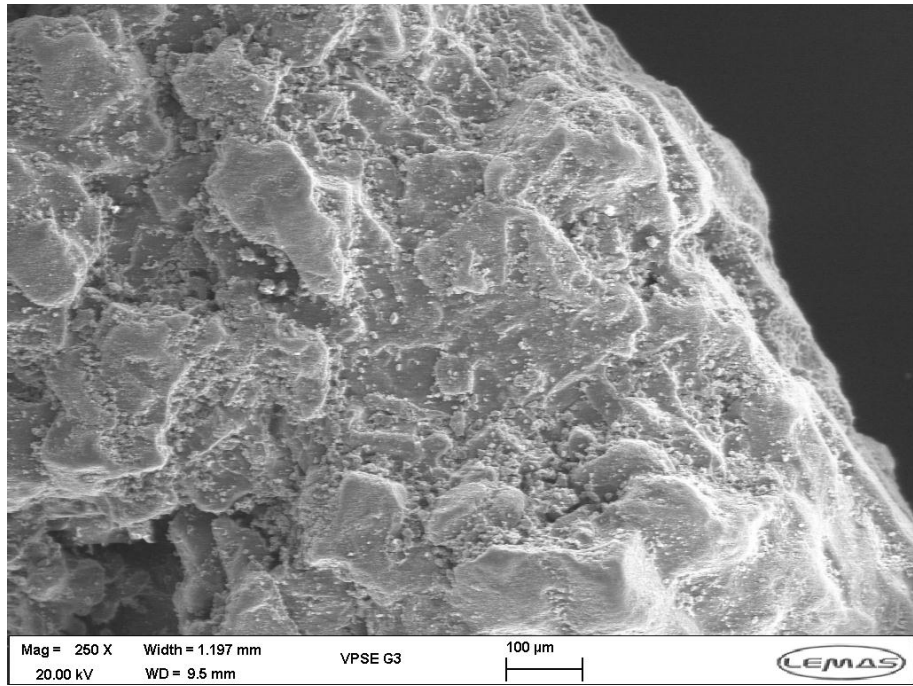
After rearranging and integrating equation (4) with the integration constant when  $t = 0$  and  $C = 0$ , the final equation of shrinking sphere model should be stated as

$$C = \frac{M_0}{V} \left[ 1 + \left( \frac{A_0}{3M_0} Kt - 1 \right)^3 \right] \quad (5)$$

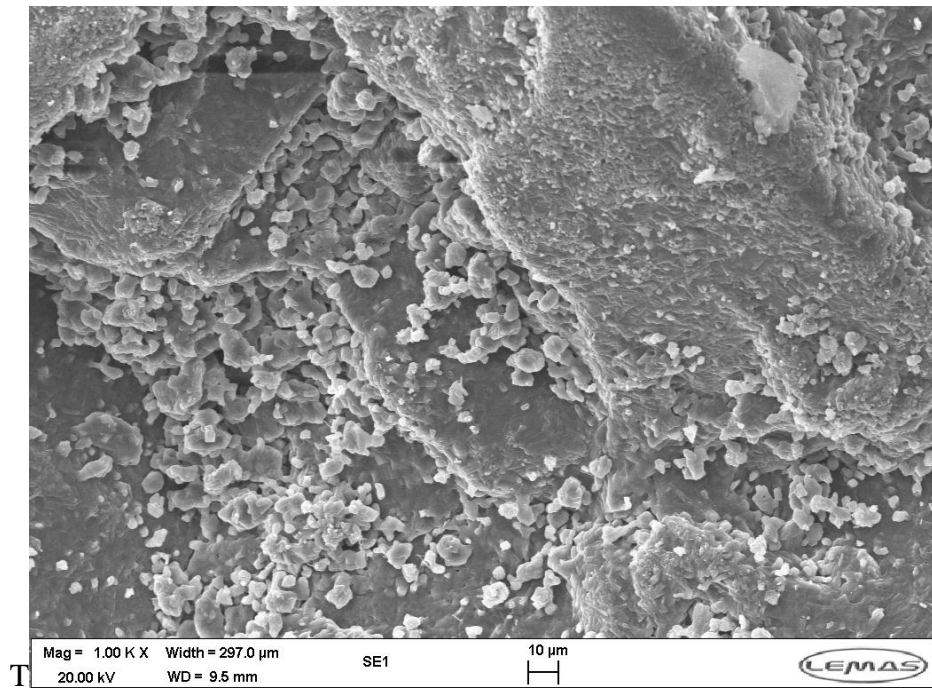
### 3.4 Results and Discussions

According to shrinking sphere mathematical model used in this work, the dissolution mechanism can be described as the dissolution reactions occurring at the surface of smooth sphere during the whole dissolution process. In this way, when the dissolving spherical particle contacts with water, the wetting and penetration process happens rapidly. As the penetration continues happening, small pieces of agglomerations disintegrate from the particle into bulk. At the same time, dissolution of sodium carbonate into irons happens at both small pieces of agglomerations and the surface of particle. This process from penetration to dissolution continually happens until the whole particle has dissolved to be solute irons into bulk.

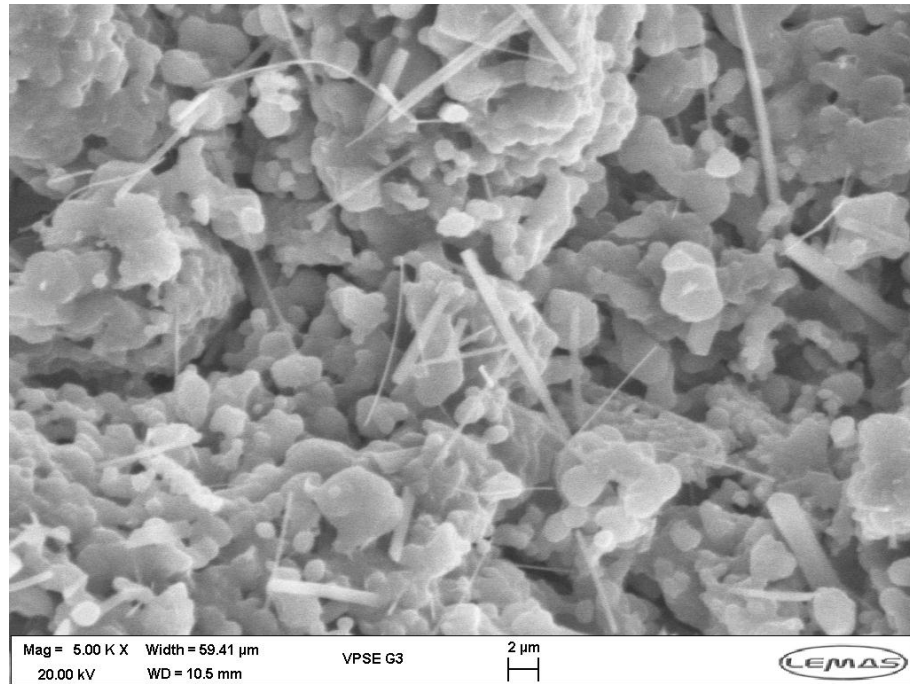
The experimental samples of sodium carbonate particles are tested by SEM and BET before the dissolution experiments. The SEM measurement for sodium carbonate particles are achieved with Camscan CS44 SEM with EDX and Cathodoluminescence facilities. The resolution of SEM used in this work can reach to 3.0nm at high vacuum mode. The SEM test images of one sodium carbonate particle is shown in Figure 3.6. It is clearly shown that the one sodium carbonate particle can be regarded as the agglomerate by many pieces with shapes of tubular-like and columnar-like. The size of these pieces is between 2 $\mu$ m to 20 $\mu$ m.



(a)



(b)



(c)

**Figure 3.6.** SEM images of one single Sodium carbonate particle with zoom-in scale of (a) 100μm, (b) 10μm, (c) 2μm.

The spherical sodium carbonate particles used in this work are test by BET to examine surface characterisation with both BET and BJH methods. BET test is carried out with Quantachrome Autosorb-1, the facility of automatic gas and vapour adsorption apparatus chemisorption. The test results are analysed with microporemodel by DFT software. The results of BET test for sodium carbonate particles of adsorption and desorption isotherm log plot is shown in Figure 3.7. The results of BET surface area plot is shown in Figure 3.8. The results of BET isotherm plot are shown in Figure 3.9. The results data of surface characteristics are shown in Figure 3.10. Based on results shown in Figure 3.10, the BET surface area is 0.2729 m<sup>2</sup>/g, the average micropore area of particles used in this work is 0.00484 m<sup>2</sup>/g. The total pore volume of pores is 0.000553 cm<sup>3</sup>/g and the average pore width is 8.10 nm.

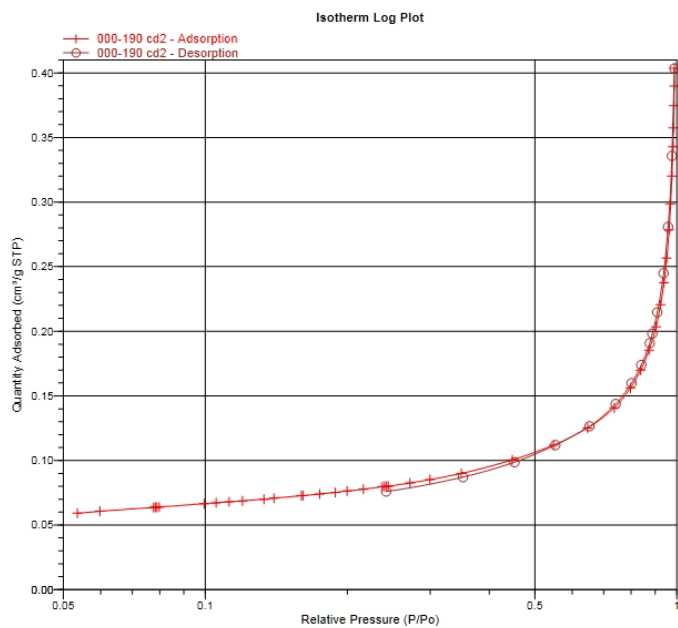


**Figure 3.7** Adsorption and desorption isotherm log plot of sodium carbonate particles

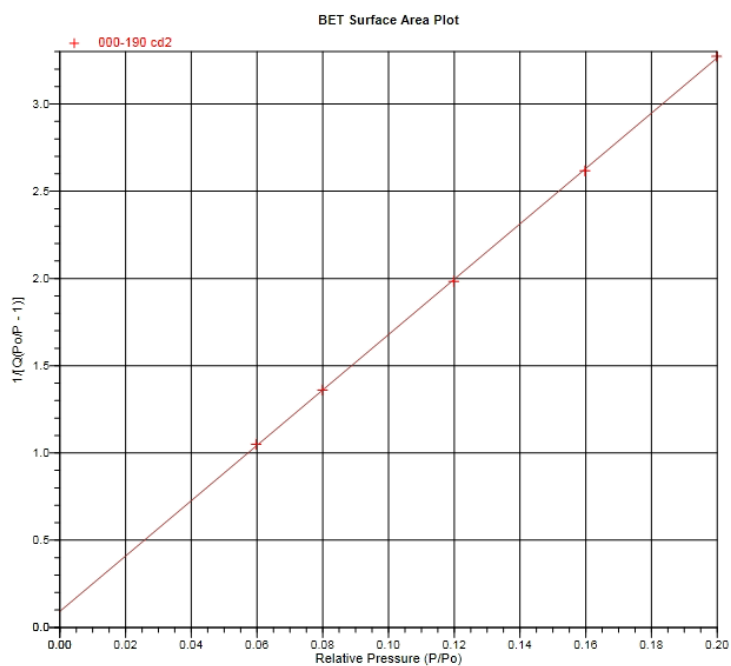


**Figure 3.8** BET surface area plot of sodium carbonate particles

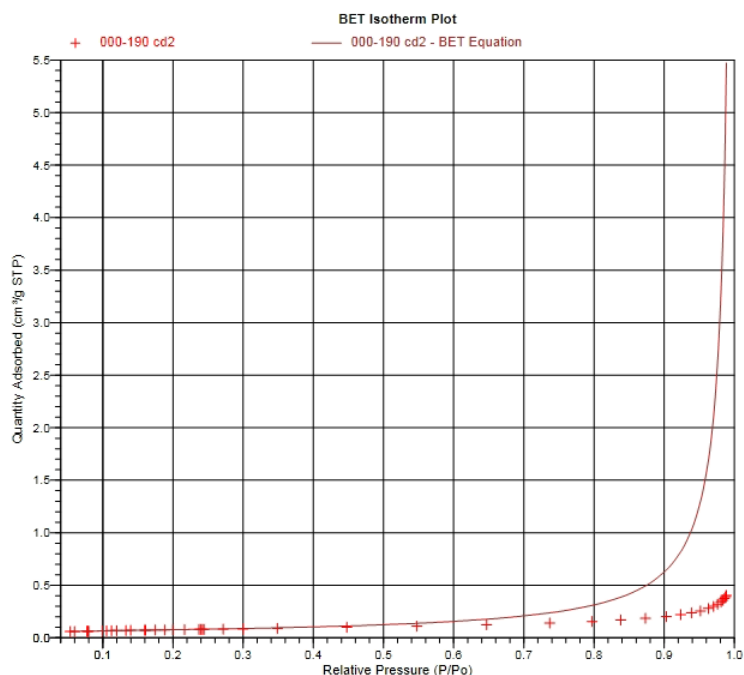


**Figure 3.9** BET isotherm plot of sodium carbonate particles

**Summary Report**

**Surface Area**

Single point surface area at  $P/P_o = 0.199775778$ : 0.2658 m<sup>2</sup>/g

BET Surface Area: 0.2729 m<sup>2</sup>/g

Langmuir Surface Area: 0.3732 m<sup>2</sup>/g

t-Plot Micropore Area: 0.0484 m<sup>2</sup>/g

t-Plot External Surface Area: 0.2246 m<sup>2</sup>/g

BJH Adsorption cumulative surface area of pores  
between 1.7000 nm and 300.0000 nm diameter: 0.1981 m<sup>2</sup>/g

BJH Desorption cumulative surface area of pores  
between 1.7000 nm and 300.0000 nm diameter: 0.2156 m<sup>2</sup>/g

**Pore Volume**

Single point adsorption total pore volume of pores  
less than 118.2576 nm diameter at  $P/P_o = 0.983352843$ : 0.000553 cm<sup>3</sup>/g

t-Plot micropore volume: 0.000020 cm<sup>3</sup>/g

BJH Adsorption cumulative volume of pores  
between 1.7000 nm and 300.0000 nm diameter: 0.000595 cm<sup>3</sup>/g

BJH Desorption cumulative volume of pores  
between 1.7000 nm and 300.0000 nm diameter: 0.000610 cm<sup>3</sup>/g

**Pore Size**

Adsorption average pore width (4V/A by BET): 8.10510 nm

BJH Adsorption average pore diameter (4V/A): 12.0216 nm

BJH Desorption average pore diameter (4V/A): 11.3178 nm

**Figure 3.10** BET test report of sodium carbonate particles

Based on IUPAC pore size classification scheme [94], micropores are the pores



with the width lower than 2nm, mesopores are the pores with the width lower between 2nm and 50nm, and macropores are the pores with the width higher than 50nm. In this way, the sodium carbonate particles used in this work are porous with mesopores. The surface properties and pores result to the highly exist of penetration of water into particle at the beginning of contacting water.

The dissolution process of each particle is recorded by the high-speed camera under different temperatures and pH. Therefore it has a clearly visual notion about the dissolution process and also the diminishing of the diameter of particle as the function of time. Through analysing the dissolution images and measuring diameter of particle at different dissolution time, the diameter of particle can be plotted versus dissolution time to show the trend of diameter diminishing. And because following the dissolution theories of diffusion layer model and the mathematical model, the shape and density of particle keep as constant during the dissolution process. Thus the remaining amount of sodium carbonate particle can be calculated and plotted versus dissolution time.

It is worth noting that the small bubbles overflow from the surface of the particle from the start of contacting with water to the end of dissolution by observation from dissolution video. That means the penetration of water into particle happens from the beginning when the particle contacts water, and still persist during the whole dissolution process because of the structure property of sample as the porous particles that are shown from SEM images.

For a typical dissolution experiment of single sodium carbonate particle, the analysis and treatment of measured data are carried out with following method. With the measurement of high speed camera, the dissolution process of one single

spherical sodium carbonate under certain solution condition is recorded per frame. Therefore, the status of the particle at different time can be determined with the recorded dissolution images. For example, a dissolution process of one spherical sodium carbonate particle under 30°C is shown in Figure 3.11.

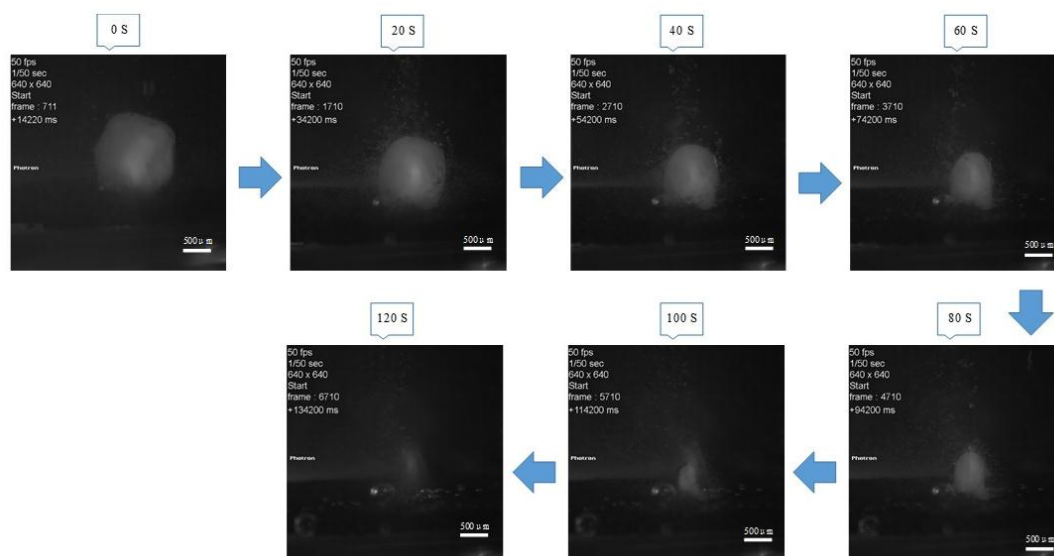


**Figure 3.11** A dissolution process of one single sodium carbonate particle under 30°C from high speed camera

With the dissolution images of particle under certain solution condition, the diameter of this particle is measured with scale bar at different time. In this work, the diameter of particle is determined as the diameter of the minimal circle that can contain the whole particle. For example, the measurements of diameter of one particle under 30°C is shown in Figure 3.12.

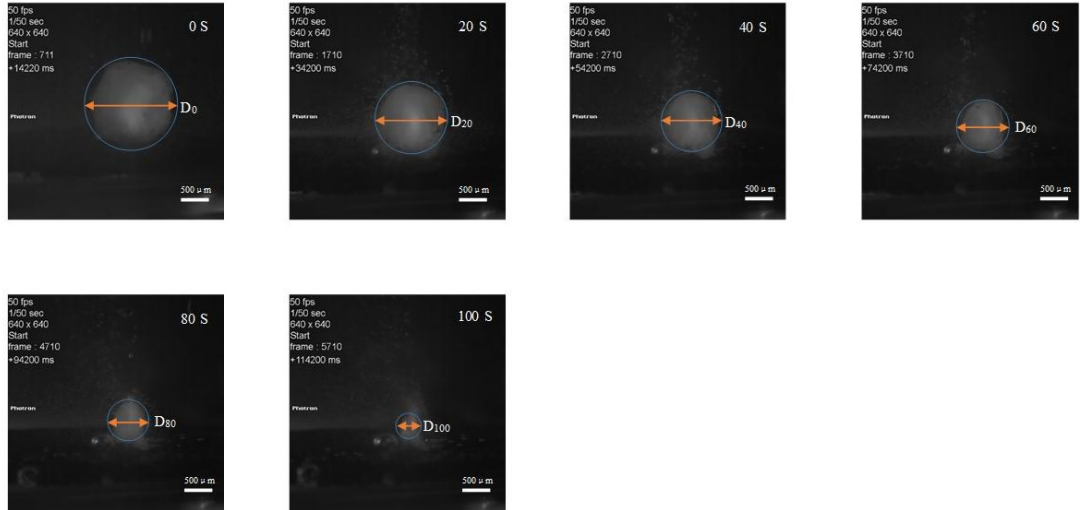


**Figure 3.12** Measurement of particle diameter under 30°C at different time

With the measurement method shown in Figure 3.12, the diameter of particle under 30°C as function of every 10 second can be determined and shown in Table 3.1.

**Table 3.1** Diameter of sodium carbonate particle as function of dissolution time under 30°C

Dissolution time (S)	Diameter of particle (mm)	Dissolution time (S)	Diameter of particle (mm)
0	1.5	70	0.82
10	1.35	80	0.7
20	1.27	90	0.56
30	1.15	100	0.48
40	1.05	110	0.33
50	0.97	120	0
60	0.9		

With the diameter shown in Table 3.1, the remaining amount of sodium carbonate particle and the concentration of dissolved sodium carbonate particle in solution can be calculated with the assumption that the density of particle will not change during dissolution process. Therefore, the remaining amount of undissolved sodium carbonate particle can be calculated with the equation below and shown in Table 3.2

$$M_t = M_0 \left( \frac{D_t}{D_0} \right)^3$$

**Table 3.2** Remaining amount of undissolved sodium carbonate as function of time

Dissolution time (S)	Remaining amount (mg)	Dissolution time (S)	Remaining amount (mm)
0	0.3	70	0.0490
10	0.2187	80	0.0305
20	0.1821	90	0.0156
30	0.2352	100	0.0098
40	0.1029	110	0.0032
50	0.0811	120	0
60	0.0648		

Based on the calculated remaining amount of undissolved sodium carbonate, the concentration of dissolved sodium carbonate in solution under 30°C as function of dissolution time is determined and shown in Table 3.3.

**Table 3.3** Concentration of sodium carbonate in solution as function of time under 30°C

Dissolution time (S)	Concentration (mg/ml)	Dissolution time (S)	Concentration (mg/ml)
0	0	70	1.255
10	0.407	80	1.348
20	0.590	90	1.422
30	0.824	100	1.451
40	0.986	110	1.484
50	1.094	120	1.5
60	1.176		

With the concentration shown in Table 3.3, the dissolution rate constant can be fitted with Equation (5). The measured data from dissolution experiment shown in Table 3.3 is fitted with Equation (5), and the fitting result is the value of dissolution rate constant for the dissolution under 30°C. The fitting result of measured dissolution data with Equation (5) is shown in Figure 3.13.

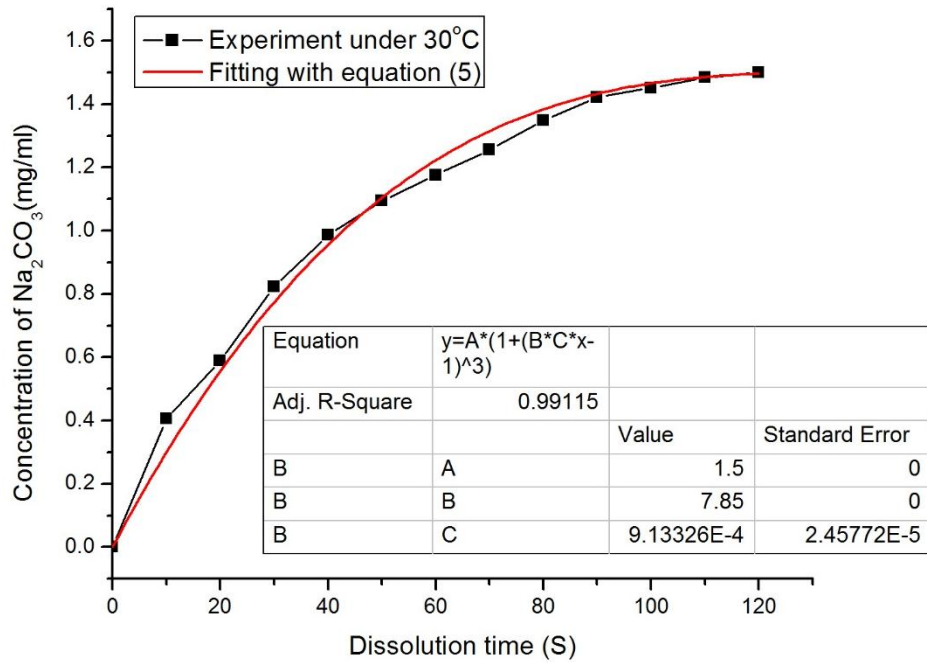


**Figure 3.13** Fitting of measured concentration of sodium carbonate under 30oC with Equation (5)

According to the fitting result shown in Figure 3.13, the dissolution rate constant of single sodium carbonate particle under 30°C is determined as **0.000913** (mg/S/mm<sup>2</sup>).

Following the same data analysis method shown above with the example of 30°C, the dissolution kinetics of single sodium carbonate particle under different temperatures and pH can be analysed and shown below.

The diameter of sodium carbonate particle as function of dissolution time under different temperature and pH based on the measurement of dissolution experiments is shown in Figure 3.14 and 3.15.

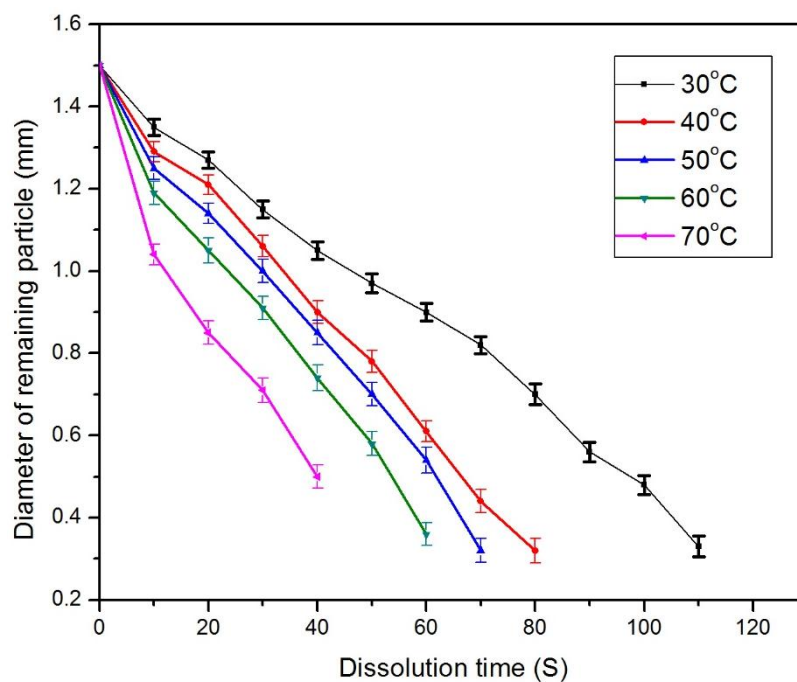


**Figure 3.14** Diameter of single sodium carbonate particle as function of time under different temperature

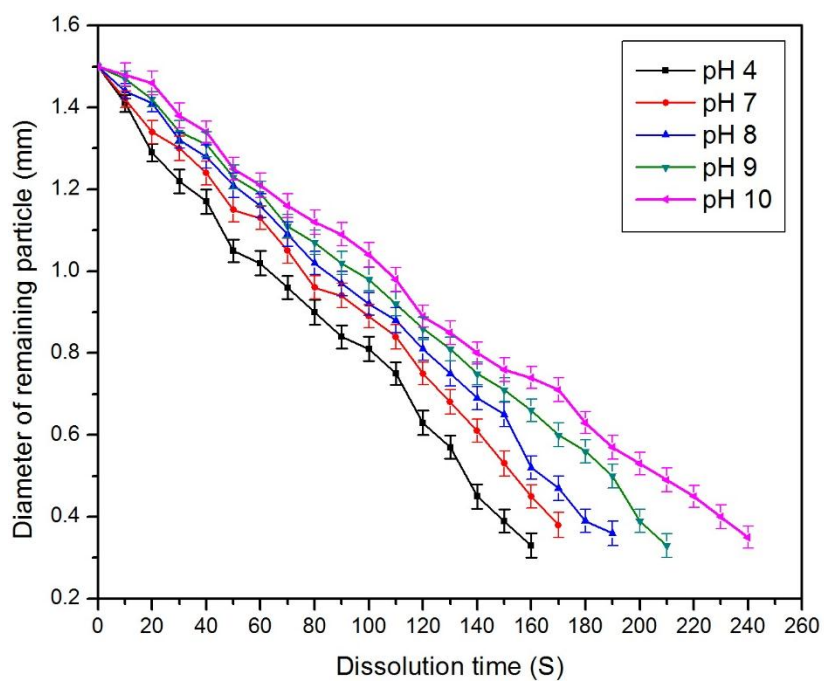


**Figure 3.15** Diameter of single sodium carbonate particle as function of time under different pH

The concentration of dissolved sodium carbonate under different temperature and pH as function of dissolution time is shown in Figure 3.16 and Figure 3.17.

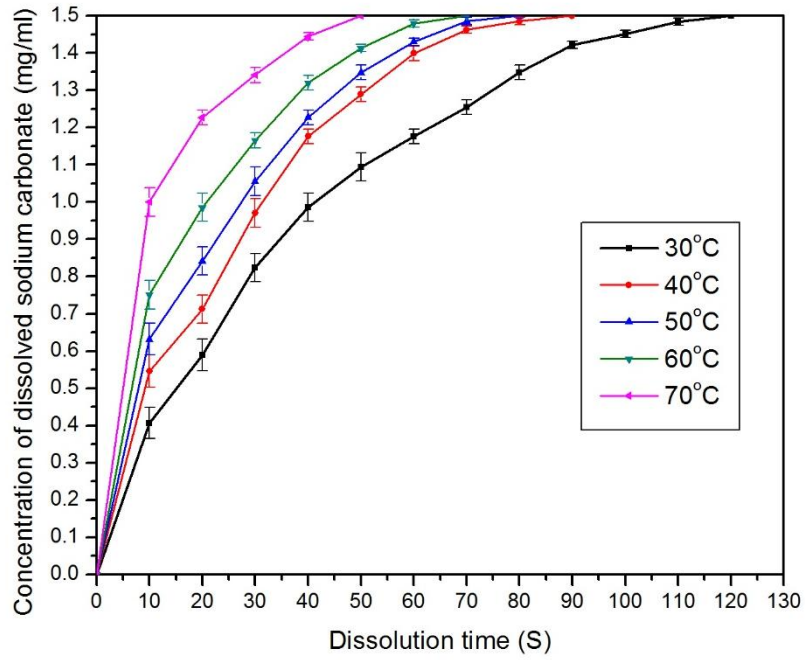


**Figure 3.16** Concentration of dissolved sodium carbonate as function of dissolution time under different temperature

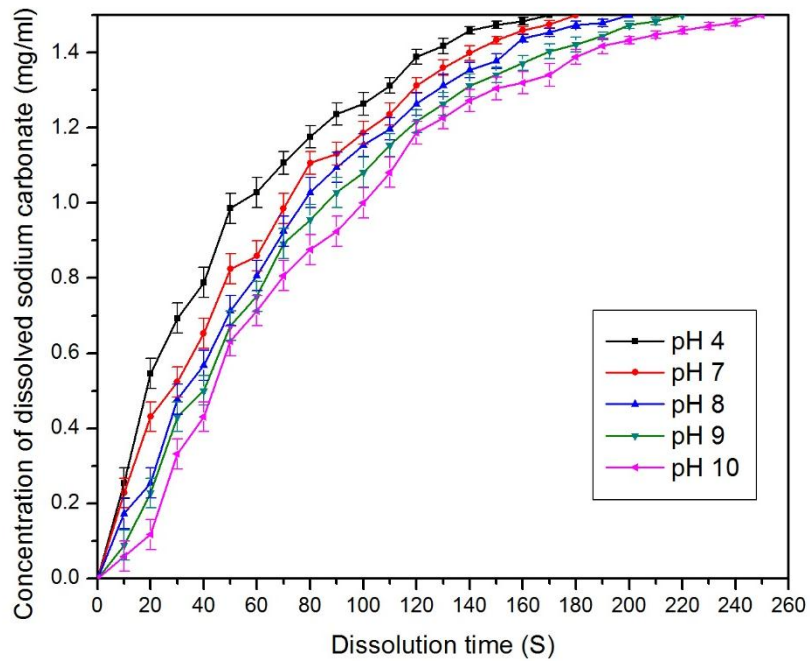
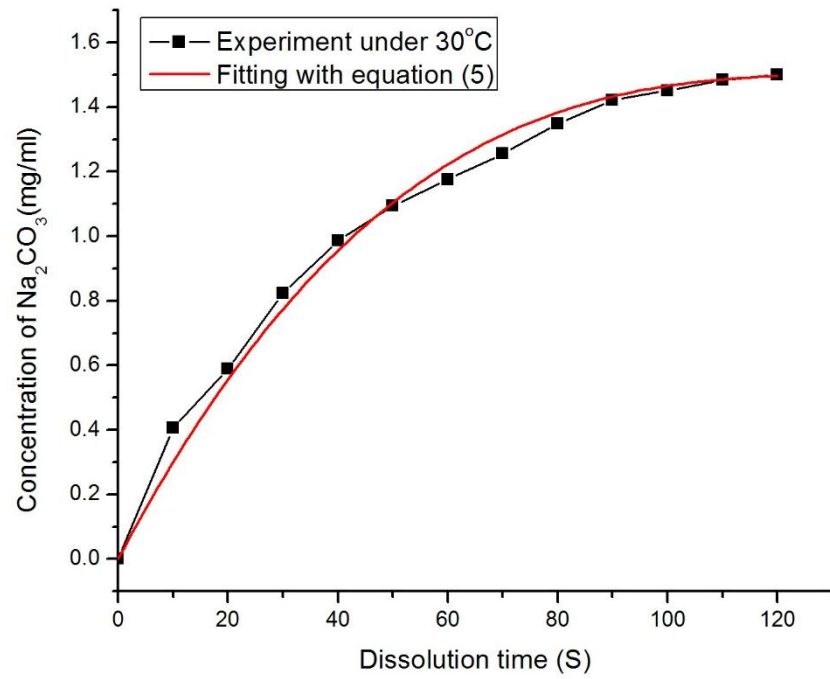


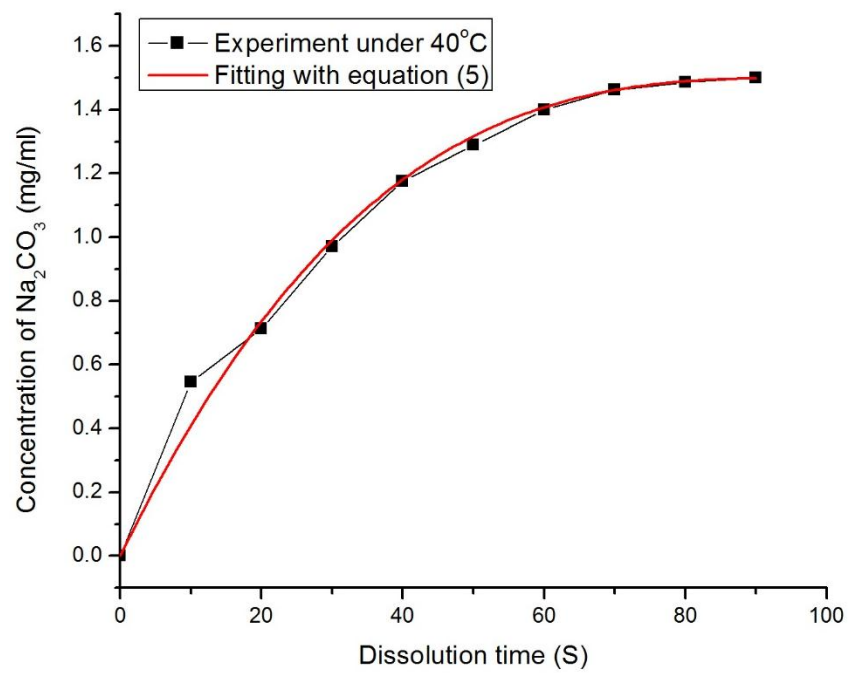
**Figure 3.17** Concentration of dissolved sodium carbonate as function of dissolution time under different pH

Based on the concentration of dissolved sodium carbonate under different temperature and pH shown in Figure 3.16 and Figure 3.17, the dissolution rate constant for each case can be fitted with Equation (5) with the same fitting method of the example shown in Figure 3.13. In this way, the fitting results with Equation (5)

under each solution condition are shown in Figure 3.18 and Figure 3.19.

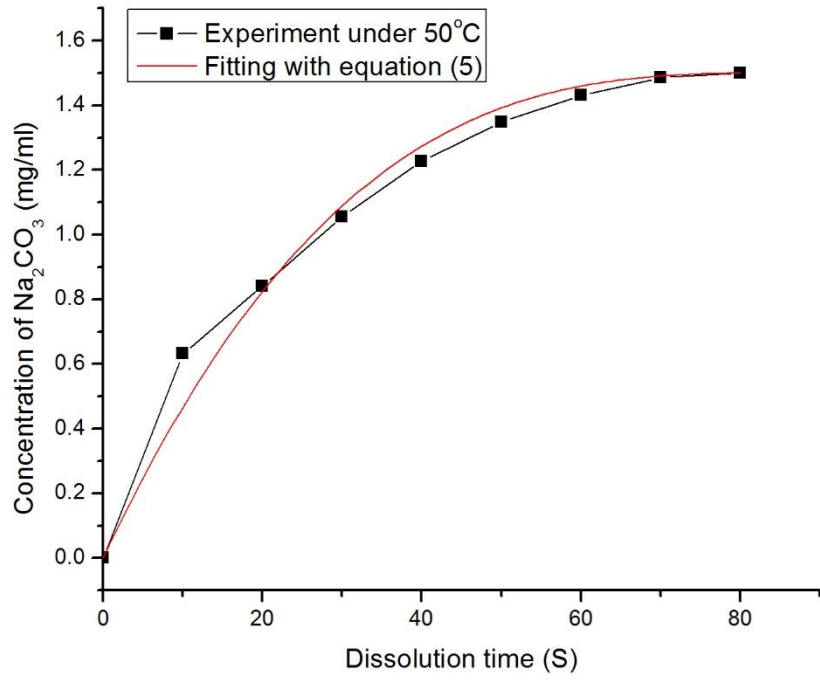


(a)

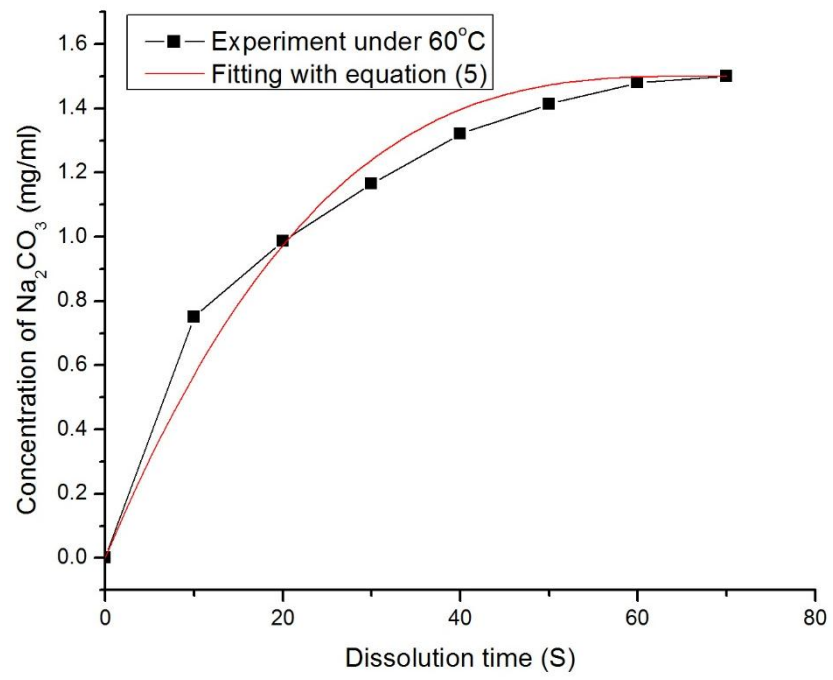


(b)

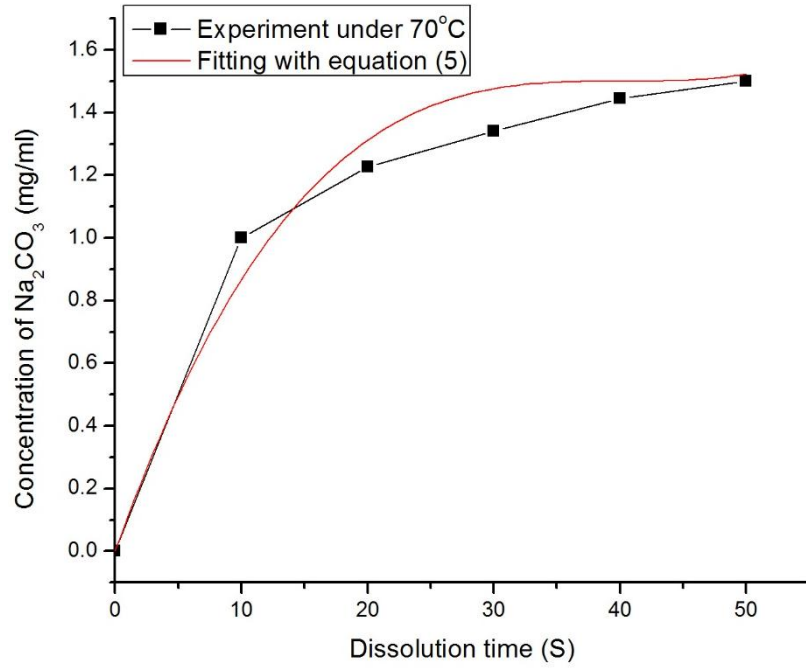




(c)

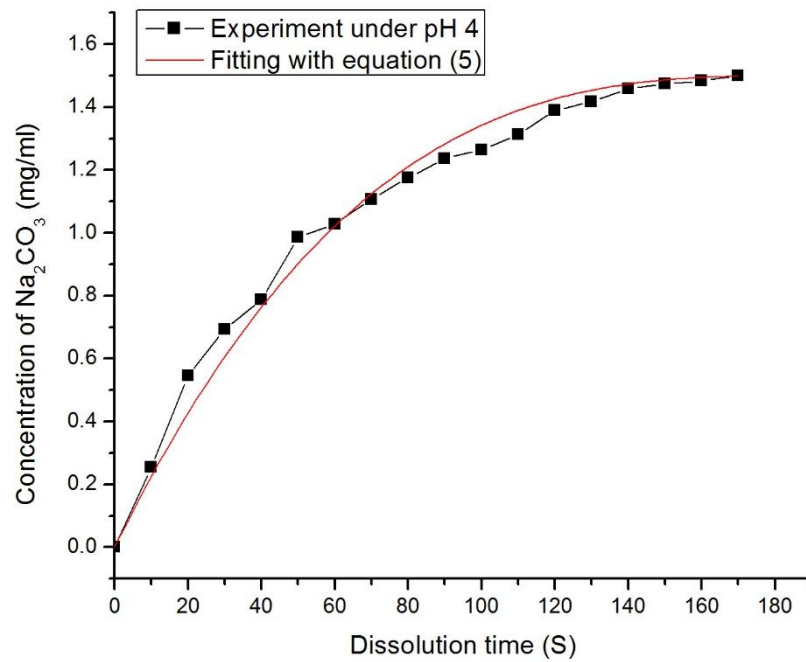


(d)

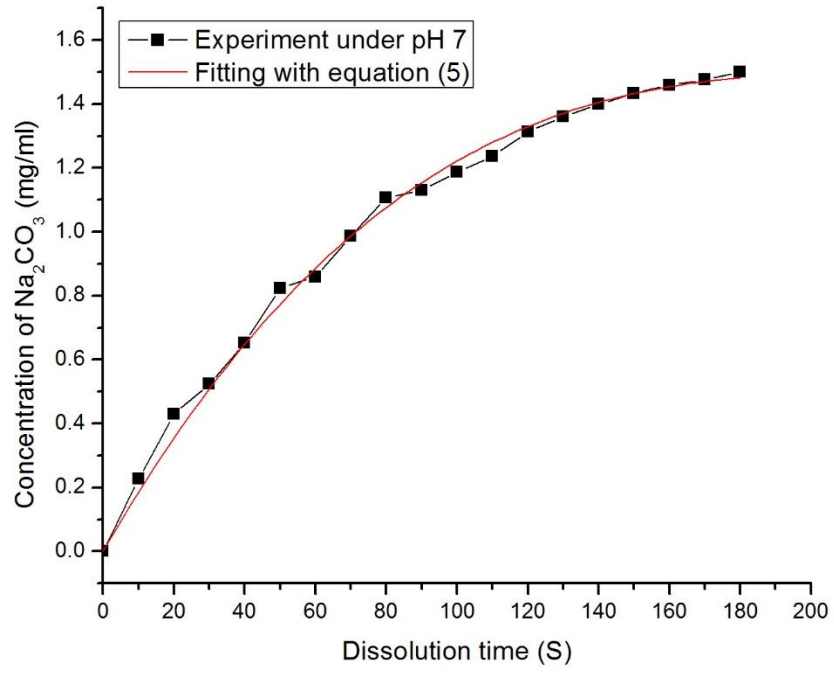


(e)

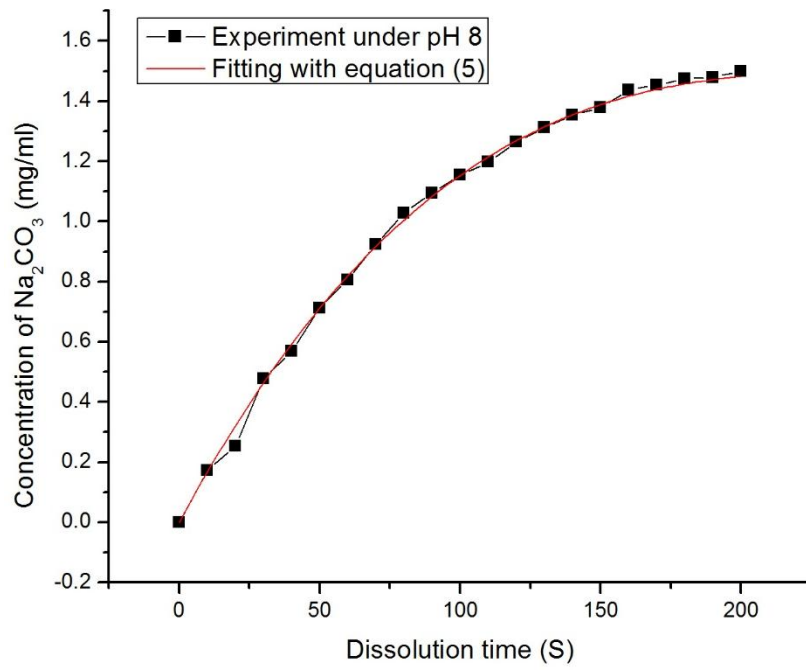
**Figure 3.18** Fitting of measured experiment concentration with equation (5) under (a) 30°C; (b) 40°C; (c) 50°C; (d) 60°C; (e) 70°C



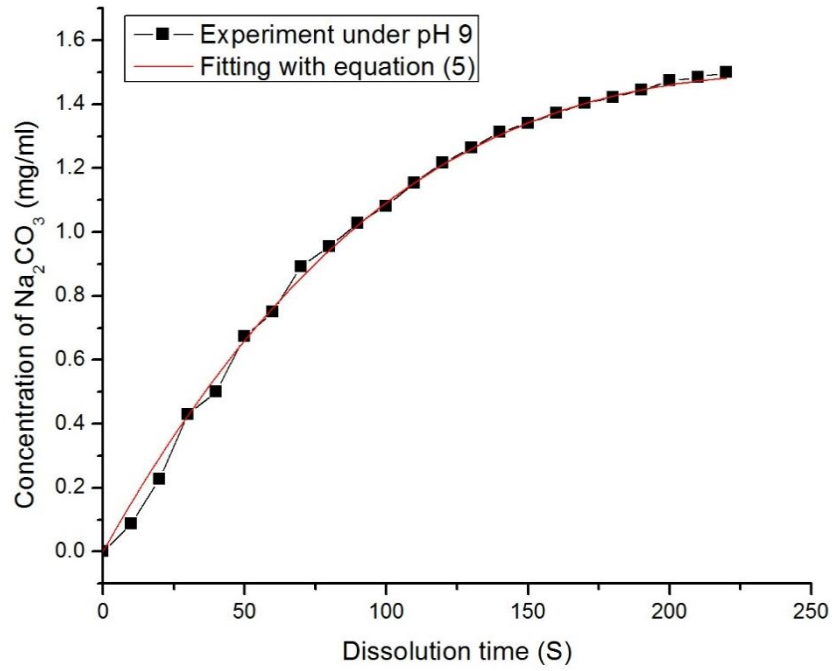
(a)



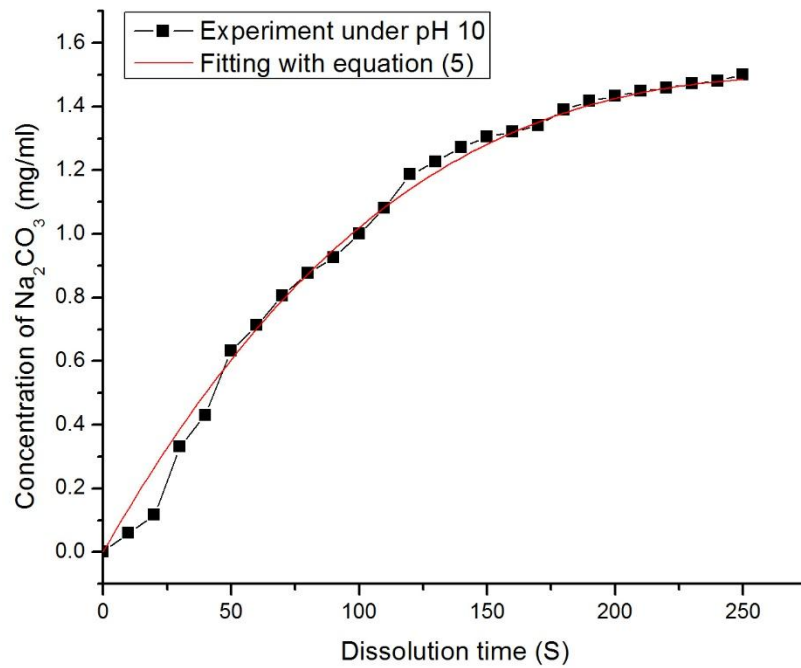
(b)



(c)



(d)



(e)

**Figure 3.19** Fitting of measured experiment concentration with equation (5) under (a) pH 4; (b) pH 7; (c) pH 8; (d) pH 9; (e) pH 10

With the fitting results shown in Figure 3.18 and Figure 3.19, the dissolution rate constant of single sodium carbonate particle under different temperature and pH are determined. The rate constant for different temperature and pH are shown in Figure

3.20 and Figure 3.21.

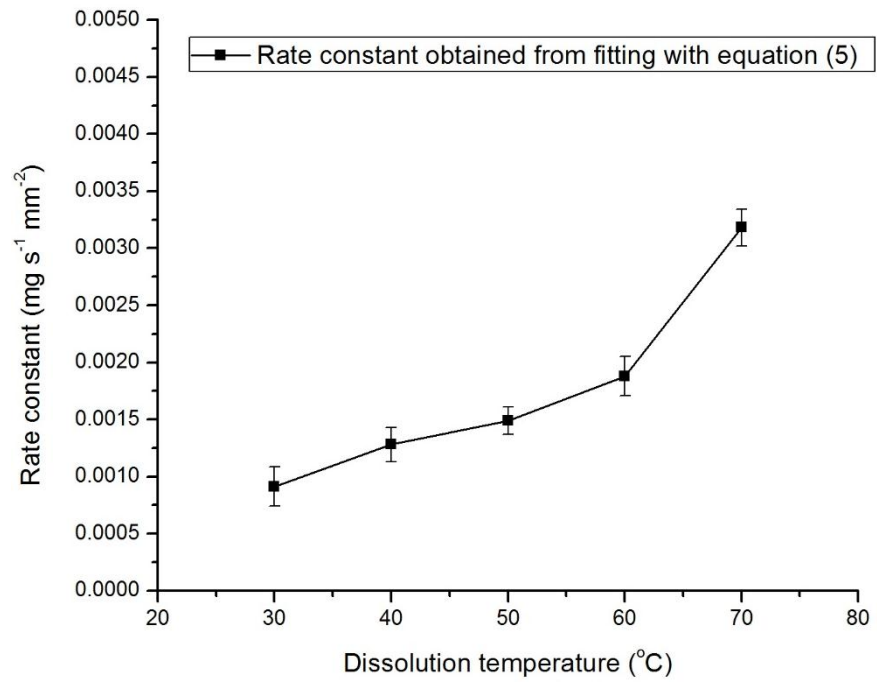


**Figure 3.20** The dissolution rate constant of single spherical sodium carbonate particle under different temperature

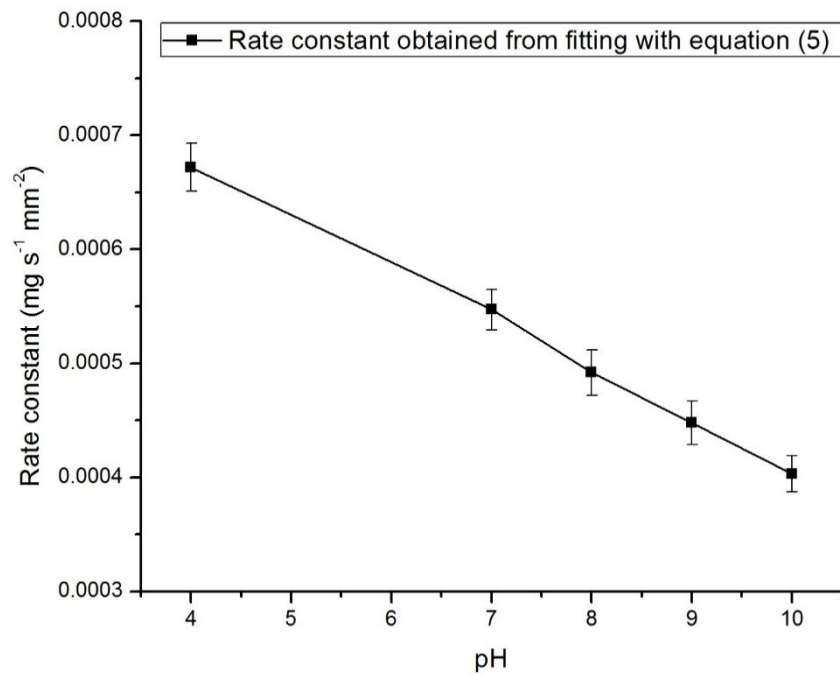


**Figure 3.21** The dissolution rate constant of single spherical sodium carbonate particle under different pH

According to the results of dissolution rate constant shown in Figure 3.20, it is

clearly represented that the dissolution rate constant increase with temperature obviously. According to the dissolution mathematical model, the dissolution process can be assumed to be related to the effective diffusion process and its coefficient in bulk. Based on Einstein-Stokes equation, the diffusion coefficient is presented as

$$D_{eff} = \frac{K_B T}{6\pi\alpha\mu}$$

Where  $K_B$  is Boltzmann's constant,  $T$  is the absolute temperature,  $\alpha$  is the hydrodynamic radius of the sucrose molecule and  $\mu$  is the viscosity of the medium.

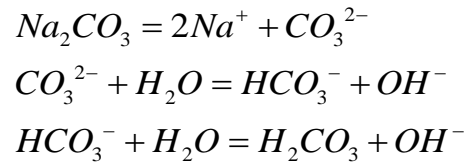
Therefore, the diffusion coefficient is derived from the value of viscosity and absolute temperature of water under different conditions. According to the measurement results of viscosity of water at temperature from 20°C to 60 °C that are shown in Table 3.4 [95], the viscosity of water decreases with the increase of temperature. This result leads to the increase of diffusion coefficient with temperature. In this way, the theoretical explanation can be said that the relationship between diffusion coefficient and temperature determines the increase of dissolution rate constant with temperature.

**Table 3.4** Viscosity of water from 30°C to 70°C

Temperature (°C)	30	40	50	60	70
Viscosity (m <sup>2</sup> /s×10 <sup>-6</sup> )	1.004	0.0081	0.658	0.553	0.475

According to the results of dissolution rate constant shown in Figure 3.21, it is clearly expressed that the rate constant decreases with the increase of pH. From the view of chemical reactions of sodium carbonate in water, the aqueous solution of sodium carbonate starts to ionize into sodium and carbonate ions when the

dissolution starts. Then a hydrolysis reaction between carbonate ions and hydrogen ions with an ionization into bicarbonate ions and hydroxide ions occurs which lead to the decrease of amount of hydrogen ions, and the left hydroxide ions lead the solution becoming alkaline. The whole ionization and hydrolysis process can be presented as [96]:



Therefore the initial concentration of hydroxide ions in water can be said to determine the speed of hydrolysis and ionization process of sodium carbonate. In this way, higher hydrogen ions accelerate this process, but higher hydroxide ions restrain it in contrast. According the experimental conditions of pH, higher pH means higher concentration of hydroxide ions. Therefore, the results that the dissolution rate constant decreases with the increase of pH can be explained from the above analysis.

### 3.5 Conclusions

To measure and quantify the dissolution process and kinetics of single special Sodium carbonate particle, the dissolution image analysis method by high speed camera is built. The dissolution process and kinetics at different temperature and pH are analyzed and quantified with the mathematical model for spherical particles. This mathematical model based on the dissolution process relating to mass transfer and diffusion is developed and used to fit the experimental data. Following this way, the dissolution rate constant at different temperatures and pH are well quantified. According to the results from quantification, the effects of temperature and pH on

dissolution rate constant are shown and discussed as the following that with the increase of temperature, it is obviously to show that the rate constant will increase with temperature due to the increase of diffusion and its coefficient. For the effect of pH, it can be noticed that the dissolution rate constant decrease with the increase of pH due to the effect of pH on chemical reactions of sodium carbonate in water that higher pH leads to the suppression on hydrolysis reactions in water.



## **CHAPTER 4. DISSOLUTION OF SODIUM CARBONATE TABLETS**

### **4.1 Introduction**

In this chapter, the dissolution process and dissolution kinetics of sodium carbonate tablet are quantified and discussed under the conditions of temperature and stirring speed. The sodium carbonate tablet is made of sodium carbonate particles by direct compression. The preparation of sodium carbonate tablet is introduced in the section of methodology. The tablets are also test by SEM to show the structure of tablet. The dissolution experiments are carried out under different temperature and stirring speed. In this way, the quantified dissolution process and kinetics are linked with temperature and stirring speed. Therefore, the effects of temperature and stirring speed can be investigated by quantification on the dissolution rate and dissolution rate constant. Because several mathematical models are applicable to be used to quantify the dissolution kinetics, the most appropriate mathematical model needs to be selected before the quantification works. Therefore, the process of selection of mathematical model is expressed in this chapter. Following this way, this chapter is organized in the following manner. Firstly, experimental methodology is introduced in Section 4.2. Experimental results are presented in Section 4.3 where the results are discussed. Finally, conclusions are given in Section 4.4.

### **4.2 Experimental Methodology**

The initial material of sodium carbonate particles used in this work are the same material particles described in Chapter 3. The work firstly involved compaction of the powder into tablets of well-defined size and shape by using a manual Baileigh Industrial compression machine with pressure of 20KN. A normal compaction force

of 20KN was applied during the fabrication of the tablets. These tablets were cylindrical shaped with 10 mm diameter and 3 mm height. Each tablet had a mass of 0.3g. As the tablets were produced using the same preparation method, the same amount of powder, and the same pressure, the internal structure of the tested samples are expected to be the same. In this way, the effect of the tablet internal structure on the dissolution process could be minimized. An example of compressed sodium carbonate tablet with mass of 0.3 mg, diameter of 10 mm and height of 3 mm is shown in Figure 4.1



**Figure 4.1** Compressed sodium carbonate tablet

For a typical dissolution experiment, a schematic diagram is shown below to state the set-up process of dissolution experiment.

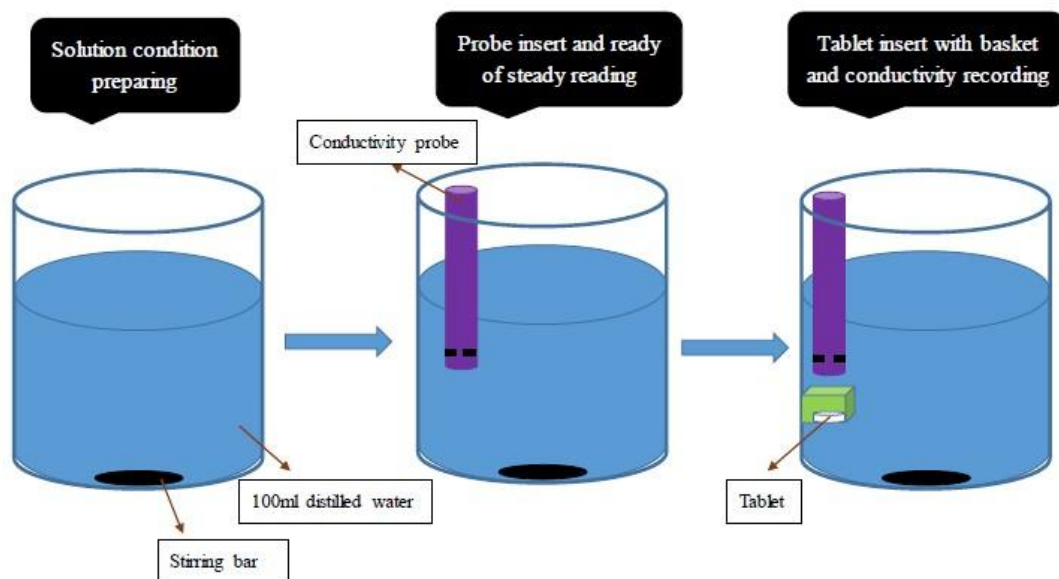


**Figure 4.2** Set-up process of typical dissolution experiment

Specifically speaking, a beaker filled with 100ml distilled water was placed in a water bath at first. The water bath was placed on the top of a Ceramic stirrer digital hot plate of Radleys for heating the water bath to a preset temperature under a magnetic stirring at a preset speed. This allowed for degassing the water before the dissolution experiment. The hotplate used in this work is shown in Figure 4.3.



**Figure 4.3** Stirring hotplate used for dissolution experiment

The water (solvent) temperature was controlled automatically to give 20°C, 30°C, 40°C, 50°C and 60°C. The control of solution temperature is achieved with digital temperature controller from this stirring hotplate which is shown in Figure 4.4. A temperature sensor is placed and contacted with solution. Therefore, the temperature of solution is controlled by this digital temperature controller. With this temperature controller, fuzzy logic microprocessor control ensures fast heating with no temperature overshoot. The set and actual temperature of solution is displayed digitally. The displays of this temperature controller are shown every temperature between -50°C and +300°C. The control accuracy of solution temperature with external temperature sensor is  $\pm 1$  K.



**Figure 4.4** Temperature controller of stirring hot plate

The dissolution process was done at different stirring speeds realized by a magnetic stirring bar placed at the bottom of the beaker induced by the hot plate device. Three stirring speeds of 300, 500 and 700 RPM were tested. The accuracy of stirring speed controlled by this hotplate is  $\pm 2\%$  RPM.

A conductivity probe from Conductivity TDS Portable Meter PHH224 was inserted vertically into the central part of the beaker to measure the conductivity as a function of time. The distance between the probe and the beaker bottom were fixed at 20mm. With this conductivity meter, the range of conductivity that can be measured at 2 mS scale is from 0.2 to 2.0 mS. The resolution of this conductivity meter at 2 mS scale is 0.001 mS, and the accuracy is  $\pm(3\%FS + 1 \text{ digital})$ . At 20 mS scale, the range of conductivity meter is from 2 to 20.0 mS. The resolution of conductivity at this scale is 0.01 mS, and the accuracy is  $\pm(3\%FS + 1 \text{ digital})$ . With this conductivity meter, the sampling time is approximately 0.8 second.

A tablet was then placed quickly at the bottom of the beaker directly below the probe and the reading of conductivity was taken through video recording until the completion of the dissolution process. The recorded data of conductivity was then processed to determine the concentration of dissolved Sodium carbonate in water

using a calibrated curve. Through repeating of the above experiments under the same conditions and different conditions, we were able to establish the measurement error bars and also the dissolution kinetics.

Before each dissolution experiment was carried out, the conductivity meter was calibrated with the calibration solutions. The calibration solutions used into calibration were provided from OMEGA with the product number of CDSA-10 and CDSA-1413. With CDSA-10 solution, the conductivity meter was calibrated to 10 $\mu$ S. With CDSA-1413 solution, the conductivity meter was calibrated to 1413 $\mu$ S. Only after calibrations with both CDSA-10 and CDSA-1413 were carried out, the conductivity meter was used to the measurement of dissolution experiment.

### **4.3 Results and Discussions**

#### **4.3.1 Structure of sodium carbonate tablet**

Because the materials used in this work are the same sodium carbonate particles introduced and analyzed in Chapter 3, the compound of sodium carbonate tablet used in this work is determined as anhydrous sodium carbonate with a very small amount of sodium carbonate hydrate. However, with the external compression to make the sodium carbonate tablet, the crystalline form of sodium carbonate tablet may have changed comparing with initial sodium carbonate particles. To identify the crystalline form of sodium carbonate tablets used in this work, the test with the same X-ray diffraction facility that is introduced in Chapter 3 is carried out. The XRD result of sodium carbonate tablet comparing with initial sodium carbonate particle is shown in Figure 4.5

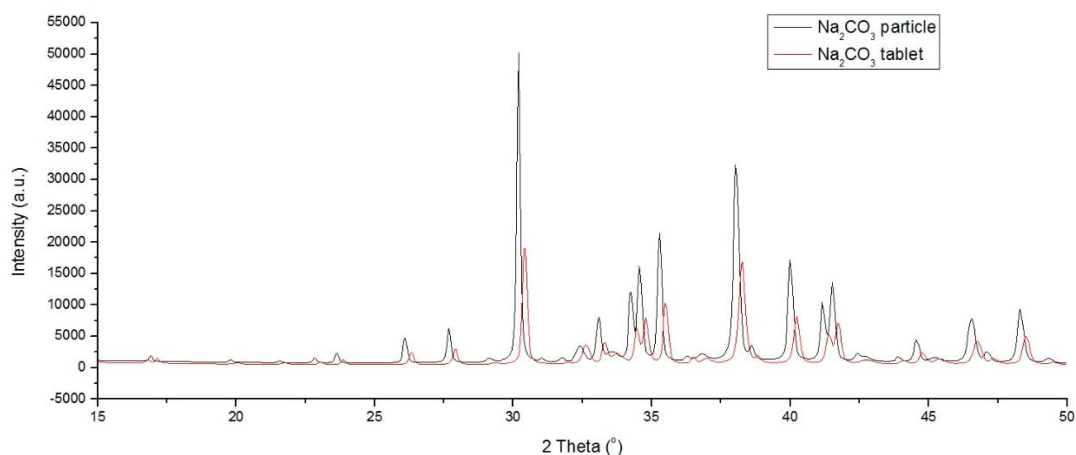
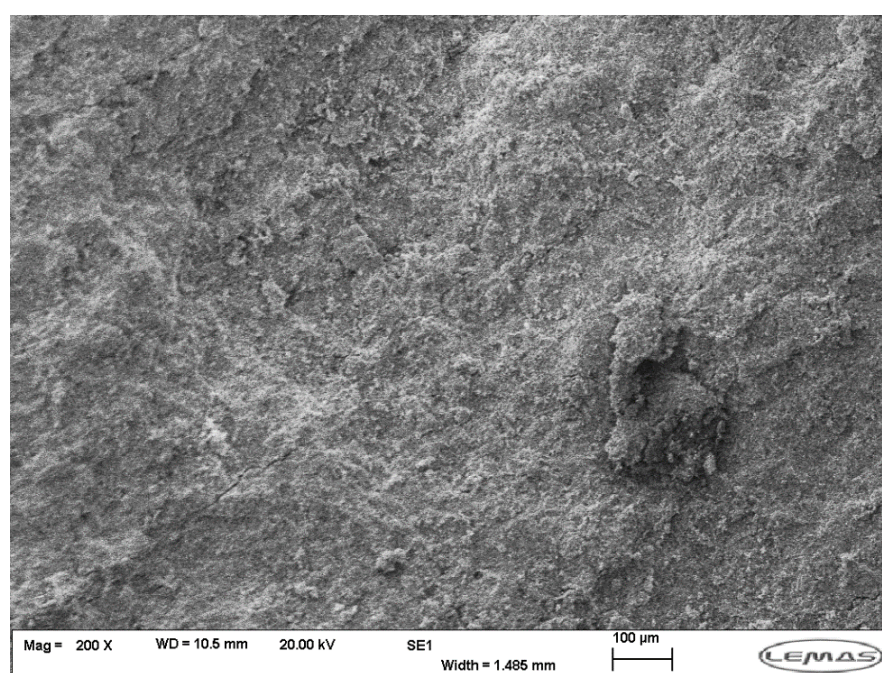


**Figure 4.5** XRD measurement of sodium carbonate tablets comparing with initial sodium carbonate particles

According to the XRD results shown in Figure 4.5, the crystalline form of sodium carbonate tablet expresses clear difference with initial sodium carbonate particle. With the XRD shown in Figure 4.5, sodium carbonate tablet shows the same peak trend and peak shape with initial sodium carbonate particle. However, the peak position of sodium carbonate tablet shows a clear rightward panning comparing with initial sodium carbonate particle, and the intensity of peak of sodium carbonate tablet is lower than initial sodium carbonate particle. According to the basic theoretical model of XRD, Bragg Law, the results shown in Figure 4.5 proves that after compression, the crystal size of sodium carbonate becomes smaller and the layer distance of diffraction surface becomes shorter. These results provide useful information to discuss that to make the dissolution happening, the energy that breaks the bond between sodium atom, carbon atom and oxygen atom for sodium carbonate tablet might be greater than the breaking energy that for initial sodium carbonate particle.

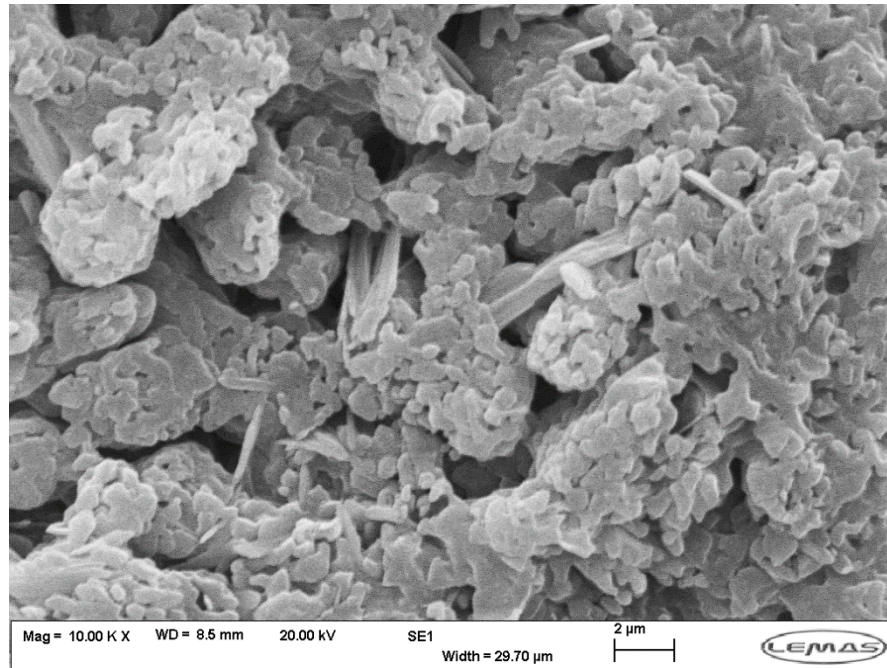
Based on the compression method for sodium carbonate tablets, every sodium carbonate tablet has the same shape and size. After the test by XRD, the test with SEM is also carried out and the SEM images are shown in Figure 4.6. The SEM

tests show that the compression has made the surface of tablet tend to be flat. Comparing with the initial sodium carbonate particle shown in Chapter 3, the structure of agglomerates is extruded in a larger extent. In this scenario, the process of water penetration into tablet is too weak to be observed during dissolution process. There are rarely bubbles coming out the tablet and floating to the surface of solution during each dissolution experiment. Therefore, the penetration process of water into tablet can be regarded as minimized.



(a)





(b)

**Figure 4.6** SEM images of Sodium carbonate tablet with scale of (a) 100μm and (b) 2μm.

#### **4.3.2 Data Analysis Method of Dissolution Experiment of Sodium Carbonate**

##### **Tablet under Temperature and Stirring speed**

Because the experimental method used in this work is conductivity tracking method, it is necessary to carry out the calibration of measured conductivity value with concentration of sodium carbonate in solution. The calibration is carried out in this work following the way as that sodium carbonate particles used in this work with specific mass are dissolved in 100ml distilled water at first. The solution containing dissolved sodium carbonate is stirred over 1 hour and then keep stationary over 1 hour. After this treatment of solution, the conductivity value of this solution is measured with the conductivity meter. This conductivity value measured from solution is determined as the conductivity of this specific amount of sodium carbonate. Then the calibrations for different amount of sodium carbonate are carried out with the same way, and the conductivities are determined as the conductivities of corresponding amount of sodium carbonate. This calibration works

are repeated 3 times and the data are shown in Table 4.1

**Table 4.1** Measured conductivity values with completely dissolved amount of sodium carbonate

Dissolved amount (g)	Conductivity (mS)	Dissolved amount (g)	Conductivity (mS)	Dissolved amount (g)	Conductivity (mS)
0.02	0.453	0.02	0.379	0.02	0.383
0.05	1.01	0.05	0.948	0.05	0.958
0.08	1.506	0.08	1.517	0.08	1.532
0.1	1.857	0.1	1.896	0.1	1.916
0.15	2.75	0.15	2.84	0.15	2.87
0.17	3.17	0.17	3.22	0.17	3.26
0.2	3.63	0.2	3.79	0.2	3.83
0.25	4.55	0.25	4.74	0.25	4.79
0.3	5.48	0.3	5.62	0.3	5.73

These conductivity values are plotted against of dissolved mass of sodium carbonate shown in Figure 4.7. According to Figure 4.7, the relation between conductivity with completely dissolved amount of sodium carbonate seems better to be shown as linear. Therefore, this linear should be used to calibrate and calculate the dissolved amount of sodium carbonate with measured conductivity value during dissolution process.

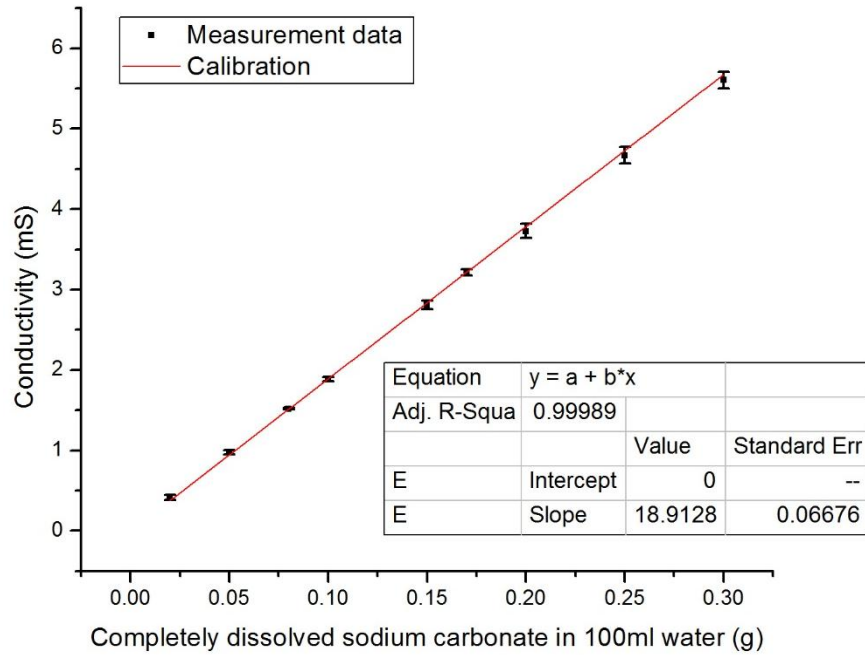


**Figure 4.7** Calibration of conductivity values with dissolved amount of sodium carbonate

With the calibration shown in Figure 4.7, it is clearly expressed that the relation of conductivity with amount of dissolved sodium carbonate is determined with the equation that

$$COND_t = 18.91M_t$$

Where  $COND_t$  means the conductivity value at time  $t$ ; and  $M_t$  means the dissolved amount of sodium carbonate at the corresponding time  $t$ .

After obtaining the calibration relation of conductivity with amount of dissolved sodium carbonate, the treatment and analysis of measured dissolution data is shown as the following method with an example of dissolution experiment under 60°C and 300RPM.

Based on the dissolution experiment, the conductivity values as function of time can be measured with the conductivity meter. The conductivity values for the dissolution experiment under 60°C and 300RPM are shown in Table 4.2

**Table 4.2** Conductivity of dissolution experiment under 60°C and 300 RPM

Time (S)	Conductivity (mS)	Time (S)	Conductivity (mS)
10	0.665	210	5.29
20	0.995	220	5.36
30	1.326	230	5.41
40	1.707	240	5.46
50	2.14	250	5.5
60	2.44	260	5.54
70	2.73	270	5.57
80	3.03	280	5.59
90	3.3	290	5.62
100	3.57	300	5.64
110	3.78	310	5.66
120	4	320	5.68
130	4.2	330	5.69
140	4.4	340	5.7
150	4.58	350	5.71
160	4.75	360	5.72
170	4.9	370	5.73
180	5.03	380	5.74
190	5.12	390	5.75
200	5.21	400	5.75

With measured conductivity values shown in Table 4.2, the amount of dissolved sodium carbonate can be calculated with the calibration relation shown as  $COND_t = 18.91M_t$ . With this calibration relation, the dissolved amount of sodium carbonate are determined and shown in Table 4.3.

**Table 4.3** Dissolved amount of sodium carbonate from experiment under 60°C and 300 RPM with calibration

Time (S)	Dissolve amount (g)	Time (S)	Dissolve amount (g)
10	0.0352	210	0.2797
20	0.0526	220	0.2834
30	0.0701	230	0.2861
40	0.0903	240	0.2887
50	0.1132	250	0.2909
60	0.129	260	0.293
70	0.1444	270	0.2946
80	0.1602	280	0.2956
90	0.1745	290	0.2972
100	0.1888	300	0.2983
110	0.1999	310	0.2993
120	0.2115	320	0.3004
130	0.2221	330	0.3009
140	0.2327	340	0.3014
150	0.2422	350	0.302
160	0.2512	360	0.3025
170	0.2591	370	0.303
180	0.266	380	0.3035

190	0.2708	390	0.3041
200	0.2755	400	0.3041

Because sodium carbonate tablet used in this work is dissolved into 100ml distilled water, the concentration of sodium carbonate under 60°C and 300RPM in solution is determined and shown in Table 4.4 based on the dissolved amount values as function of dissolution time. And the ratio of dissolved amount of sodium carbonate as function of time is shown in Figure 4.8.

**Table 4.4** Concentration of sodium carbonate in solution as function of time under 60°C and 300 RPM

Time (S)	Concentration (g/ml)	Time (S)	Concentration (g/ml)
10	0.000352	210	0.002797
20	0.000526	220	0.002834
30	0.000701	230	0.002861
40	0.000903	240	0.002887
50	0.001132	250	0.002909
60	0.00129	260	0.00293
70	0.001444	270	0.002946
80	0.001602	280	0.002956
90	0.001745	290	0.002972
100	0.001888	300	0.002983
110	0.001999	310	0.002993
120	0.002115	320	0.003004
130	0.002221	330	0.003009
140	0.002327	340	0.003014
150	0.002422	350	0.00302
160	0.002512	360	0.003025
170	0.002591	370	0.00303
180	0.00266	380	0.003035
190	0.002708	390	0.003041
200	0.002755	400	0.003041

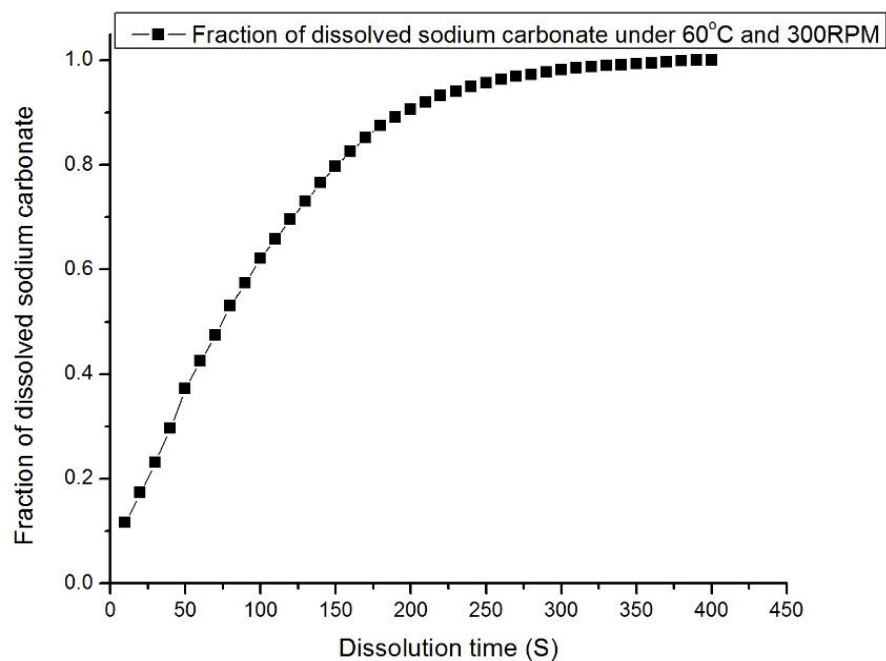


**Figure 4.8** Ratio of dissolved sodium carbonate as function of time under 60°C and 300RPM

With the measured dissolution data above, the next step is the analysis of dissolution rate constant with mathematical model. Due to the diversity of dissolution mathematical models, it is significant to select the appropriate model to study and quantify the dissolution kinetics. The process of quantification generally based on the model dependent methods which include zero-order kinetics model, first-order kinetics model, Higuchi model and Hixson-Crowell model. The details of these four mathematical models have been expressed in the chapter of literature review.

The method of selecting the mathematical models is based on the statistical treatments with different criteria. The most widely used method is to apply the coefficient of determination to assess the fit of equation. But when the number of parameters of each equation is different, an adjusted coefficient of determination is more appropriate to be used to compare different models and equations. Therefore, the most appropriate model is the one with the biggest value of adjusted coefficient

of determination.

With the measured dissolution data, the values of adjusted coefficient of determination are obtained for zero-order model, first-order model, Higuchi model and Hixson-Crowell model respectively under the 300RPM. These values are listed in Table 4.5.

**Table 4.5** Values of adjusted coefficient of determination from measurement data for dissolution models at different temperatures under the stirring speed of 300RPM.

	20°C	30°C	40°C	50°C	60°C
<b>Zero-order model</b>	0.9787	0.97192	0.97364	0.97028	0.98084
<b>First-order model</b>	0.85114	0.87135	0.87942	0.87663	0.87155
<b>Higuchi model</b>	0.88532	0.87786	0.87405	0.86727	0.88862
<b>Hixson-Crowell model</b>	0.99699	0.99963	0.99983	0.99893	0.99546

According to the values which are shown in Table 4.4, Hixson-Crowell model represents the biggest adjusted coefficient of determination. Therefore, Hixson-Crowell model is selected as the most appropriate dissolution model to research the dissolution kinetics of Sodium carbonate tablet in this case.

In this way, the dissolution rate constant is fitted with the equation of Hixson-Crowell model that

$$W_0^{1/3} - W^{1/3} = K_H t \quad (4.1)$$

Where  $W_0$  is the initial amount of sodium carbonate tablet;  $W$  is the remaining undissolved amount of sodium carbonate from experimental measurement; and  $K_H$

is the dissolution rate constant.

Therefore, based on the measured dissolution data of sodium carbonate tablet under 60°C and 300RPM, the fitting with equation (4.1) is shown in Figure 4.9.

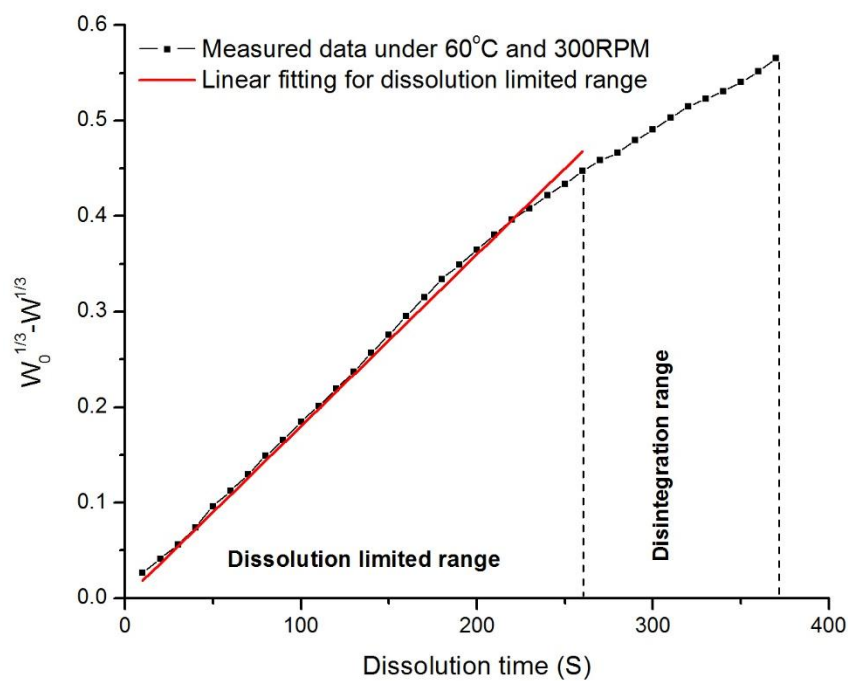


**Figure 4.9** Fitting of dissolution experiment with Hixson-Crowell model under 60°C and 300RPM

With Hixson-Crowell model, a linear should be obtained for the experimental data if the dissolution process is matching the assumptions of mathematical model during the whole dissolution process that the shape factor of dissolved tablet should keep as a constant and only the diminishing of size of tablet happens during dissolution process. However, according to the observation of dissolution experiment, the dissolution of sodium carbonate tablet is not following the assumption of Hixson-Crowell model for the whole dissolution process.

When the undissolved sodium carbonate tablet is thinner and smaller enough, the sodium carbonate tablet is very unlikely to keep as a whole tablet under stirring conditions. That means once the remaining sodium carbonate tablet is lower than a possible amount, the tablet will be disintegrated into pieces due to the external



stirring force from solution. Therefore, the practical dissolution of sodium carbonate tablet in this work can be said has two ranges that the tablet will dissolve with dissolution limited process as a whole, and once the tablet starts to disintegrate, the dissolution steps into disintegration process. In this way, the fitting of measured experimental data with Hixson-Crowell model should be carried out for two ranges. One is the dissolution limited range, and another is disintegration range. However, the assumptions of mathematical model during the whole dissolution process that the shape factor of dissolved tablet should keep as a constant and only the diminishing of size of tablet happens during dissolution process is only applied within dissolution limited range. Therefore, the linear fitting with Hixson-Crowell model for dissolution limited range is the appropriate method to quantify the dissolution rate constant for dissolution of experiment with Hixson-Crowell model.

According to the measurements of dissolution experiments and the observation of dissolution process, the time period for disintegration range can be recorded and used to determine the time period of dissolution limited range and disintegration range for each case. In this way, the linear fitting with Hixson-Crowell model for dissolution limited range of each case is carried out to quantify the dissolution rate constant of corresponding experiment. According to Figure 4.9, the dissolution rate constant for sodium carbonate tablet under 60°C and 300RPM can be determined as *0.00180* (g<sup>1/3</sup>/S).

#### **4.3.3 Dissolution Kinetics of Sodium Carbonate Tablet under Temperatures and Stirring speeds**

With Hixson-Crowell model used in this work, the mechanism of dissolution process of tablet can be regarded as the dissolution reactions that happen at tablet

surface as function of time. With the dissolution reactions, sodium carbonate hydrolyzes into iron species at tablet surface and sodium carbonate tablet then may disintegrate successively depending on external stirring conditions. Also during this period, the tablet dimensions are assumed to diminish proportionally and the initial tablet geometrical form keeps as constant. After dissolution reaction process, the diffusion process is the way that dissolved iron species diffuse through the diffusion layer into bulk. With this dissolution mechanism of tablet with Hixson-Crowell model, the dissolution rate of sodium carbonate tablet is greatly limited by the dissolution reaction rate of sodium carbonate particle in solution.

With the same analysis method shown in last section, the dissolution data measured from dissolution experiments under different temperature and stirring speed are shown, and the dissolution kinetics for each case is quantified as follows.

With the calibration relationship shown in Figure 4.6, the ratio of dissolved amount of sodium carbonate to initial amount of sodium carbonate tablet can be calculated for each case with the calibration equation. Therefore, the ratio of dissolved amount of sodium carbonate of each temperature are shown at different stirring speed in Figure 4.10, Figure 4.11 and Figure 4.12.

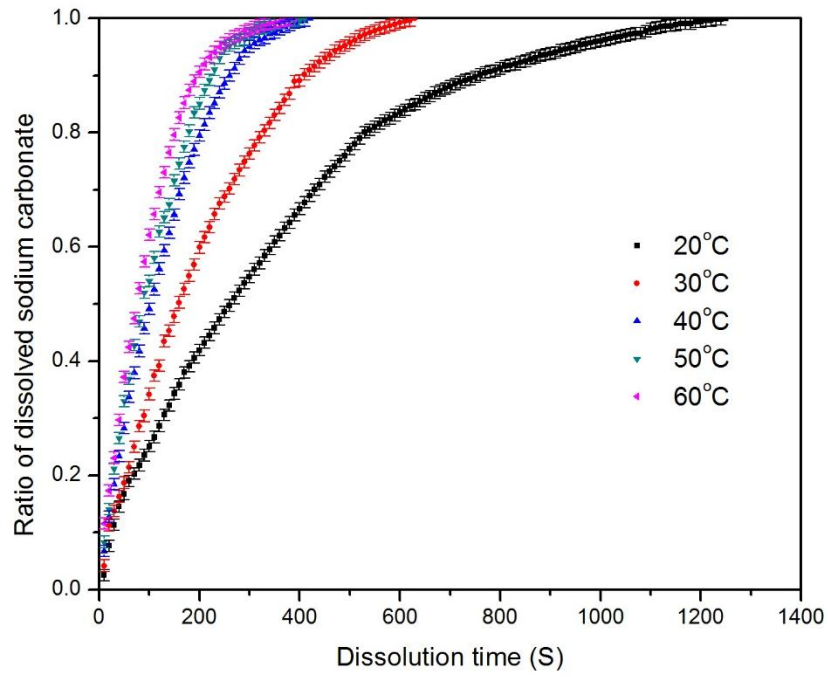


**Figure 4.10.** Ratio of dissolved sodium carbonate under 300RPM.

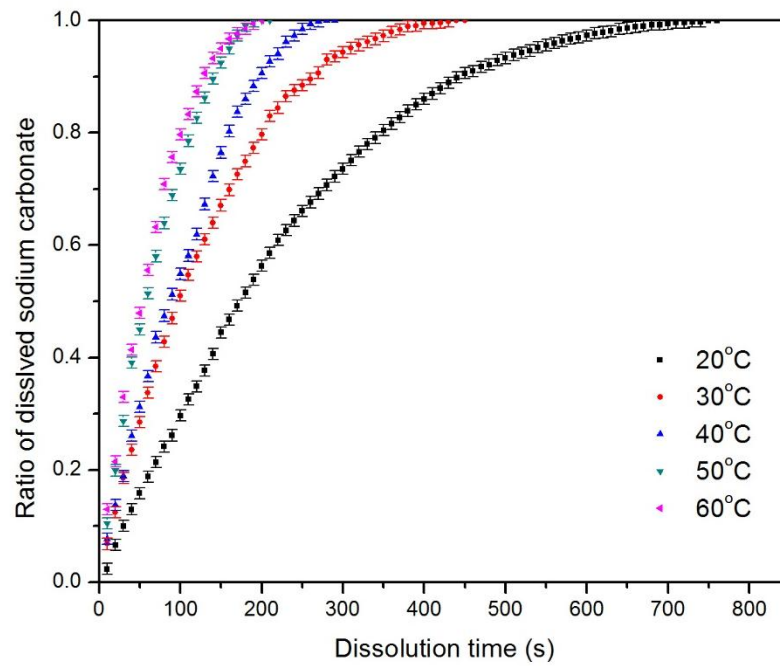


**Figure 4.11.** Ratio of dissolved sodium carbonate under 500RPM.

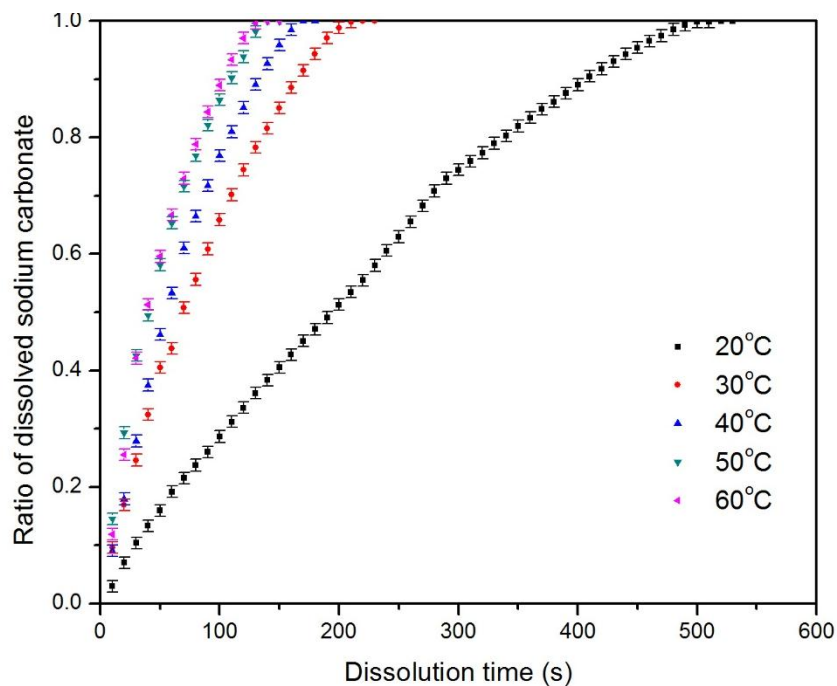


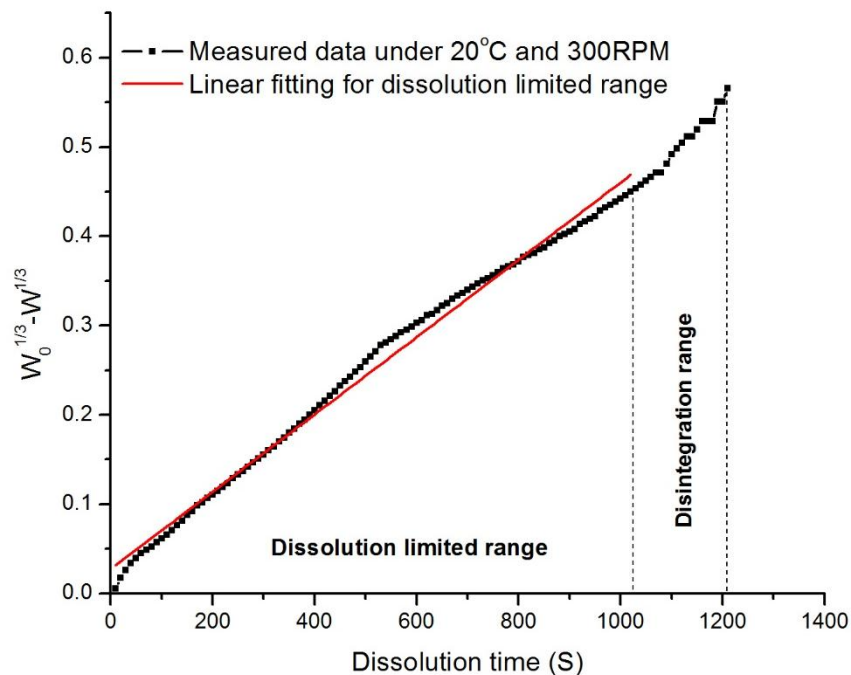
**Figure 4.12.** Ratio of dissolved sodium carbonate under 700RPM.

It is obviously shown that all the dissolution processes present the similar trend under different temperatures and stirring speeds. The dissolution time is shortened significantly by increasing temperature and stirring speed. That means increasing temperature and stirring speed have the great effect to accelerate the dissolution process.

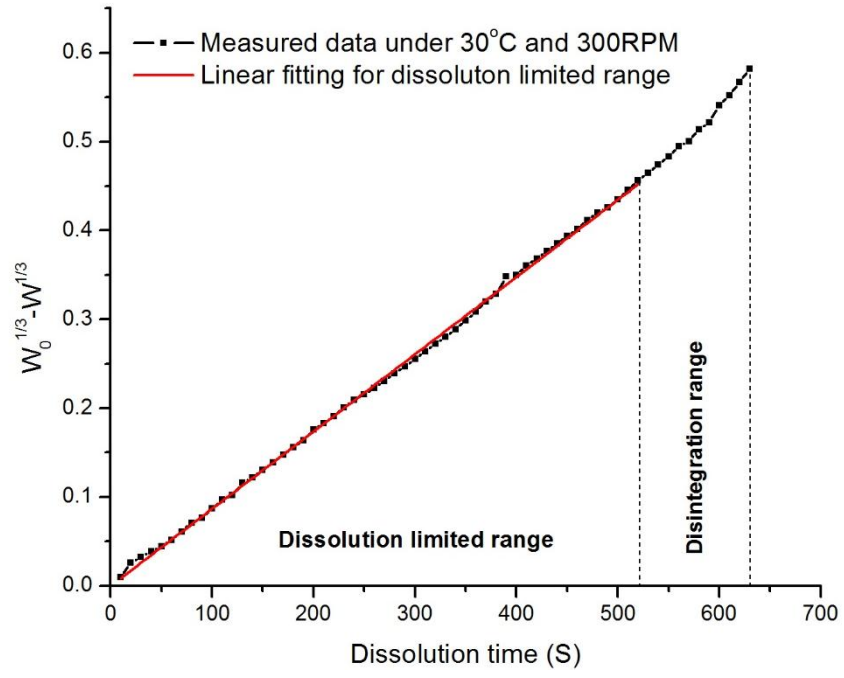
For every dissolution curve, it is clearly to show that the highest dissolution rate is at the start time point and then will decrease to 0 gradually till the end of dissolution. Through the whole dissolution curve, higher temperature and stirring speeds leads to the higher dissolution rate at the same time point. Therefore, based on the overall evaluation of dissolution curve, it can be regarded that the dissolution rate will increase with temperature and stirring speed.

Based on the analysis of fitting for dissolution limited range with Hixson-Crowell model, the fitting for each case are shown in Figure 4.13, Figure 4.14 and Figure 4.15. In this way, a linear is fitted with Hixson-Crowell model in dissolution limited

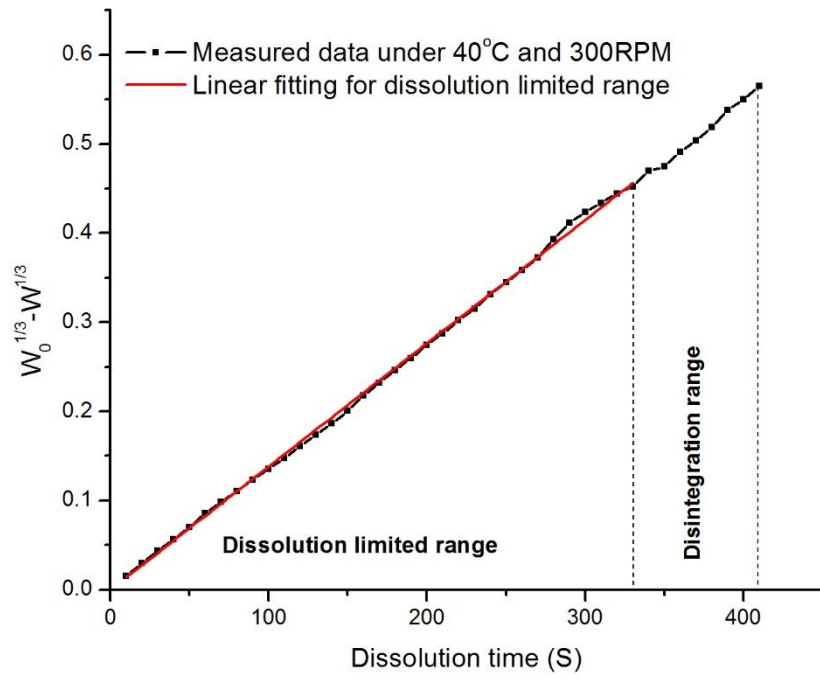
range. The fitting results for dissolution limited range of each case can be regards as the dissolution rate constant for corresponding solution conditions. Therefore, the dissolution rate constant of sodium carbonate tablet under different temperature and pH is shown in Figure 4.16.



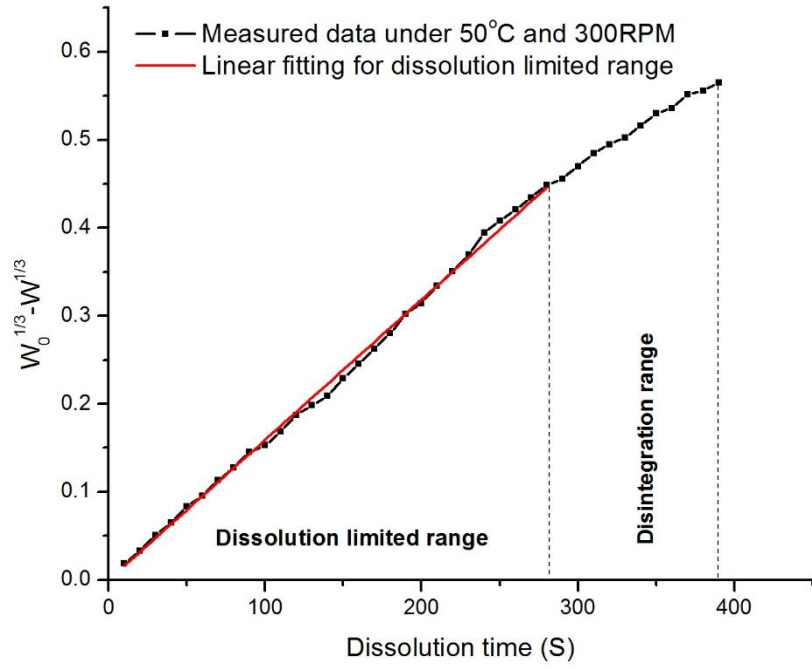
(a)



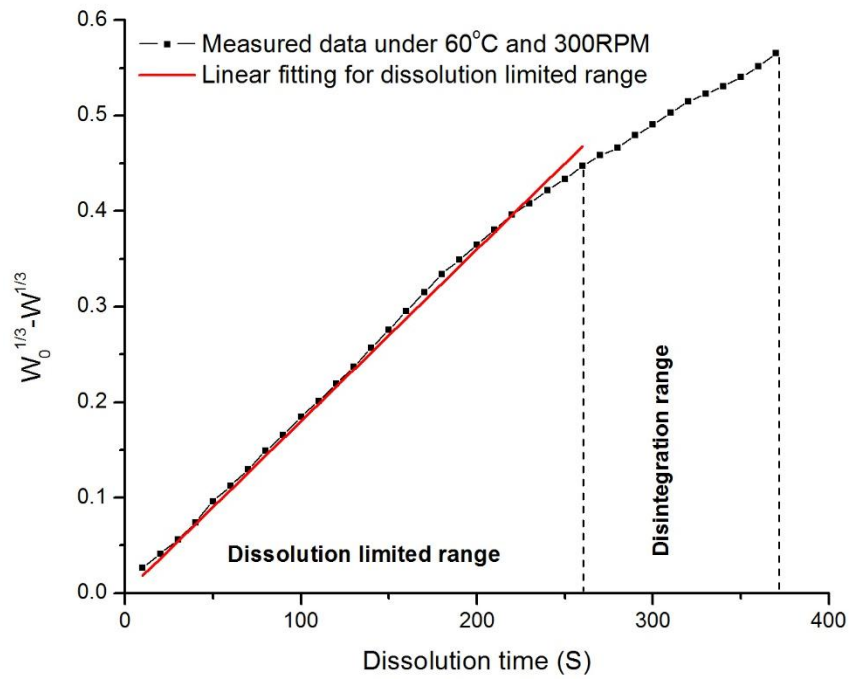
(b)



(c)

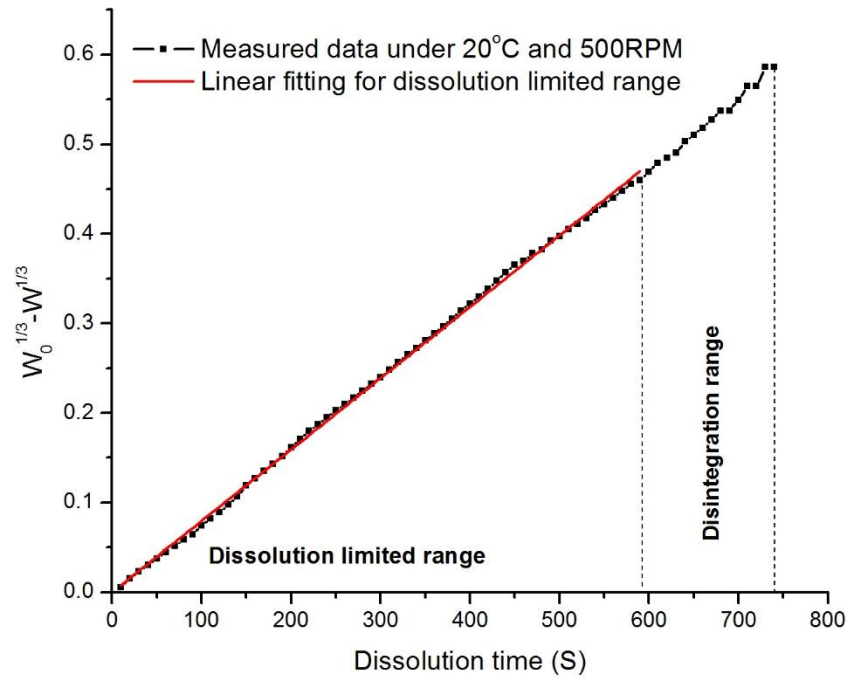


(d)

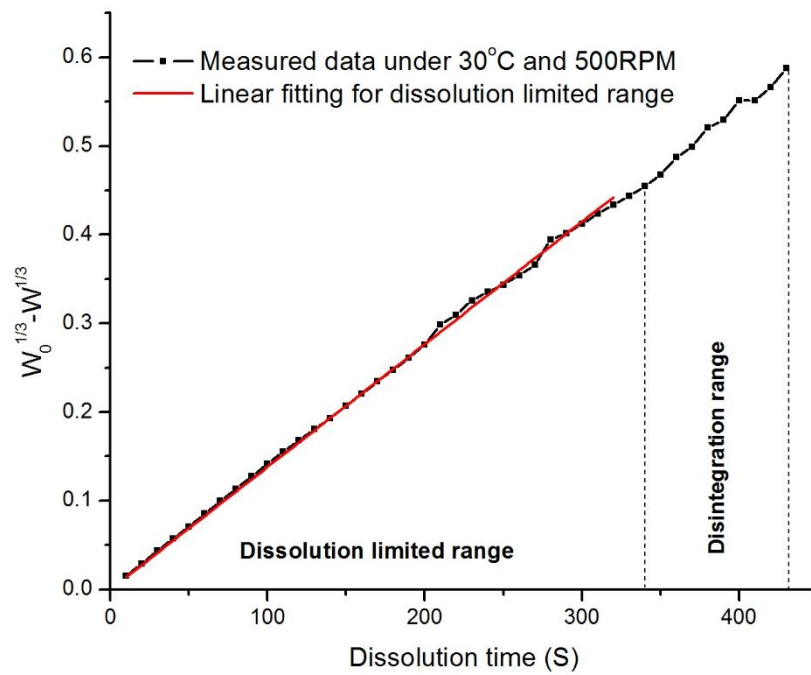


(e)

**Figure 4.13.** Fitting with Hixson-Crowell model on dissolution experimental data of sodium carbonate tablet under 300RPM and (a) 20°C; (b) 30°C; (c) 40°C; (d) 50°C; (e) 60°C.

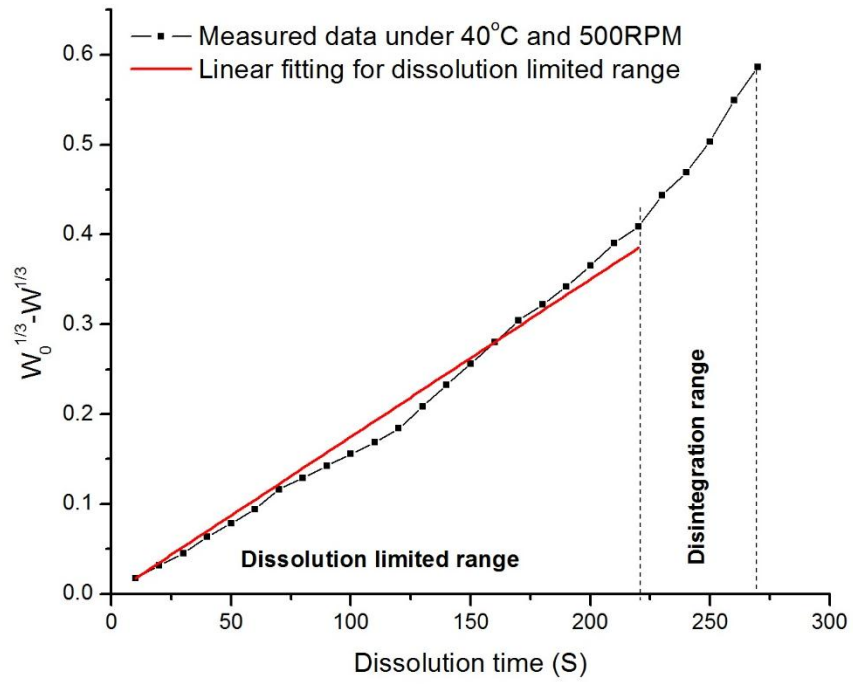


(a)

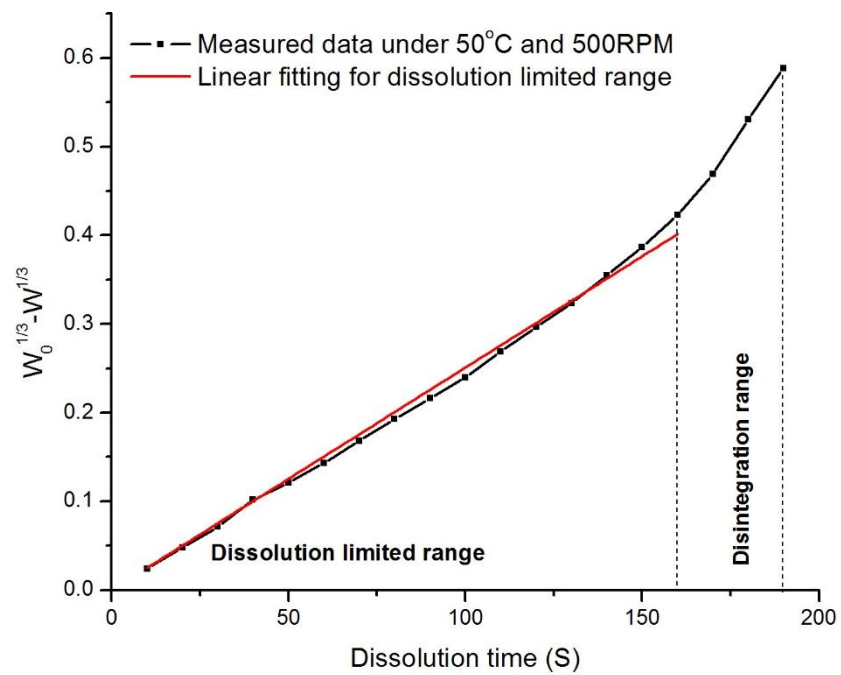


(b)

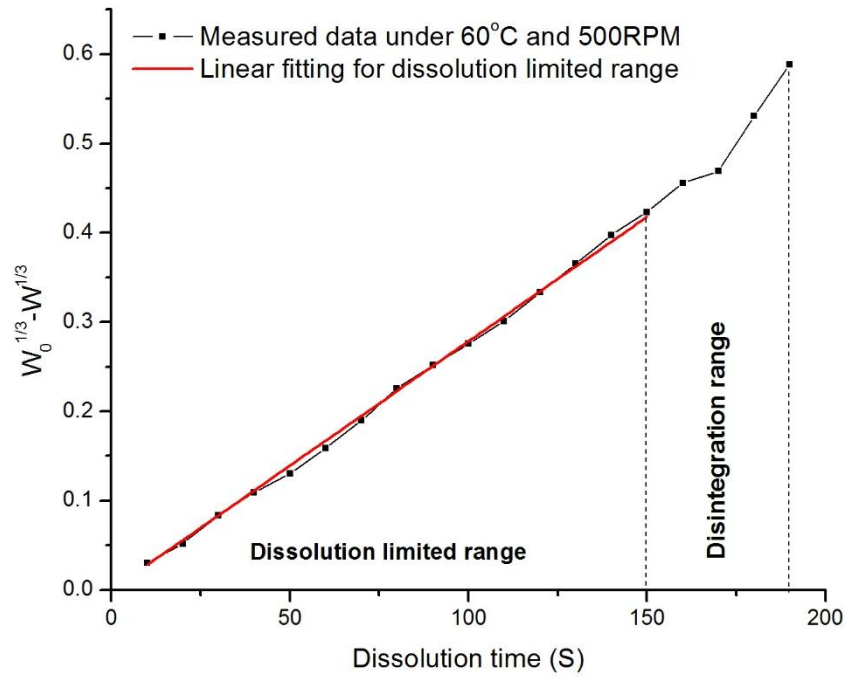




(c)

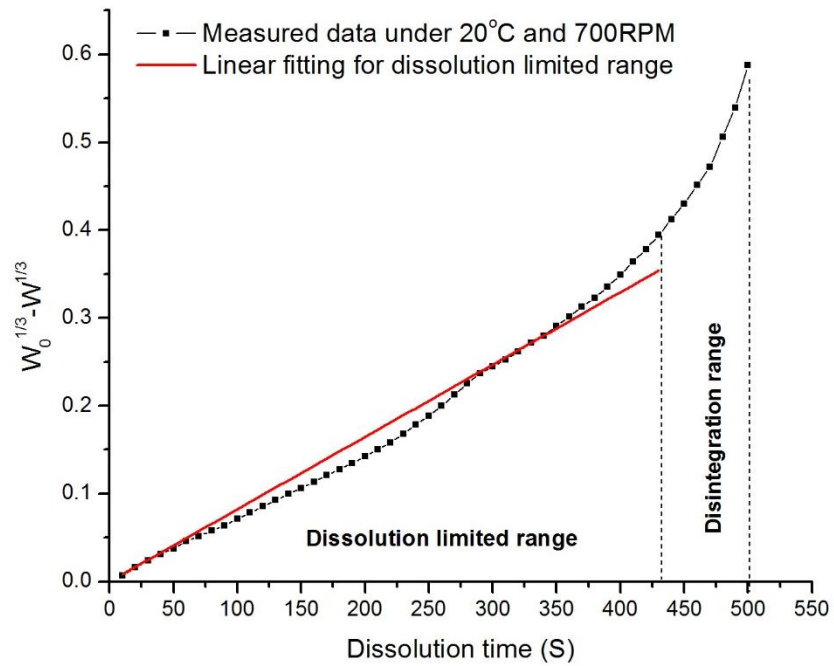


(d)

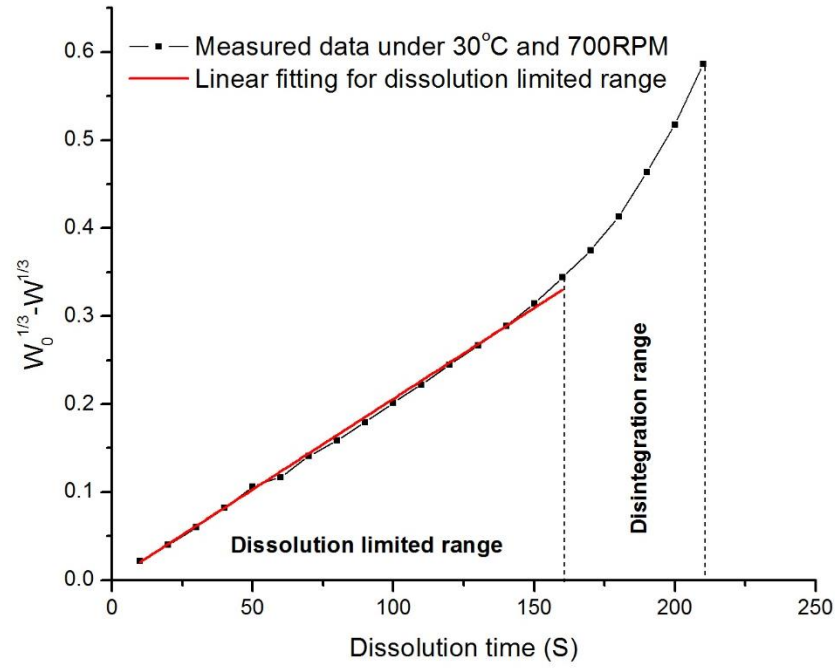


(e)

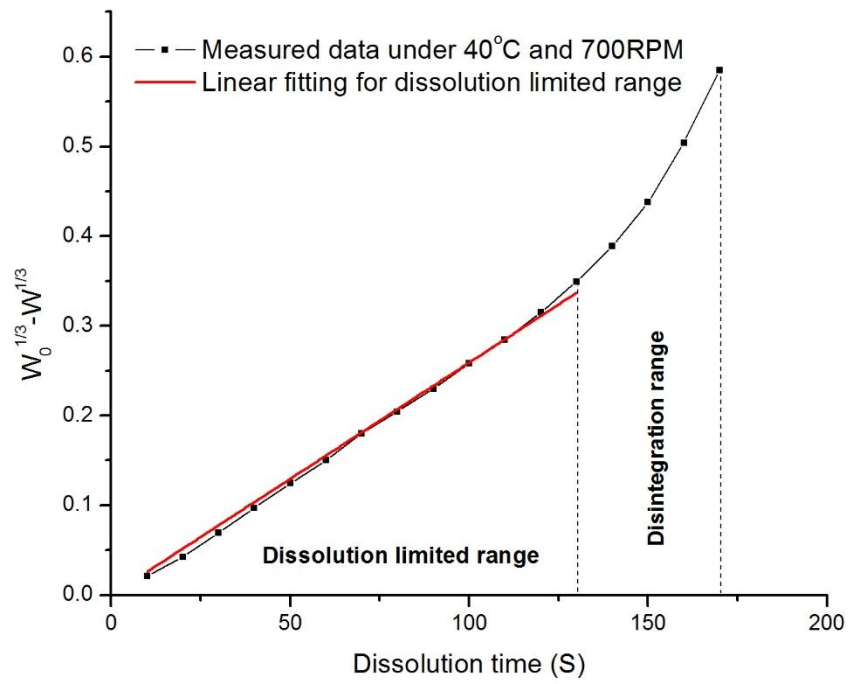
**Figure 4.14.** Fitting with Hixson-Crowell model on dissolution experimental data of sodium carbonate tablet under 500RPM and (a) 20°C; (b) 30°C; (c) 40°C; (d) 50°C; (e) 60°C.



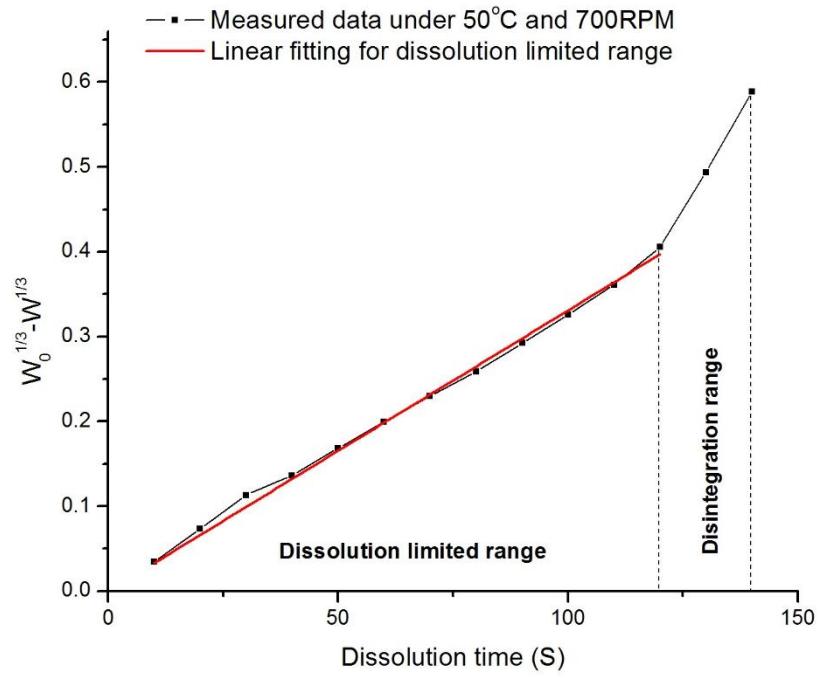
(a)



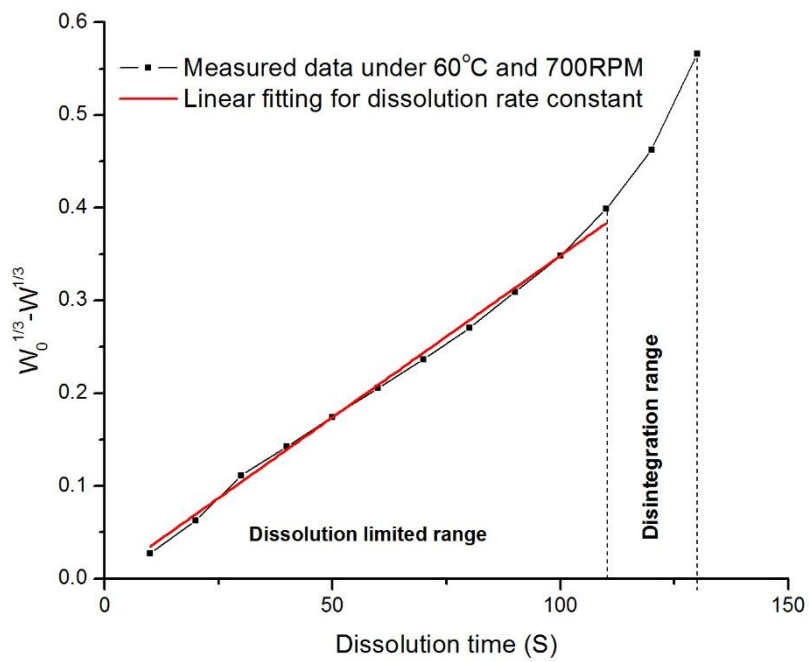
(b)



(c)



(d)



(e)

**Figure 4.15.** Fitting with Hixson-Crowell model on dissolution experimental data of sodium carbonate tablet under 700RPM.

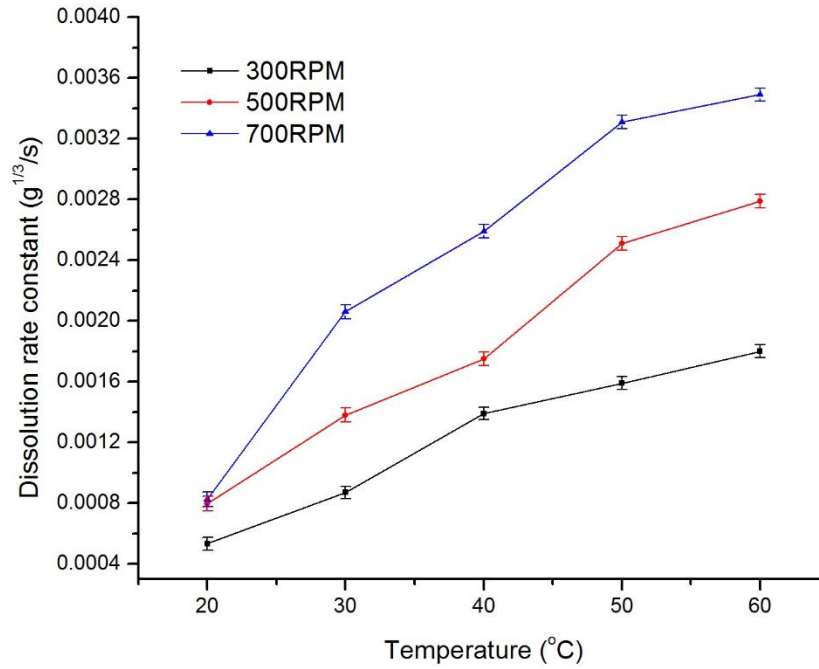


**Figure 4.16.** Dissolution rate constant of sodium carbonate tablet fitting with Hixson-Crowell model under different temperature and pH

According to Figure 4.16, the dissolution rate constant will increase with the increase of temperature, and similarly the rotation speed increasing will lead to increase of the dissolution rate constant. Based on the fitting mathematical model of Hixson-Crowell model used in this work, the mathematical equation also can be written as

$$w_0^{1/3} - w^{1/3} = \frac{k' N^{1/3} D C_s t}{\delta}$$

Where  $k'$  is a constant related to the shape factor and density of tablet,  $N$  is the number of particles,  $D$  is the diffusion coefficient through the diffusion layer,  $C_s$  is the saturated amount of Sodium carbonate and  $\delta$  is the thickness of diffusion layer.

According to the assumption of this model that the density and volume shape factor keep as a constant, the Hixson-Crowell dissolution rate constant can be

reformed as

$$k_h = \frac{k' N^{1/3} DC_s}{\delta}$$

that represents the inverse relationship with the diffusion layer thickness.

The diffusion layer thickness at the interface was derived by Levich [97] under the stirring conditions into the equation shown as

$$\delta = 1.612 D^{1/3} \nu^{1/6} \omega^{-1/2}$$

Where  $\nu$  is the kinematic viscosity of medium which decreases with temperature and  $\omega$  is angular velocity in medium which increase with stirring speed.

According to studies and analysis of diffusion layer thickness by Levich, the thickness of diffusion layer decreases with the increase of temperature and stirring speed. Therefore, combining the relationship between dissolution rate constant and diffusion layer thickness, the dissolution rate constant theoretically increased with temperature and stirring speed, and which also matches the results from experiments and quantifications.

#### 4.4 Conclusions

The process of dissolution of sodium carbonate tablet at different temperatures and stirring speeds are studied by conductivity measurement method. The effects of temperature and stirring speed on tablet dissolution and dissolution rate constant are quantified. Hixson-Crowell model which is developed from Noyes-Whitney equation is selected as the dissolution mathematical model to quantify the dissolution kinetics of sodium carbonate tablet by the adjusted coefficient of determination method, and this model is proved by the experimental results to be the

appropriate model for this study. The quantifications of dissolution rate constant and tablet dissolution represent clearly that they increase significantly with the increase of temperature and stirring speed due to the increasing diffusion properties with temperature and stirring speed.

## **CHAPTER 5. DISSOLUTION OF TABLETS CONTAINING SODIUM CARBONATE AND POLYMERS**

### **5.1 Introduction**

In this chapter, three kinds of polymers are mixed with sodium carbonate particles respectively to form the 2-component tablets that are used into dissolution experiments that are carried out under different temperatures. Through the results from dissolution experiments, the dissolution process of every tablet containing different components are determined and analyzed. The dissolution rate constant of every tablet is quantified by the appropriate mathematical model. Following this, the effect of every kind of polymer and also temperature on dissolution process and dissolution kinetics can be investigated. Based on these analyses, the conclusions are summarized to provide the accurate data about how these polymers affect the dissolution of tablets. These conclusions are further expected to provide useful information to the practical production of detergent.

Before the expression of the experimental works, an introduction about these polymers is necessary to be shown in this chapter. As known, every ingredient of detergent has its specific role in the performance of detergent such as dissolution performance and utility performance. The main ingredients of detergent normally have three parts including builders which take 50% by weight approximately, surfactants which take 15% by weight and bleaches which take 7%. Apart from the three main ingredients, the other ingredients are usually added depending on different applications. Therefore the specific research of dissolution kinetics of different ingredients plays a significant role in the development of detergent productions and applications. The ingredient polymers used in this chapter include



carboxymethyl cellulose, croscarmellose sodium and crospovidone.

Carboxymethyl cellulose (CMC) is the very important concentration of surfactants to form micelles [98]. The functions of surfactants can be described as dividing the interface and reducing the free energy of system by lowering the interface energy and removing the hydrophobic of surfactant. Specifically for CMC, it is usually used as the anti-redisposition agent in detergent. This highly water-soluble polymer can minimize the redisposition of soil that has been removed by washing. The molecular structural formula of CMC can be expressed as  $C_6H_7O_2(OR_1)(OR_2)(OR_3)$  where  $R_1$ ,  $R_2$  and  $R_3$  can be  $-H$ ,  $-CH_2COONa$  or  $CH_2COOH$  which is shown in Figure 5.1 [99]. Previous research and applications of CMC are widely from food industry, pharmaceutical industry, daily chemical industry and micro-particle science. Li [100] expressed the study of CMC to be a potential binder for Li-Ion battery and shown a better performance in cycling. He [101] used CMC as the stabilizers to manipulate the size and dispersibility of zerovalent iron nanoparticles and led to more effective utility of these nanoparticles used in soil and groundwater. Rossi [102] investigated the drug release and wash ability of gels based on sodium CMC and polyacrylic acid, and shown sodium CMC had a better performance.

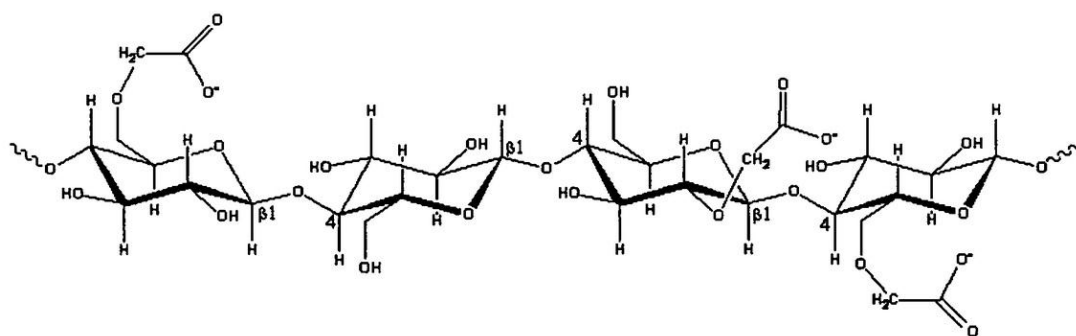


**Figure 5.1.** Molecular structural formula of CMC [99]

Croscarmellose sodium (CCMC) is the cross linked type of sodium carboxymethyl cellulose which is usually used as the superdisintegrant [103]. The function of cross-linking is to reduce the water solubility and also let the material swell and absorb much more than before to get a better contact with the solution. Croscarmellose sodium also can be used to solve the functional stability issues and reduce the effectiveness of tablets at high hardness level. Previous research mainly focused on the application of croscarmellose sodium in pharmaceutical productions. Ferrero and Munoz et al. [104] evaluated the effect of croscarmellose sodium on disintegration of a compression formulations. Zhao and Augsburger [105] investigated the effect of different croscarmellose sodium brands on the superdisintegrant performance from the aspects of size distribution, water uptake and swelling properties. Gordon and Chatterjee et al. [106] studied the effect of the form of croscarmellose sodium on tablet dissolution and friability and shown the fast dissolution rate with the form of intragranully.

Crospovidone (PVPP) is a kind of cross linked polyvinyl N-pyrrolidone which plays an important role in detergent due to its excellent surface activity [107]. The function of PVPP is to enhance the dispersion effect on liquid-solid phase as an agent. Crospovidone is insoluble in water, however it also can absorb water and swell quickly. Therefore crospovidone can be used effectively as disintegrate especially in tablets. Previous research mainly focuses on the effect of crospovidone on pharmaceutical dosage forms and tablets. Shu and Suzuki et al. [108] attempted to develop the fast disintegration tablets in oral use by mixing mannitol and crospovidone and crospovidone provided a great effect on the tablet hardness. Shin and Sang-Chul et al. [109] studied the effect of crospovidone to improve the dissolution rate of furosemide by co-precipitating or co-grinding, and the results

shown an increasing on dissolution rate. Fujili and Makiko et al. [110] aimed to solve the difficulties of solid dispersion on dosage forms preparations and achieve the goals by using crospovidone as the carrier.

As the important ingredients of detergent, very few research and studies are implemented to report the effect of carboxymethyl cellulose, croscarmellose sodium and crospovidone on the dissolution behaviors of tablets, and the effectiveness of these 3 polymers on dissolution rate are rare to be quantified and compared. Therefore, this chapter focuses on the dissolution of tablet containing sodium carbonate and these 3 kinds of polymers respectively by the experimental method of conductivity measurement method. The dissolution process and kinetics are quantified for every kind of 2-component tablet. In this way, the effects of these 3 kinds of polymers on the dissolution kinetics of tablets are discussed. The polymer particles and sodium carbonate particles are mixed respectively and compressed into tablet directly with the same size and shape. The different weight ratio of polymer in tablet is also studied and the effectiveness of each polymer with different weight ratio on dissolution kinetics is therefore investigated and quantified. Furthermore a comparison of the effect of these 3 kinds of polymers and the effect of different weight ratios on dissolution kinetics is done in this chapter.

## **5.2 Material and Preparation**

### **5.2.1 Materials**

The polymers of carboxymethyl cellulose, croscarmellose sodium and crospovidone used in the experiments in this chapter are the ingredients which are used in the realistic detergent products that are provided from the same supplier with the above experimental works. The GCAS of carboxymethyl cellulose is 10070788

NP-025 and the activity is 72.6% which is tested by Procter & Gamble. The GCAS of Croscarmellose sodium is 74811-65-7 and the activity is 100% which is tested by Procter & Gamble. Crospovidone powders are provided by BASF SE Chemical Company from the product of Kollidon® CL. The Art. of this product is 50000696 and Lot. is 18942636W0. The chemical structure of Kollidon® CL is the cross-linked homopolymer of N-vinyl-2-pyrrolidone.

The particles of these 3 kinds of polymers are tested respectively by SEM to show the different structure. According to the SEM results shown in Figure 5.2, 5.3 and 5.4, it is clearly shown that all these 3 kinds of polymers can be regarded as agglomerations. PVPP has the most compaction structure but CMC shows the loosest structure. The agglomerates in CMC presents the different shapes and sizes, however the agglomerates in CCMC and PVPP have a relatively uniform shape and size. In another word, the structure of CMC can be said as loose irregular agglomerations, the structure of CCMC is related to the tubular agglomerations and PVPP has the compacted structure with floccule agglomerates.

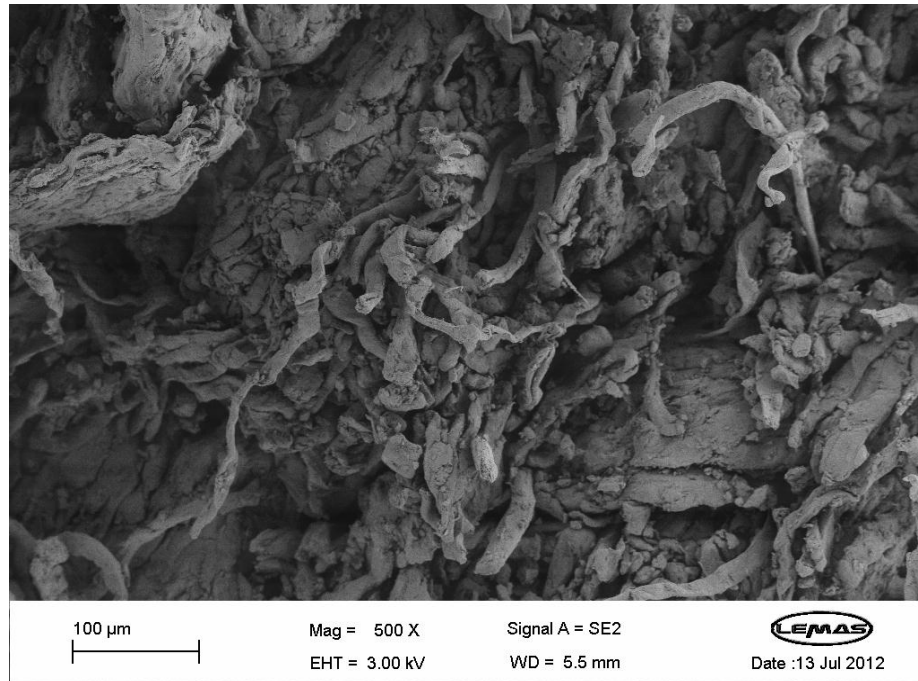


**Figure 5.2.** SEM image of carboxymethyl cellulose

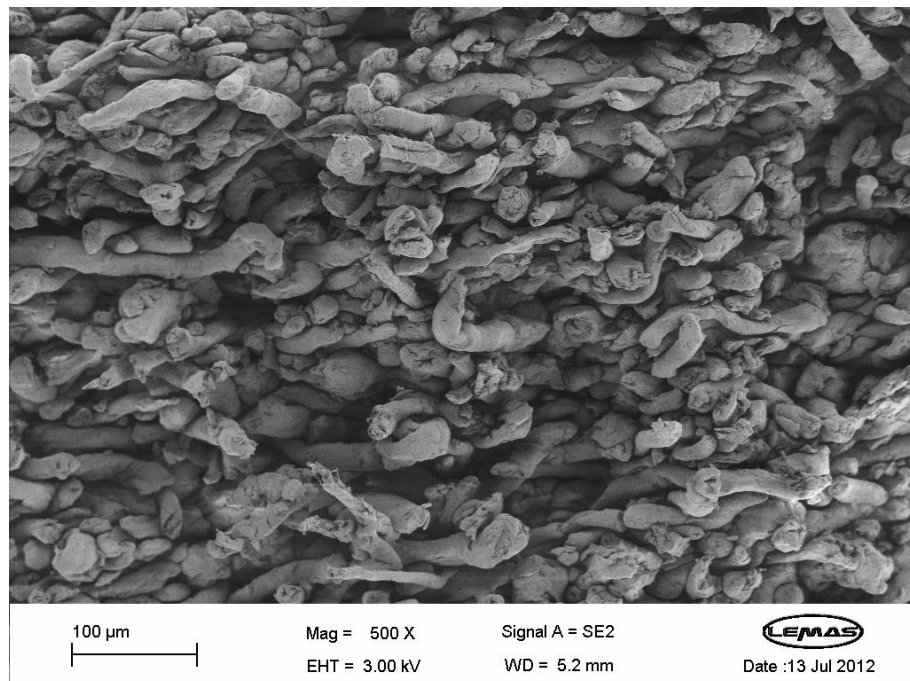


**Figure 5.3.** SEM image of croscarmellose sodium

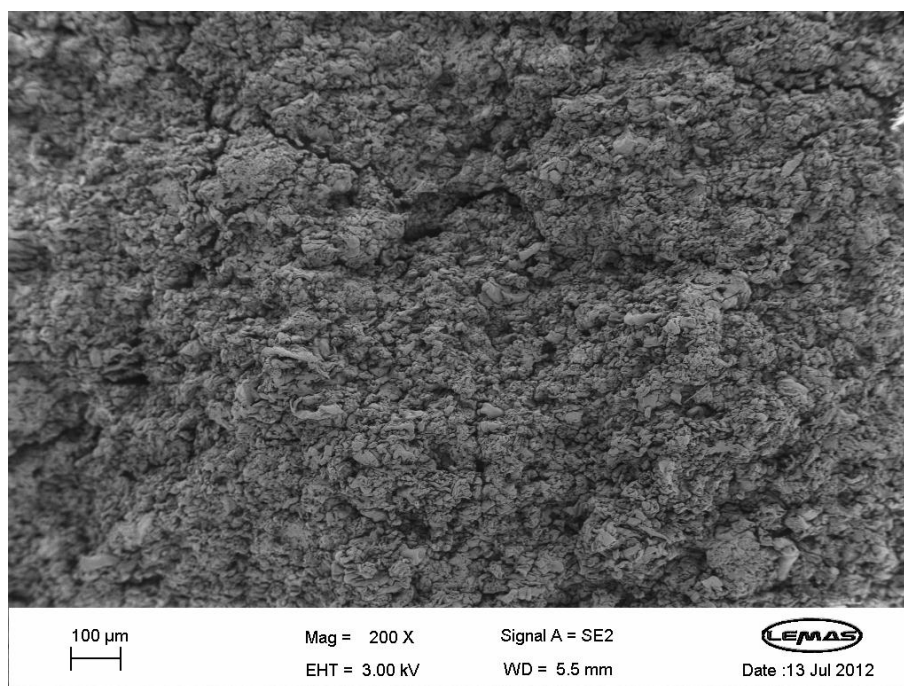


**Figure 5.4.** SEM image of crospovidone

### **5.2.2 Preparation of Materials**

The tablets used in dissolution experiments are 3 kinds of 2-component tablet with 2 different weight ratios. Therefore, the materials are prepared into 6 groups depending on different ingredients and weight ratios. The weight ratios of polymer in one tablet are 3% and 5% respectively which are suggested according from the practical production of Procter & Gamble. The prepared sample particles of each group are placed in a glass bottle which can be sealed to avoid of wetting with the label of No. 1-6.

The prepared particles in bottle 1-6 are: 0.3g carboxymethyl cellulose mixed with 9.7g sodium carbonate, 0.3g croscarmellose sodium mixed with 9.7g sodium carbonate, 0.3g crospovidone mixed with 9.7g sodium carbonate, 0.5g carboxymethyl cellulose mixed with 9.5g sodium carbonate, 0.5g croscarmellose sodium mixed with 9.5g sodium carbonate and 0.5g crospovidone mixed with 9.5g

sodium carbonate respectively.

To ensure the mixture of ingredients in every bottle is sufficient and polymer particles are well enough in sodium carbonate powders, every bottle is placed in the dry powder rotator (Glas-Col® Dry Powder Rotator) to be rotated with 40rpm over 12 hours. The mixed particles from each bottle are directly compressed into tablet of well-defined size and shape by a manual tablet compressor (Baileigh Industrial Compression Machine) with the same compressing pressure of 20KN. The compaction force of 20KN is applied during the fabrication of tablets. Every tablet has the same mass of 0.3g, and has the cylindrical shape with 10mm diameter and 3mm height. The tablet from every bottle is produced with the same amount of mass and preparation method of pressure and mold. Therefore the tablet from every bottle is expected to have the same internal structure. In this way, the effect of internal structure can be minimized.

To define and examine the mixture quality of every type of polymer within composite tablet, the random dissolution tests with conductivity measurement are carried out at first. For each type of composite tablet, three tablets are picked out randomly to be dissolved under the totally same dissolution situations. With measured values, the final conductivity of these three tablets are recorded and compared. In this work, the random tablet dissolution test of final conductivity value for each type of composite tablet is shown within 0.1mS. Based on the calibration of dissolved amount of sodium carbonate with conductivity shown previously, the amount of sodium carbonate from every tablet from the same group could be controlled within 1%. That can be regarded as that the composite tablets from same group own the same proportion of polymer and sodium carbonate.

### **5.3 Experimental Methodology**

The experiment is undertaken in this work with the aim of investigating and quantifying the dissolution kinetics of 2-component tablets by the experimental conductivity method under different temperatures. Therefore, the effect of carboxymethyl cellulose, croscarmellose sodium and crospovidone on the dissolution kinetics of tablet can be studied and quantified respectively under different temperatures. Also the effect of these 3 kinds of polymer on dissolution kinetics can be compared from different weight ratios to show how the weight ratio of ingredients influencing the utility of polymer on dissolution kinetics. Because the tablets are dissolved under different temperatures, the effect of temperature on dissolution kinetics of tablet can be quantified and investigated in this way. It is noting that the effect of these 3 kinds of polymer on dissolution kinetics is studied by comparing with the dissolution kinetics of pure sodium carbonate tablets, therefore the dissolution experiments of pure sodium carbonate tablet are needed to be done with the same experimental method.

A typical dissolution experiment for composite tablet can be processed as the same experimental method and same experimental equipment including hot plate, temperature controller and conductivity meter shown in Chapter 4.2. The dissolution experiments for each case are carried out with same set-up process of experiments of pure sodium carbonate tablets and shown in Figure 5.5.



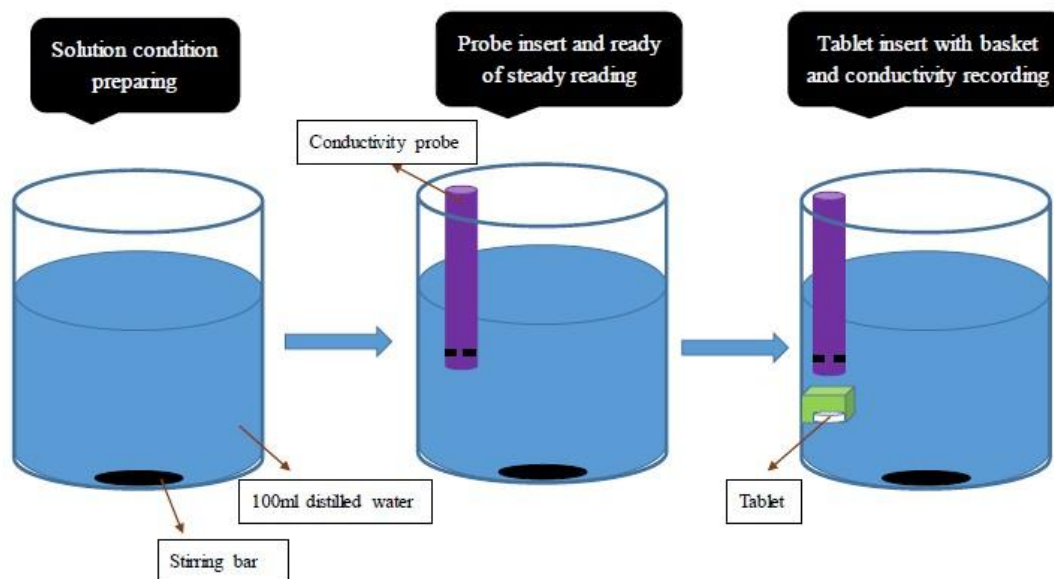


**Figure 5.5** Set-up process of typical dissolution experiment of composite tablet

A clean beaker is firstly prepared and filled with 100ml distilled water. The beaker is then placed in a water bath. The water bath is placed on Ceramic Stirrer Digital Hot Plate to heat the water bath to a preset temperature. This allowed for degassing the water before the experiment. The temperature of distilled water as solvent is controlled by the temperature controller automatically given at 20°C, 30°C, 40°C, 50°C and 60°C. The accuracy of temperature control is within  $\pm 1$  k. Also the solution is stirred at 300RPM for all cases by a magnetic stirring bar at the bottom of the beaker induced by the hot plate.

A conductivity probe from a portable conductivity meter of Conductivity TDS Portable Meter PHH244 is inserted vertically into the beaker to measure the conductivity with function of time. The distance from the sensor on the probe to the bottom of beaker is fixed at 20mm. When the probe and conductivity meter is set accurately, a tablet is placed very rapidly at the bottom of the beaker just below the probe. The reading of the conductivity in solvent is recording from the meter through the whole experiment process until the completion of tablet dissolution.

## **5.4 Mathematical Model**

According to the experiments used to analyze the dissolution of sodium carbonate tablets that are represented in Chapter 4, the preferred mathematical model for quantifying the dissolution kinetics of tablets is Hixson-Crowell model. Comparing with the pure sodium carbonate tablets, the physical behaviors of sample tablets including shape, size, weight and structure used in this chapter have the minimized differences. The addition of polymers in sodium carbonate tablets may affect the dissolution kinetics greatly, however the physical dissolution process related to the assumptions of mathematical model used to quantify the dissolution kinetics have not changed. In this way, the mathematical model applied to pure sodium carbonate tablet experiments is also appropriate to be used to quantify the dissolution kinetics of polymer-sodium carbonate tablets. Therefore, Hixson-Crowell mathematical model is chosen to be used in this work.

## **5.5 Results and Discussions**

For the discussion of dissolution mechanism of composite tablet in solution, the mechanism of dissolution process of composite tablet with Hixson-Crowell model used in this work can be also regarded as the dissolution reactions that happen at the tablet surface as function of time. With the dissolution reactions, sodium carbonate hydrolyzes into ions occurs at tablet surface. and sodium carbonate tablet then may disintegrate successively depending on external stirring conditions, as well as the effect of polymers used in this work on disintegration of tablet such as the effect of croscopolone as super integration agent. Also during this period, the tablet dimensions are assumed to diminish proportionally and the initial tablet geometrical form keeps as constant. After dissolution reaction process, the diffusion process is

the way that dissolved ions diffuse through the diffusion layer into bulk. With this dissolution mechanism of tablet with Hixson-Crowell model, the dissolution rate of sodium carbonate tablet is greatly limited by the dissolution reaction rate of sodium carbonate particle in solution.

### **5.5.1 Dissolution Kinetics of Sodium Carbonate- Carboxymethyl Cellulose**

#### **Composite Tablet**

The sodium carbonate-carboxymethyl cellulose composite tablets used in this work are tested with SEM at first shown in Figure 5.5. According to Figure 5.5, the sodium carbonate-carboxymethyl cellulose composite tablet after compression show a relative similar surface as pure sodium carbonate tablet shown in Chapter 4. That means the adding of carboxymethyl cellulose has not shown apparent impact on SEM to change the surface property of tablet. Then the sodium carbonate-carboxymethyl cellulose composite tablets used in this work are tested with XRD to show the crystalline forms of each kind of composite tablet that are shown in Figure 5.6 and Figure 5.7. The measurement equipment and method of XRD is the same as shown in Chapter 4 for pure sodium carbonate tablet. According to Figure 5.6 and Figure 5.7, it is clearly shown sodium carbonate-carboxymethyl cellulose composite tablet shows the same peak trend and peak shape with pure sodium carbonate tablet. However, the peak position of sodium carbonate tablet shows a clear leftward panning comparing with pure sodium carbonate tablet, and the intensity of peak of sodium carbonate-carboxymethyl cellulose composite tablet is higher than pure sodium carbonate tablet. According to the basic theoretical model of XRD, Bragg Law, the results shown in Figure 5.6 and Figure 5.7 prove that after compression with adding carboxymethyl cellulose, the crystal size of sodium carbonate becomes larger and the layer distance of diffraction surface becomes longer. These results

provide useful information to discuss that to make the dissolution happening, the energy that breaks the bond between sodium atom, carbon atom and oxygen atom from sodium carbonate-carboxymethyl cellulose composite tablet might be smaller than the breaking energy that for pure sodium carbonate tablet.

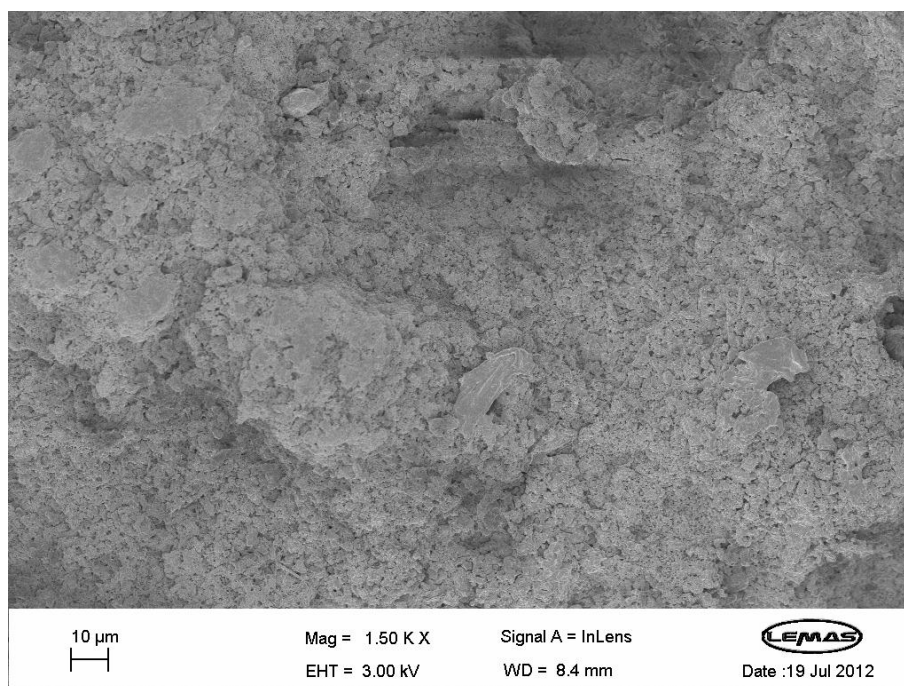


**Figure 5.5.** SEM image of tablet with mixture of sodium carbonate and carboxymethyl cellulose

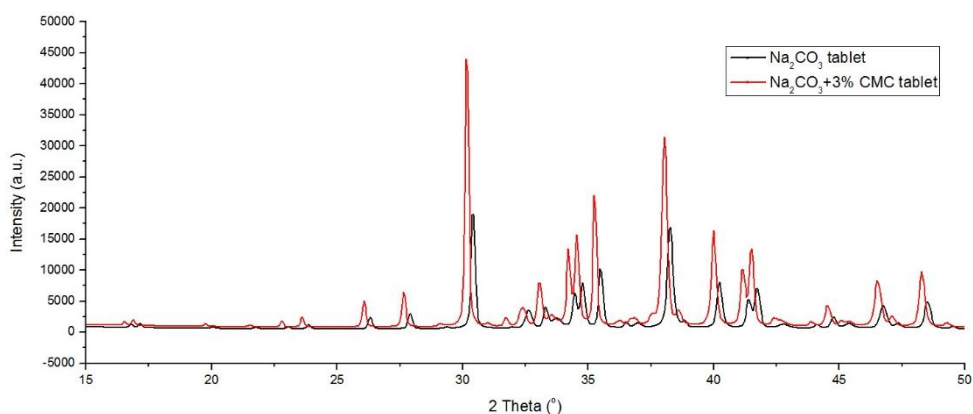


**Figure 5.6** XRD test of composite tablet containing 3% carboxymethyl cellulose comparing with pure sodium carbonate tablet

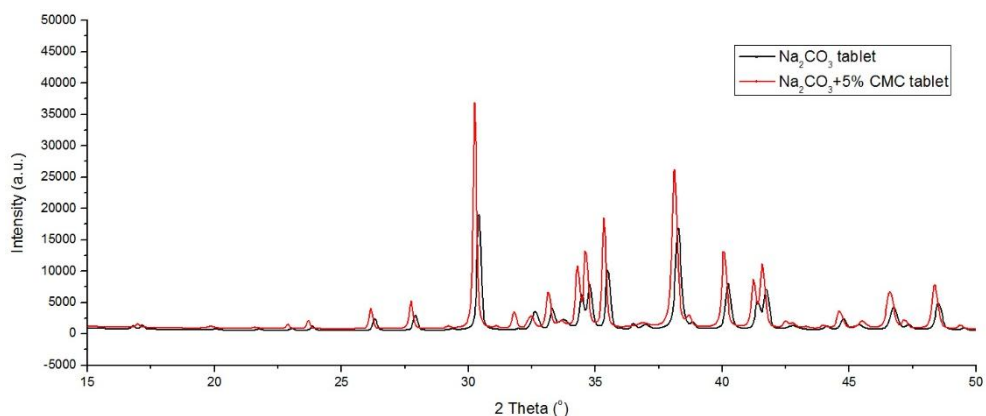


**Figure 5.7** XRD test of composite tablet containing 5% carboxymethyl cellulose comparing with pure sodium carbonate tablet

To analyze the dissolution experiment and measured dissolution data, an example of composite tablet containing 3% carboxymethyl cellulose dissolving under 30°C is expressed to show the analysis method and step of measured dissolution data. Based on the dissolution experiments, the conductivity values of composite tablet containing 3% carboxymethyl cellulose are recorded as function of time. The measured conductivity values of composite tablet containing 3% carboxymethyl cellulose under 30°C are shown in Table 5.1.

**Table 5.1** Conductivity values of composite tablet containing 3% carboxymethyl cellulose under 30°C

Dissolution time (S)	Conductivity (mS)	Dissolution time (S)	Conductivity (mS)
10	0.114	240	3.6
20	0.36	250	3.69
30	0.544	260	3.78
40	0.722	270	3.92
50	0.907	280	4.01
60	1.063	290	4.09
70	1.246	300	4.17
80	1.38	310	4.26
90	1.543	320	4.34
100	1.704	330	4.43
110	1.86	340	4.5
120	2.03	350	4.59
130	2.14	360	4.66
140	2.27	370	4.75
150	2.42	380	4.79
160	2.57	390	4.83
170	2.72	400	4.89
180	2.9	410	4.92

190	3.03	420	4.97
200	3.14	430	4.99
210	3.27	440	5.02
220	3.38	450	5.03
230	3.49		

With measured conductivity values shown in Table 5.1, the amount of dissolved sodium carbonate can be calculated with the calibration relation shown in Figure 4.7 as  $COND_t = 18.91M_t$ . With this calibration relation, the dissolved amount of sodium carbonate are determined and shown in Table 5.2.

**Table 5.2** Dissolved amount of sodium carbonate within composite tablet containing 3% carboxymethyl cellulose under 30°C

Dissolution time (S)	Dissolved amount (g)	Dissolution time (S)	Dissolved amount (g)
10	0.006	240	0.1904
20	0.019	250	0.1951
30	0.0288	260	0.1999
40	0.0382	270	0.2073
50	0.048	280	0.2121
60	0.0562	290	0.2163
70	0.0659	300	0.2205
80	0.073	310	0.2253
90	0.0816	320	0.2295
100	0.0901	330	0.2343
110	0.0984	340	0.238
120	0.1074	350	0.2427
130	0.1132	360	0.2464
140	0.12	370	0.2512
150	0.128	380	0.2533
160	0.1359	390	0.2554
170	0.1438	400	0.2586
180	0.1534	410	0.2602
190	0.1602	420	0.2628
200	0.166	430	0.2639
210	0.1729	440	0.2655
220	0.1787	450	0.266
230	0.1846		

Because composite tablet used in this work is dissolved into 100ml distilled water, the concentration of sodium carbonate from dissolved composite tablet containing 3% carboxymethyl cellulose under 30°C in solution is determined and shown in Table 5.3. And the ratio of dissolved amount of sodium carbonate from dissolved composite tablet containing 3% carboxymethyl cellulose as function of time is shown in Figure 5.8.

**Table 5.3** Concentration of sodium carbonate from composite tablet containing 3% carboxymethyl cellulose in solution under 30°C

Dissolution time (S)	Concentration (g/ml)	Dissolution time (S)	Concentration (g/ml)
10	6.03E-05	240	0.001904
20	0.00019	250	0.001951
30	0.000288	260	0.001999
40	0.000382	270	0.002073
50	0.00048	280	0.002121
60	0.000562	290	0.002163
70	0.000659	300	0.002205
80	0.00073	310	0.002253
90	0.000816	320	0.002295
100	0.000901	330	0.002343
110	0.000984	340	0.00238
120	0.001074	350	0.002427
130	0.001132	360	0.002464
140	0.0012	370	0.002512
150	0.00128	380	0.002533
160	0.001359	390	0.002554
170	0.001438	400	0.002586
180	0.001534	410	0.002602
190	0.001602	420	0.002628
200	0.00166	430	0.002639
210	0.001729	440	0.002655
220	0.001787	450	0.00266
230	0.001846		

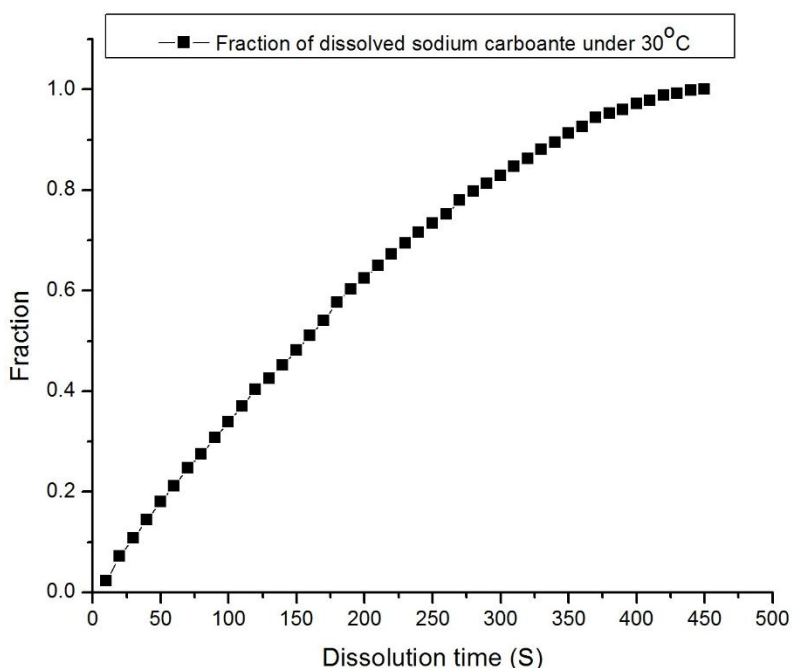


**Figure 5.8** Ratio of dissolved sodium carbonate from composite tablet containing 3% carboxymethyl cellulose under 30°C

With the measured dissolution data above, the next step is the analysis of dissolution rate constant with Hixson-Crowell model. In this way, the dissolution

rate constant is fitted with the equation of Hixson-Crowell model that

$$W_0^{1/3} - W^{1/3} = K_H t \quad (5.1)$$

Where  $W_0$  is the initial amount of sodium carbonate tablet;  $W$  is the remaining undissolved amount of sodium carbonate from experimental measurement; and  $K_H$  is the dissolution rate constant.

As it has been discussed for quantifying tablet dissolution rate constant, a linear should be obtained for the experimental data if the dissolution process is matching the assumptions of mathematical model during the whole dissolution process that the shape factor of dissolved tablet should keep as a constant and only the diminishing of size of tablet happens during dissolution process. However, according to the observation of dissolution experiment of composite tablet, the tablet dissolution process is not following the assumption of Hixson-Crowell model for the whole dissolution process when the undissolved composite tablet is thinner and smaller enough as it is very unlikely to keep as a whole tablet. That means once the remaining sodium carbonate tablet is lower than a possible amount, the tablet will be disintegrated into pieces due to the external stirring force from solution. The disintegration is not only from the effect of external stirring condition, but also comes from the effect of polymers used in this work. As adding carboxymethyl cellulose, the important dispersion functions of carboxymethyl cellulose leading to the disintegration of composite tablet becomes more likely. Therefore, the practical dissolution of sodium carbonate-carboxymethyl cellulose composite tablet in this work can be said has two ranges that the tablet will dissolve with dissolution limited process as a whole, and once the tablet starts to disintegrate, the dissolution steps into disintegration process. In this way, the fitting of measured experimental data



with Hixson-Crowell model should be carried out for two ranges. One is the dissolution limited range, and another is disintegration range. Therefore, the linear fitting with Hixson-Crowell model for dissolution limited range is the appropriate method to quantify the dissolution rate constant for dissolution of experiment with Hixson-Crowell model.

According to the measurements of dissolution experiments and the observation of dissolution process, the time period for disintegration range can be recorded and used to determine the time period of dissolution limited range and disintegration range for each case. In this way, the linear fitting with Hixson-Crowell model for dissolution limited range of each case is carried out to quantify the dissolution rate constant of corresponding experiment. In this way, based on the measured data, the fitting with equation (5.1) for dissolution limited range is shown in Figure 5.9.

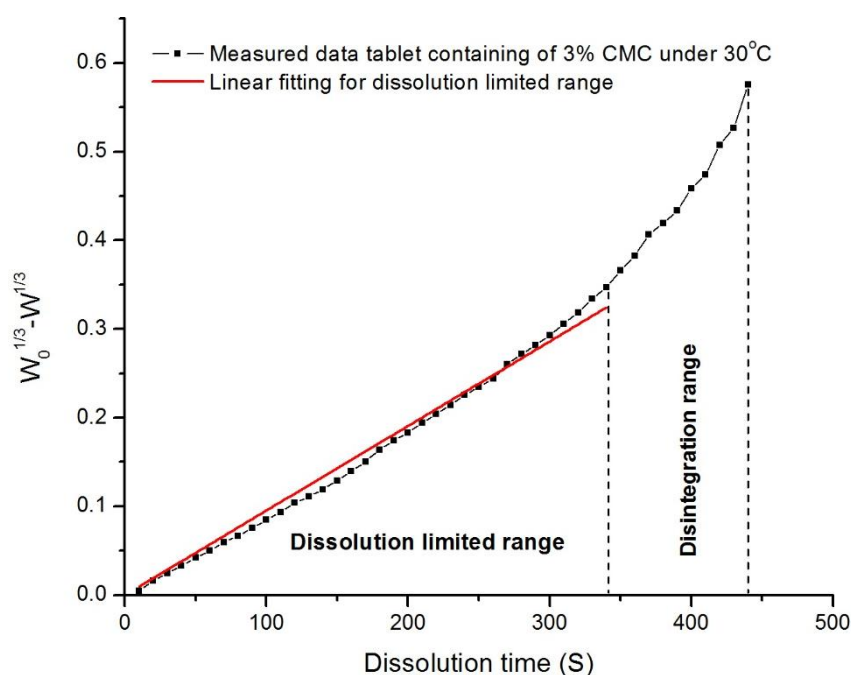
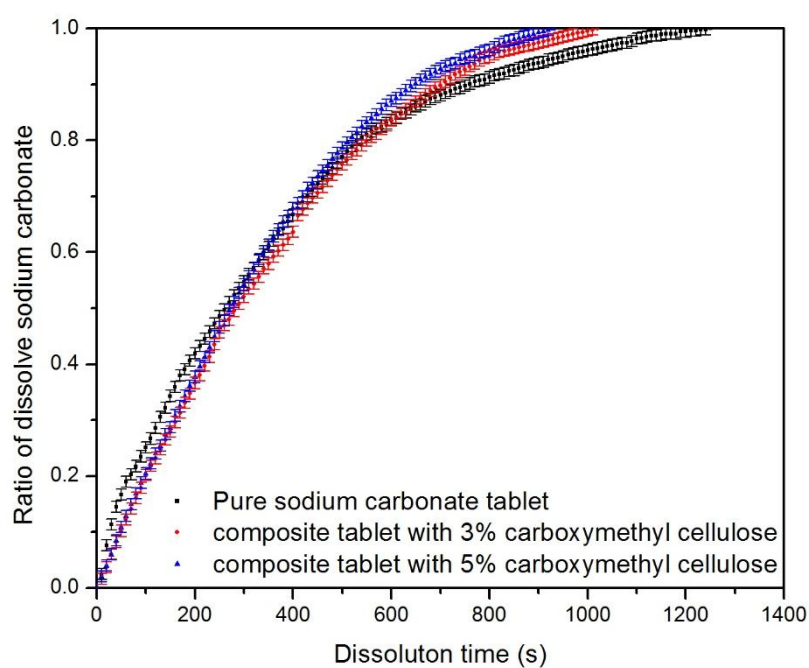


**Figure 5.9** Fitting of dissolution experiment for composite tablet containing 3% CMC under 30°C

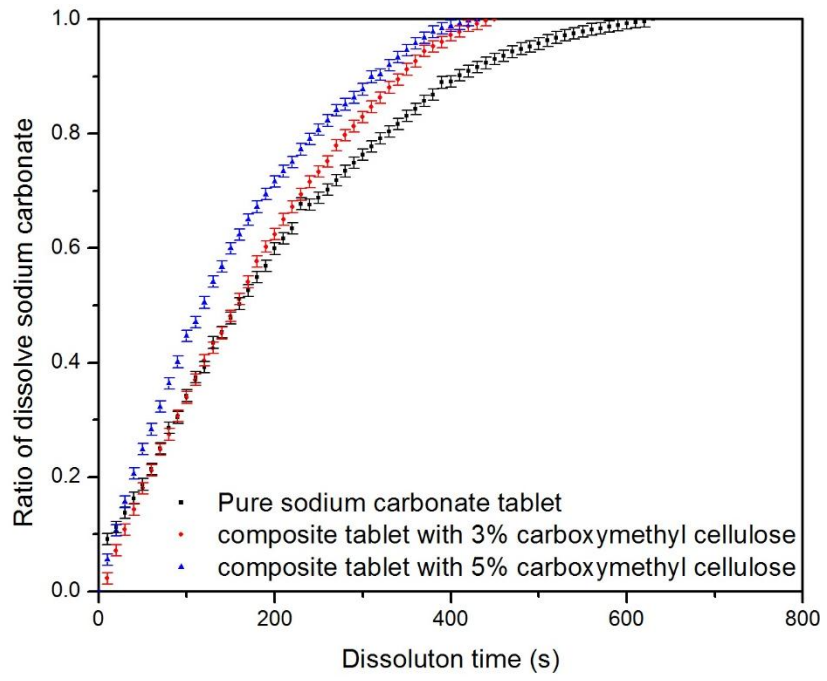
Based on the analysis for quantifying tablet dissolution rate constant, the fitting result in dissolution limited range is the dissolution rate constant of measured

composite tablet with Hixson-Crowell model. According to Figure 5.9, the dissolution rate constant for composite tablet containing 3% carboxymethyl cellulose under 30°C is **0.000954** (g<sup>1/3</sup>/S).

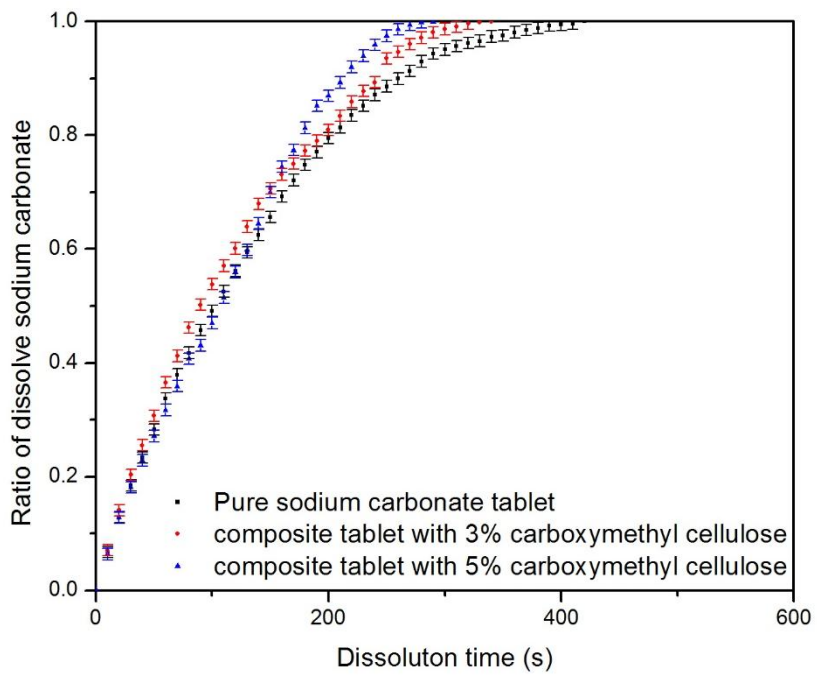
Following the same analysis method and step shown above of the example of composite tablet containing 3% carboxymethyl cellulose under 30°C, the measured dissolution data for each case in this work are shown below. The ratio of dissolved amount of sodium carbonate for each case are shown in Figure 5.10.



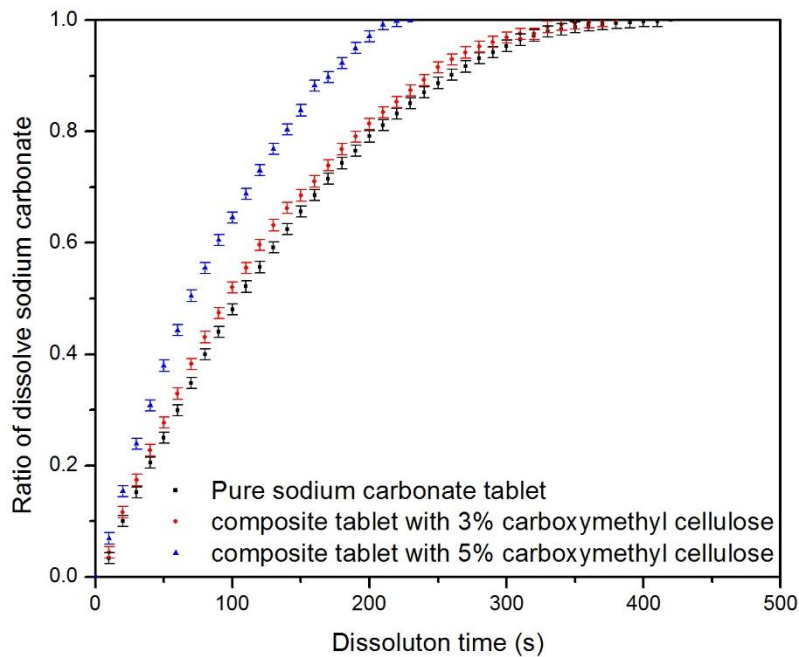
(a)



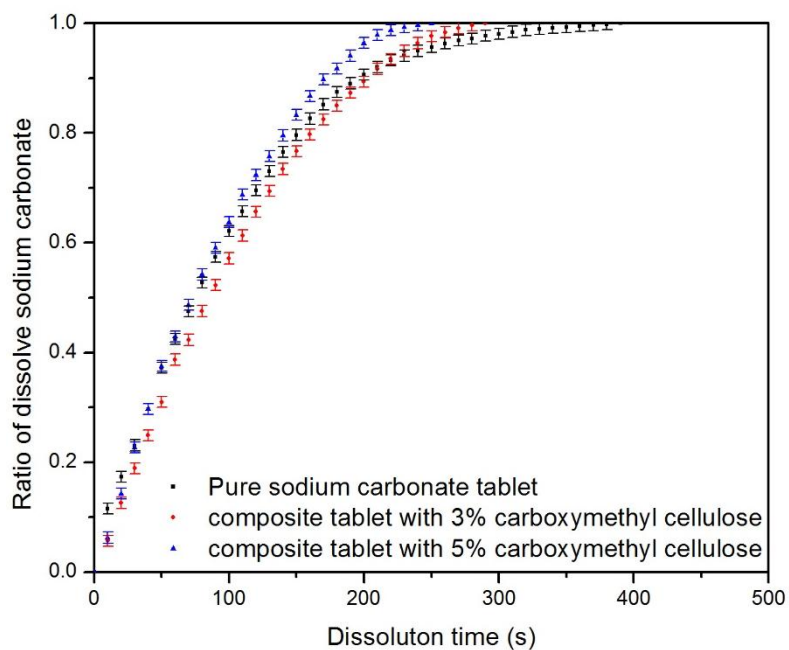
(b)



(c)



(d)



(e)

**Figure 5.10.** Ratio of dissolved amount of sodium carbonate from pure sodium carbonate tablet, composite tablet containing 3% carboxymethyl cellulose and 5% carboxymethyl cellulose under (a) 20°C; (b) 30°C; (c) 40°C; (d) 50°C; (e) 60°C.

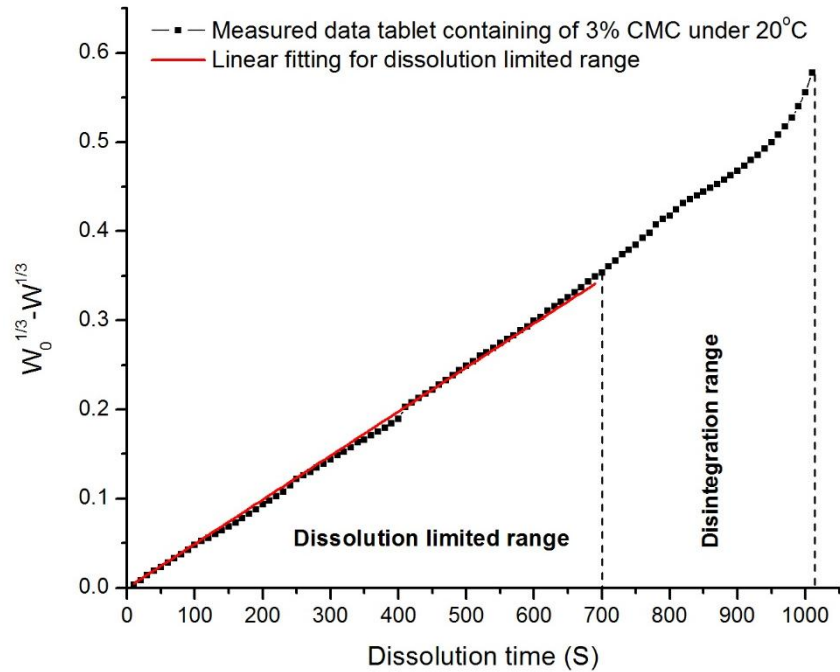
Through the results in Figure 5.10, it is clearly shown that the sodium carbonate-carboxymethyl cellulose composite tablets has shorter dissolution time comparing

with pure sodium carbonate tablets. Evidently, the dissolution time of composite tablet containing 5% carboxymethyl cellulose is shorter than the composite tablets containing 3% carboxymethyl cellulose.

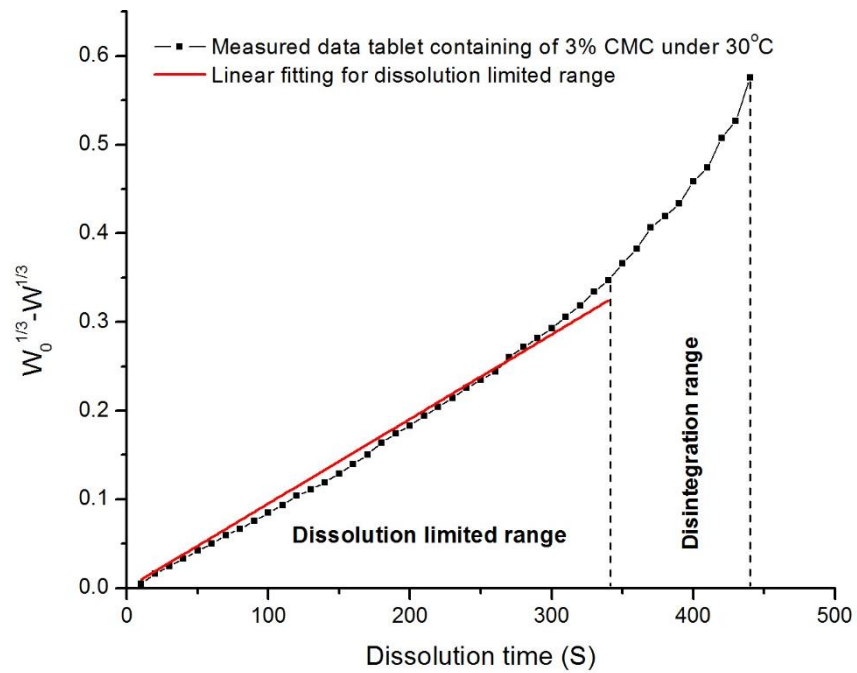
According to Figure 5.10, the dissolution speed is regarded as the gradient of each time point and it is changing with the function of dissolution time. Therefore, it is impracticable to evaluate the effect of carboxymethyl cellulose on dissolution rate from one specific time to another. The evaluation of effect of carboxymethyl cellulose is therefore suggested to be viewed from the overall effect through the whole dissolution process. According to the results shown in Figure 5.10, the highest dissolution rate for every kind of tablet is at the starting dissolution time, and then decreases through the dissolution process till almost 0. For the overall evaluation of dissolution rate of every kind of tablet, adding carboxymethyl cellulose has the positive effect to enhance the dissolution rate of tablet, and more amount of carboxymethyl cellulose shows a better enhancement. It is worth noting that adding carboxymethyl cellulose seems to be finite on the effect on dissolution rate. This conclusion is based on the overall general evaluation of dissolution curve. Therefore the dissolution rate constant in this case is needed to be quantified by Hixson-Crowell model to show the effect of carboxymethyl cellulose on dissolution kinetics accurately.

Hixson-Crowell model is applied to quantify the dissolution rate constant in this case following the same method which is discussed previously. The fitting with Hixson-Crowell model for each case is suitable for dissolution limited range because of the phenomenon of tablet disintegration when the remaining tablet is lower than a possible certain amount. Therefore, the fitting with Hixson-Crowell model applied for dissolution limited range is applied in this work. In this way, a linear in

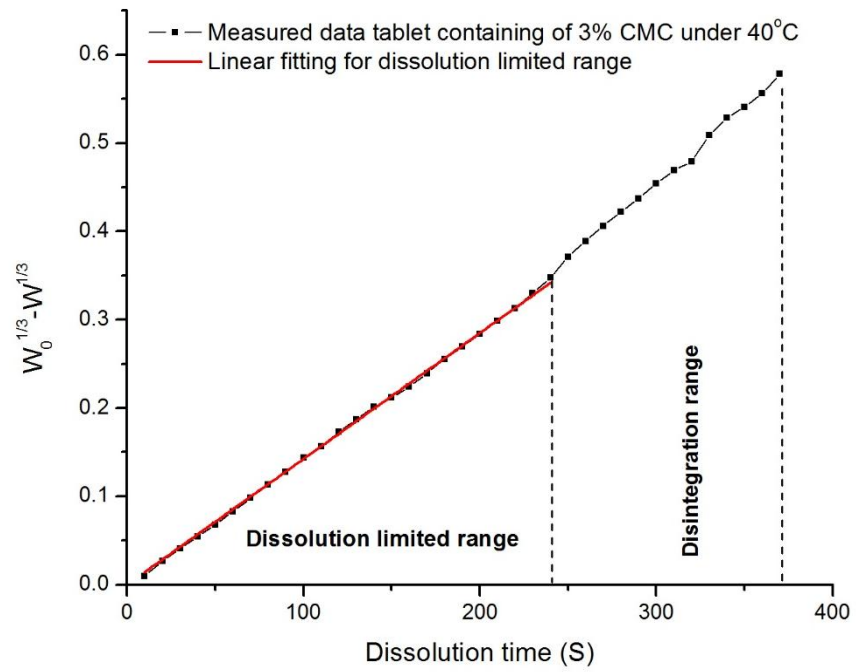
dissolution limited range is fitted and the gradient of this linear is regarded as the dissolution rate constant for corresponding dissolution experiment. The fitting results for each case are shown in Figure 5.11 and Figure 5.12.



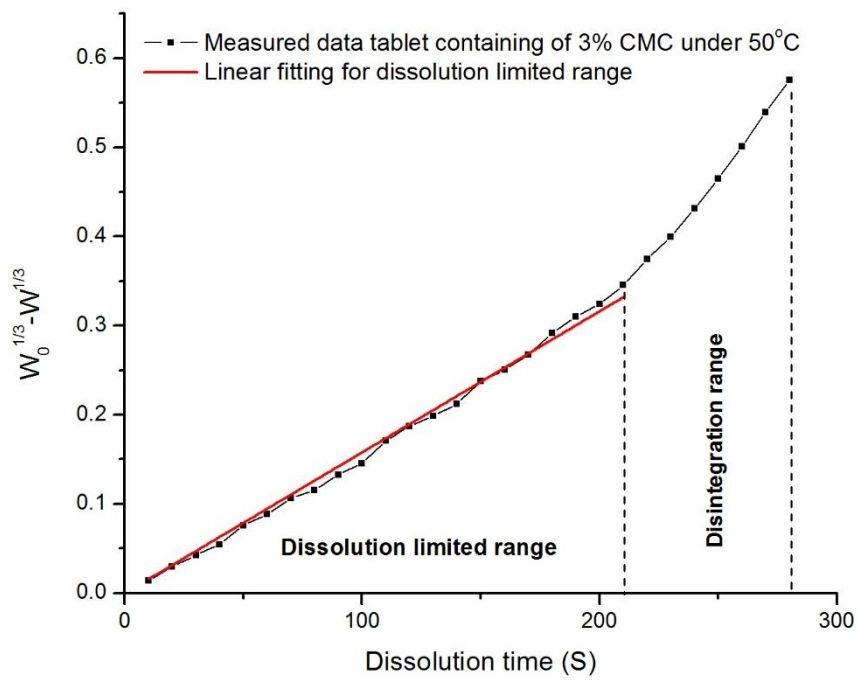
(a)



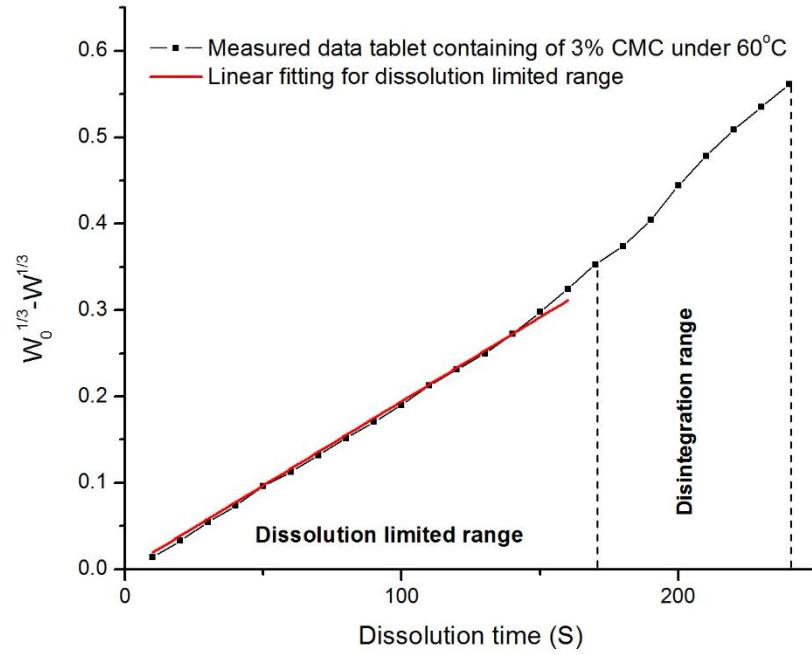
(b)



(c)

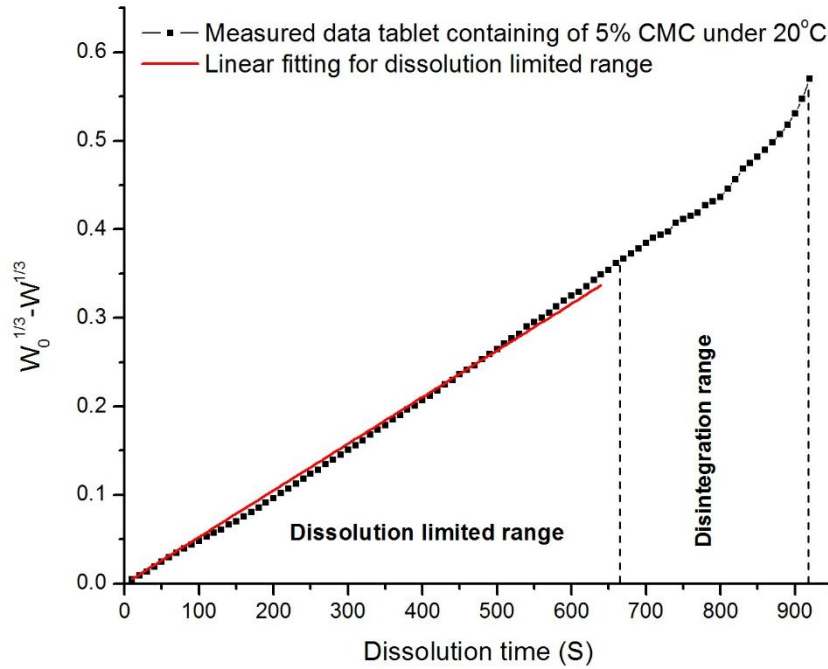


(d)



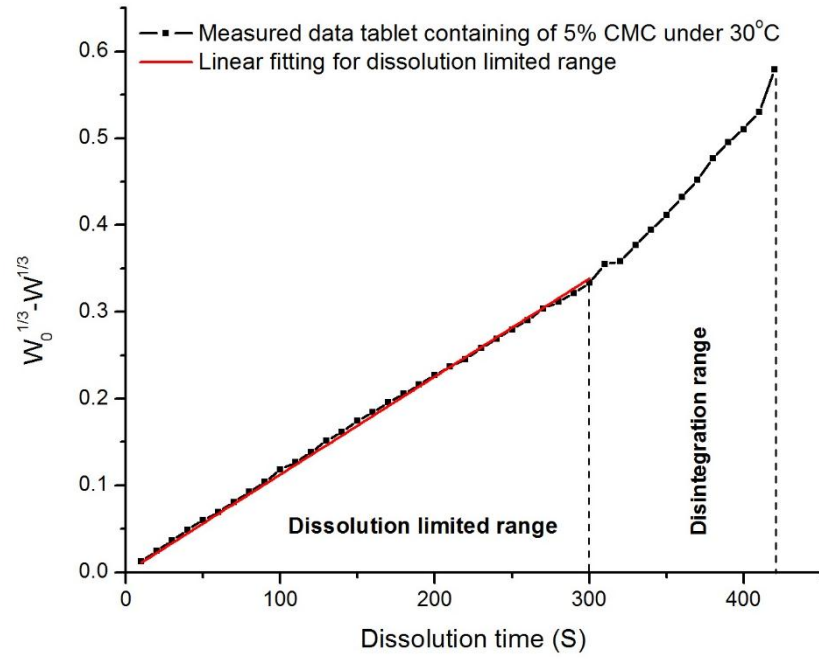
(e)

**Figure 5.11** Linear fitting of dissolution limited range with Hixson-Crowell model for composite tablet containing 3% carboxymethyl cellulose under (a) 20°C; (b) 30°C; (c) 40°C; (d) 50°C; (e) 60°C

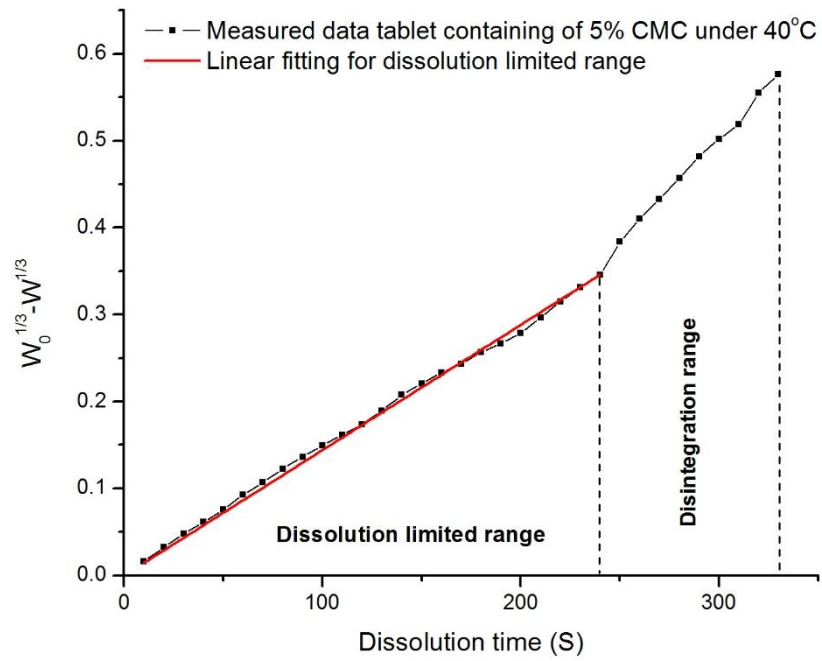


(a)

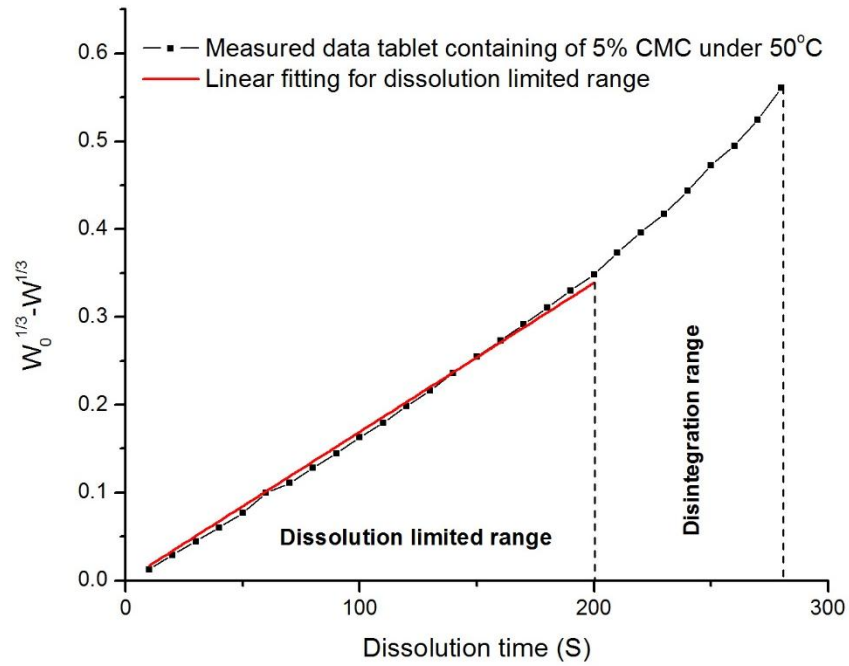




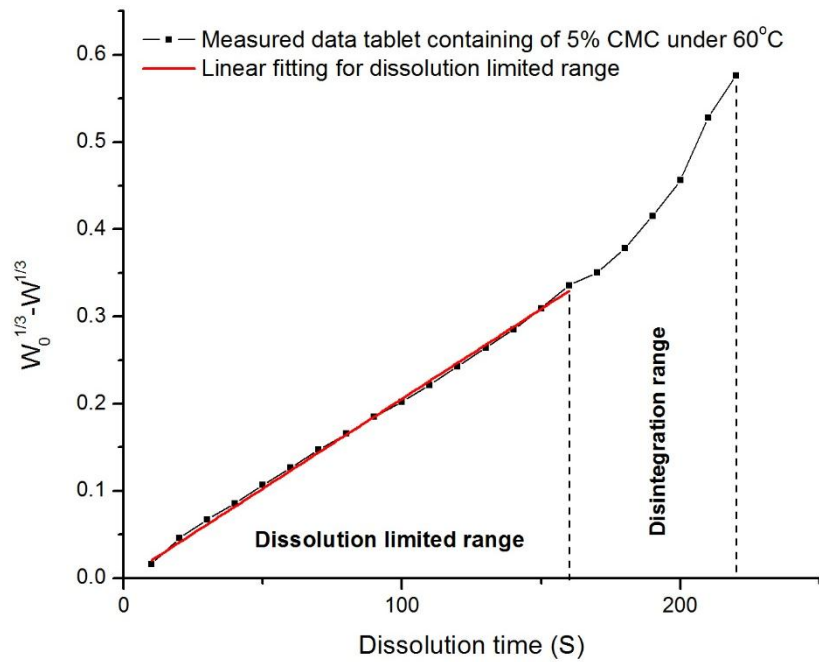
(b)



(c)



(d)



(e)

**Figure 5.12** Linear fitting of dissolution limited range with Hixson-Crowell model for composite tablet containing 5% carboxymethyl cellulose under (a) 20°C; (b) 30°C; (c) 40°C; (d) 50°C; (e) 60°C

According to the fitting results for dissolution limited range with Hixson-Crowell model of each case shown in Figure 5.11 and Figure 5.12, the dissolution rate

constant of every kind of tablet including pure sodium carbonate tablet, composite tablet containing 3% carboxymethyl cellulose tablet and 5% carboxymethyl cellulose tablet is quantified and represented in Figure 5.13.

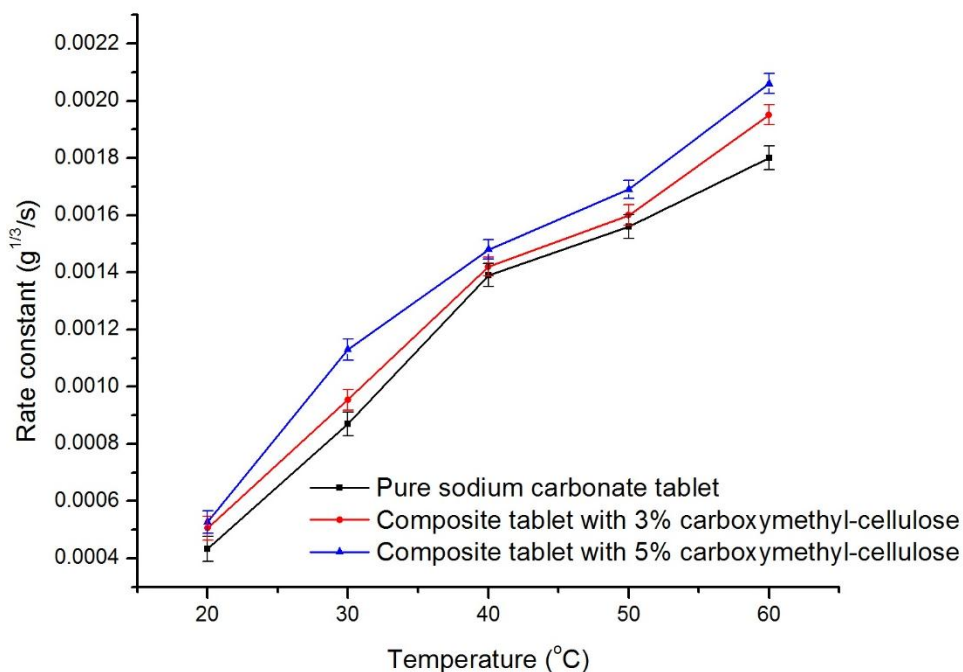


**Figure 5.13** Dissolution rate constant for pure sodium carbonate tablet, composite tablet with 3% carboxymethyl cellulose 5% carboxymethyl cellulose

Through the quantification of dissolution rate constant for 3 kinds of tablets in this work which is shown in Figure 5.13, the effect of carboxymethyl cellulose on dissolution rate constant shows a clear enhancement at every temperature. And also the more amount of carboxymethyl cellulose leads to a greater dissolution rate constant. These results proves the unique properties of carboxymethyl cellulose which are used as the dispersive additives in detergent due to its chemical structure of cellulose derivative with carboxymethyl groups bound to some hydroxyl groups. This chemical structure makes carboxymethyl cellulose own high water soluble and dispersion functions. The strong dispersion function of carboxymethyl cellulose accelerates the dispersion of particles apart of the tablet from tablet starting to

dissolve. That explains why the dissolution rate constant is accelerated by adding carboxymethyl cellulose.

It also needs to be noticed that the dissolution rate constant increases with temperature significantly for every kind of tablet. The effect of temperature is easy to understand due to the aggravation of particle motions from the increasing of temperature. When the solvent temperature is at 20°C, the enhancement on dissolution rate constant by adding more carboxymethyl cellulose exists, however the scale of this enhancement is in a small range. When the temperature keeps increasing, the enhancement of carboxymethyl cellulose from becomes more clearly and greater.

### **5.5.2 Dissolution Kinetics of Sodium Carbonate-Croscarmellose Sodium**

#### **Composite Tablet**

The composite tablets used in this work are sodium carbonate-croscarmellose sodium composite tablets containing 3% and 5% croscarmellose sodium respectively. As the dissolution experimental method and measured data analysis method have been detailed expressed in Chapter 5.5.1 of sodium carbonate-carboxymethyl cellulose composite tablet, and the dissolution experiments and data analysis used in this work are the same method as last section. Therefore, the measured data analysis from dissolution experiments of this work will be expressed directly.

The sodium carbonate-croscarmellose sodium composite tablets used in this work are tested with SEM at first shown in Figure 5.14. According to Figure 5.14, the sodium carbonate- croscarmellose sodium composite tablet after compression show a relative similar surface as pure sodium carbonate tablet shown in Chapter 4. That means the adding of croscarmellose sodium has not shown apparent impact on SEM

to change the surface of tablet. Then the sodium carbonate- croscarmellose sodium composite tablets used in this work are tested with XRD to show the crystalline forms of each kind of composite tablet that are shown in Figure 5.15 and Figure 5.16. The measurement equipment and method of XRD is the same as shown in Chapter 4 for pure sodium carbonate tablet. According to Figure 5.15 and Figure 5.16, it is shown sodium carbonate-croscarmellose sodium composite tablet shows the same peak trend and peak shape with pure sodium carbonate tablet. However, the peak position of sodium carbonate-croscarmellose sodium composite tablet shows a slightly leftward panning comparing with pure sodium carbonate tablet, and the intensity of peak of sodium carbonate-croscarmellose sodium composite tablet is higher than initial sodium carbonate particle. According to the basic theoretical model of XRD, Bragg Law, the results shown in Figure 5.15 and Figure 5.16 prove that after compression with adding croscarmellose sodium, the crystal size of sodium carbonate becomes larger and the layer distance of diffraction surface becomes slightly longer. These results provide useful information to discuss that to make the dissolution happening, the energy that breaks the bond between sodium atom, carbon atom and oxygen atom from sodium carbonate-croscarmellose sodium composite tablet might be slightly smaller than the breaking energy that for pure sodium carbonate tablet.

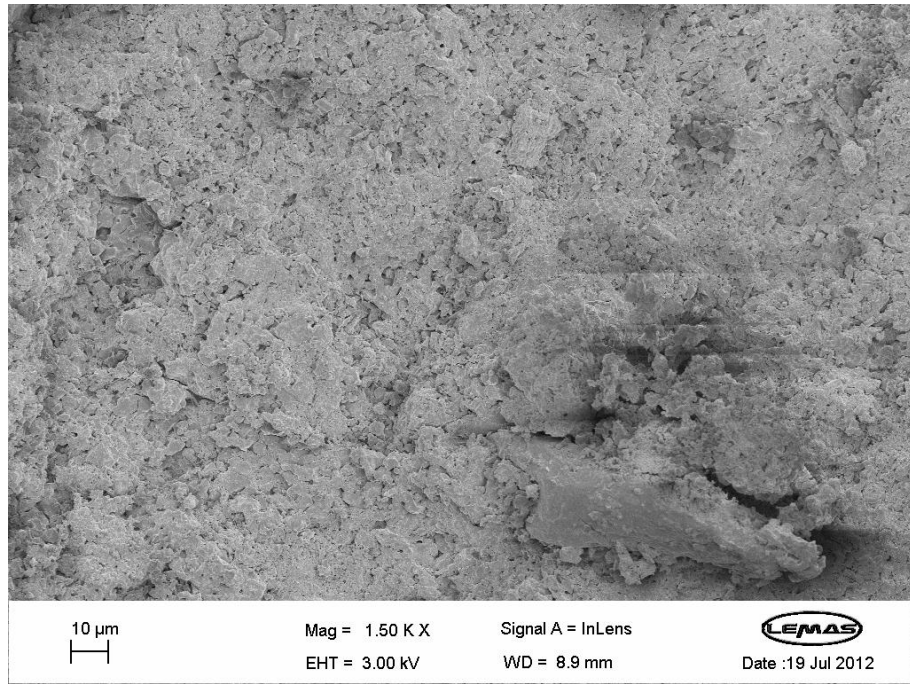


**Figure 5.14.** SEM image of sodium carbonate-crosscarmellose sodium composite tablet

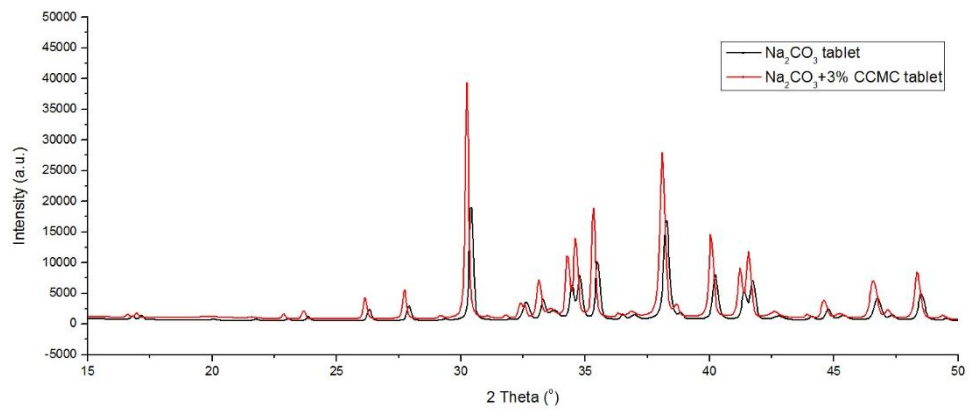


**Figure 5.15** XRD test of composite tablet containing 3% crosscarmellose sodium comparing with pure sodium carbonate tablet

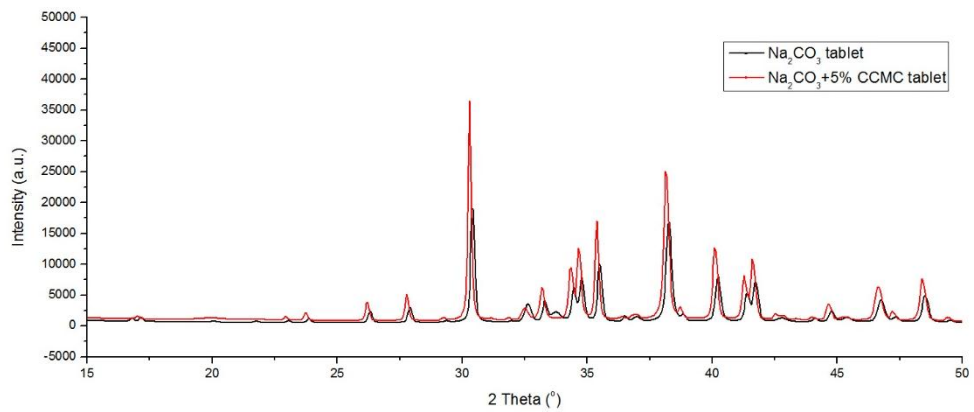


**Figure 5.16** XRD test of composite tablet containing 5% croscarmellose sodium comparing with pure sodium carbonate tablet

An example of dissolution experimental data of sodium carbonate-croscarmellose sodium composite tablets containing 3% croscarmellose sodium under 30°C are shown as the measured dissolution data analysis method. In this way, the conductivity values measured from dissolution experiment under 30°C are shown in Table 5.4.

**Table 5.4** Conductivity values of composite tablet containing 3% croscarmellose sodium under 30°C

Dissolution time (S)	Conductivity (mS)	Dissolution time (S)	Conductivity (mS)
10	0.0621	360	4.1
20	0.264	370	4.11
30	0.443	380	4.18
40	0.62	390	4.25
50	0.781	400	4.29
60	0.932	410	4.33
70	1.026	420	4.36
80	1.219	430	4.44
90	1.372	440	4.47
100	1.568	450	4.55
110	1.708	460	4.58
120	1.809	470	4.6
130	1.979	480	4.67
140	2.01	490	4.74
150	2.18	500	4.76
160	2.35	510	4.78
170	2.47	520	4.8
180	2.58	530	4.81
190	2.64	540	4.83
200	2.84	550	4.84
210	2.88	560	4.85
220	3.03	570	4.86
230	3.12	580	4.88
240	3.23	590	4.89
250	3.29	600	4.89
260	3.35	610	4.9
270	3.41	620	4.91
280	3.51	630	4.92
290	3.58	640	4.93
300	3.66	650	4.94
310	3.73	660	4.95
320	3.85	670	4.96
330	3.88	680	4.99
340	3.95	690	5.01
350	4.03		

With measured conductivity values shown in Table 5.4, the amount of dissolved

sodium carbonate can be calculated with the calibration relation shown in Figure 4.7 as  $COND_t = 18.91M_t$ . With this calibration relation, the dissolved amount of sodium carbonate from composite tablet are shown in Table 5.5.

**Table 5.5** Dissolved amount of sodium carbonate from composite tablet containing 3% croscarmellose sodium under 30°C

Dissolution time (S)	Dissolved amount (g)	Dissolution time (S)	Dissolved amount (g)
10	0.0033	360	0.2168
20	0.014	370	0.2173
30	0.0234	380	0.221
40	0.0328	390	0.2247
50	0.0413	400	0.2269
60	0.0493	410	0.229
70	0.0543	420	0.2306
80	0.0645	430	0.2348
90	0.0726	440	0.2364
100	0.0829	450	0.2406
110	0.0903	460	0.2422
120	0.0957	470	0.2433
130	0.1047	480	0.247
140	0.1063	490	0.2507
150	0.1153	500	0.2517
160	0.1243	510	0.2528
170	0.1306	520	0.2538
180	0.1364	530	0.2544
190	0.1396	540	0.2554
200	0.1502	550	0.2559
210	0.1523	560	0.2565
220	0.1602	570	0.257
230	0.165	580	0.2581
240	0.1708	590	0.2586
250	0.174	600	0.2586
260	0.1772	610	0.2591
270	0.1803	620	0.2597
280	0.1856	630	0.2602
290	0.1893	640	0.2607
300	0.1935	650	0.2612
310	0.1973	660	0.2618
320	0.2036	670	0.2623
330	0.2052	680	0.2639
340	0.2089	690	0.2649
350	0.2131		

Because composite tablet used in this work is dissolved into 100ml distilled water, the concentration of sodium carbonate from dissolved composite tablet containing 3% croscarmellose sodium under 30°C in solution is determined and shown in Table 5.6. And the ratio of dissolved amount of sodium carbonate from dissolved composite



tablet containing 3% croscarmellose sodium as function of time is shown in Figure 5.17.

**Table 5.6** Concentration of sodium carbonate from composite tablet containing 3% croscarmellose sodium in solution under 30°C

Dissolution time (S)	Concentration (g/ml)	Dissolution time (S)	Concentration (g/ml)
10	3.28E-05	360	0.002168
20	0.00014	370	0.002173
30	0.000234	380	0.00221
40	0.000328	390	0.002247
50	0.000413	400	0.002269
60	0.000493	410	0.00229
70	0.000543	420	0.002306
80	0.000645	430	0.002348
90	0.000726	440	0.002364
100	0.000829	450	0.002406
110	0.000903	460	0.002422
120	0.000957	470	0.002433
130	0.001047	480	0.00247
140	0.001063	490	0.002507
150	0.001153	500	0.002517
160	0.001243	510	0.002528
170	0.001306	520	0.002538
180	0.001364	530	0.002544
190	0.001396	540	0.002554
200	0.001502	550	0.002559
210	0.001523	560	0.002565
220	0.001602	570	0.00257
230	0.00165	580	0.002581
240	0.001708	590	0.002586
250	0.00174	600	0.002586
260	0.001772	610	0.002591
270	0.001803	620	0.002597
280	0.001856	630	0.002602
290	0.001893	640	0.002607
300	0.001935	650	0.002612
310	0.001973	660	0.002618
320	0.002036	670	0.002623
330	0.002052	680	0.002639
340	0.002089	690	0.002649
350	0.002131		

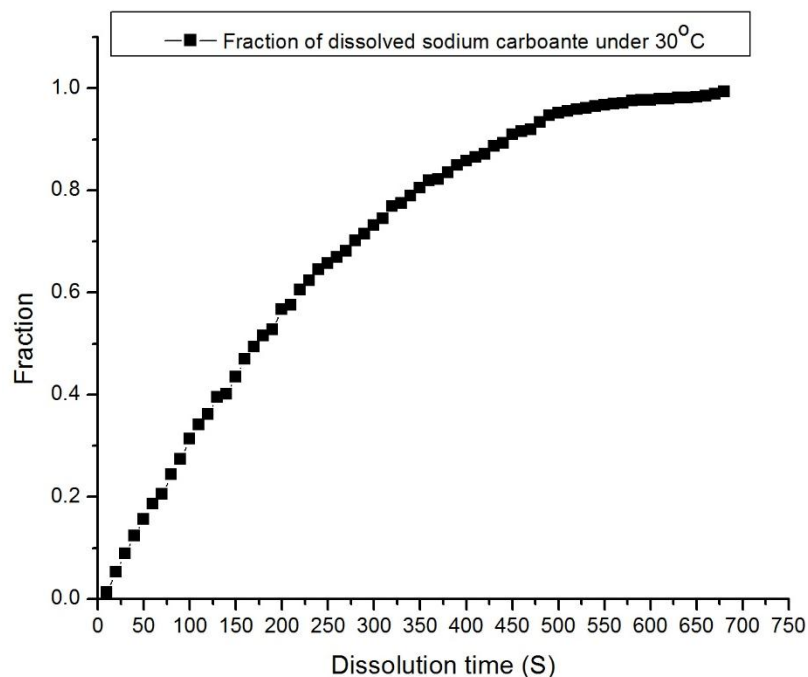


**Figure 5.17** Ratio of dissolved sodium carbonate from composite tablet containing 3% croscarmellose sodium under 30°C

As it has been discussed for the fitting of dissolution experiment data of tablet, a linear should be obtained for the experimental data if the dissolution process is matching the assumptions of mathematical model during the whole dissolution process that the shape factor of dissolved tablet should keep as a constant and only the diminishing of size of tablet happens during dissolution process. However, according to the observation of dissolution experiment of composite tablet, the tablet dissolution process is not following the assumption of Hixson-Crowell model for the whole dissolution process when the undissolved composite tablet is thinner and smaller enough as it is very unlikely to keep as a whole tablet. That means once the remaining sodium carbonate tablet is lower than a possible amount, the tablet will be disintegrated into pieces due to the external stirring force from solution. The disintegration is not only from the effect of external stirring condition, but also comes from the effect of polymers used in this work. As adding croscarmellose sodium, the important swelling functions of croscarmellose sodium leading to the

disintegration of composite tablet becomes more likely. Therefore, the practical dissolution of sodium carbonate-crosscarmellose sodium composite tablet in this work can be said has two ranges that the tablet will dissolve with dissolution limited process as a whole, and once the tablet starts to disintegrate, the dissolution steps into disintegration process. In this way, the fitting of measured experimental data with Hixson-Crowell model should be carried out for two ranges. One is the dissolution limited range, and another is disintegration range. Therefore, the linear fitting with Hixson-Crowell model for dissolution limited range is the appropriate method to quantify the dissolution rate constant for dissolution of experiment with Hixson-Crowell model. In this way, based on the measured dissolution data, the fitting with equation (5.1) for two ranges is shown in Figure 5.18.

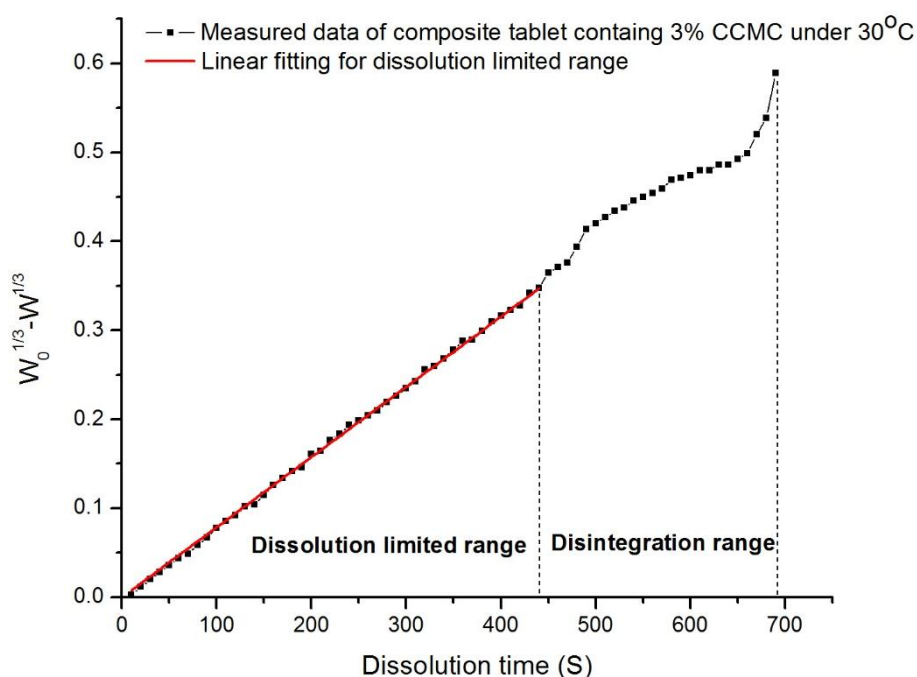
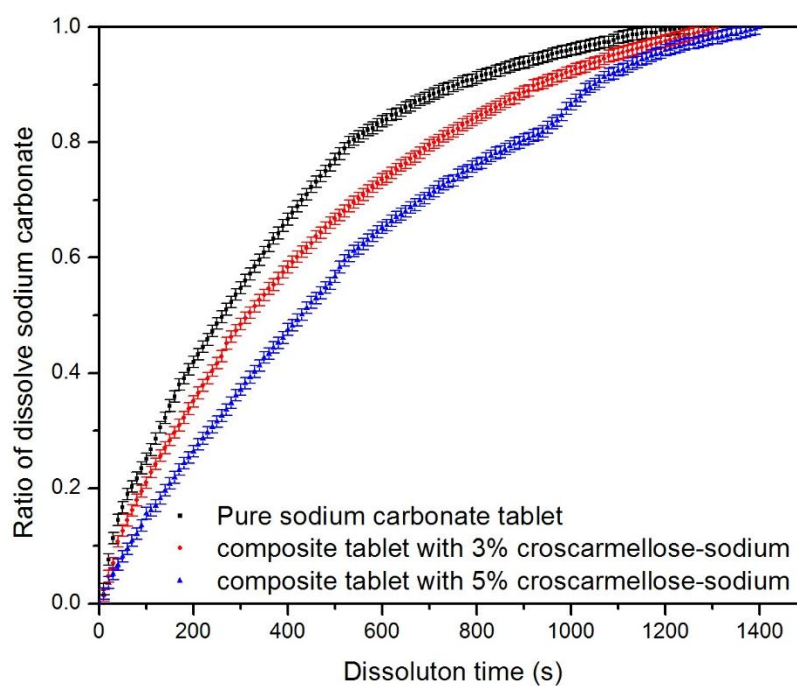


**Figure 5.18** Fitting of dissolution experiment for composite tablet containing 3% croscarmellose sodium under 30°C

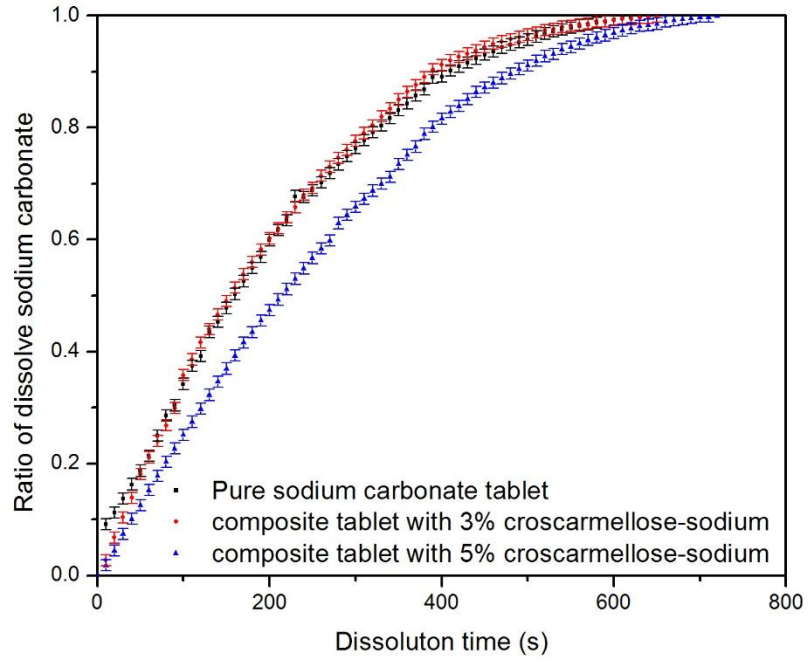
Based on the analysis for quantifying tablet dissolution rate constant, the fitting result in dissolution limited range is the dissolution rate constant of measured composite tablet with Hixson-Crowell model. According to Figure 5.18, the

dissolution rate constant for composite tablet containing 3% croscarmellose sodium under 30°C is **0.000788** ( $\text{g}^{1/3}/\text{S}$ ).

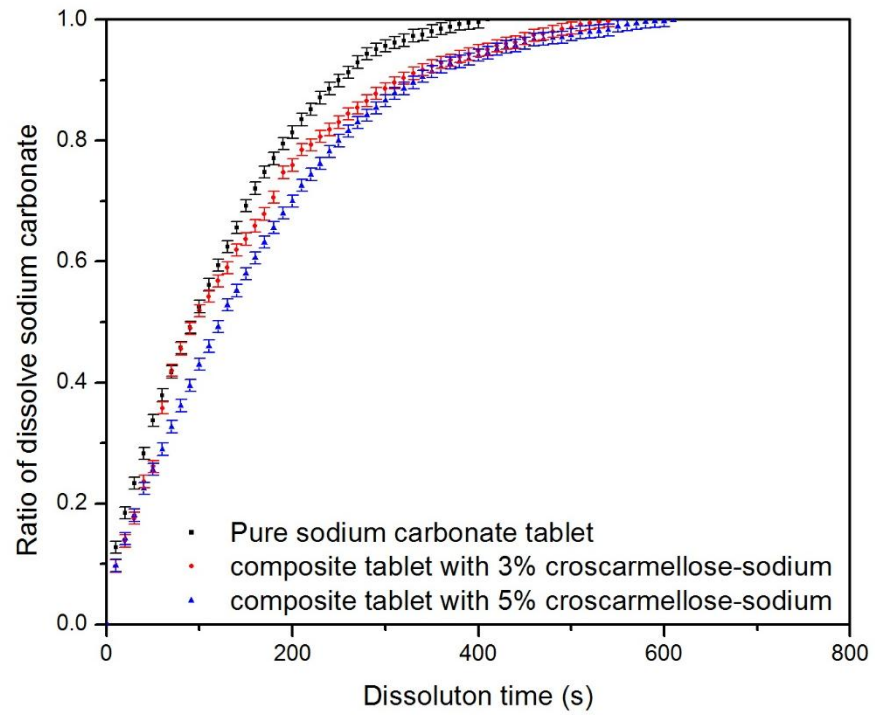
Following the same analysis method and step shown above of the example of composite tablet containing 3% croscarmellose sodium under 30°C, the measured dissolution data for each case in this work are shown below. The ratio of dissolved amount of sodium carbonate for each case are shown in Figure 5.19.



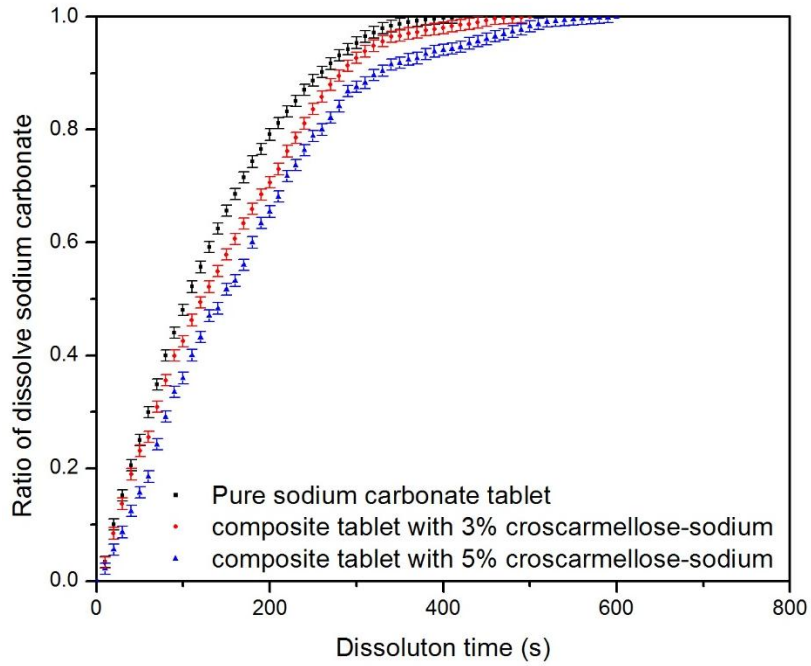
(a)



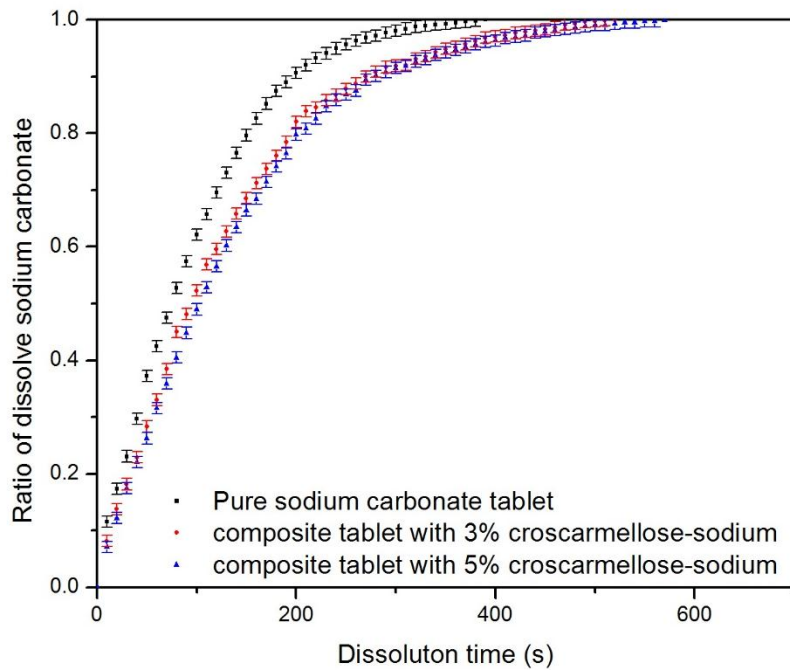
(b)



(c)



(d)



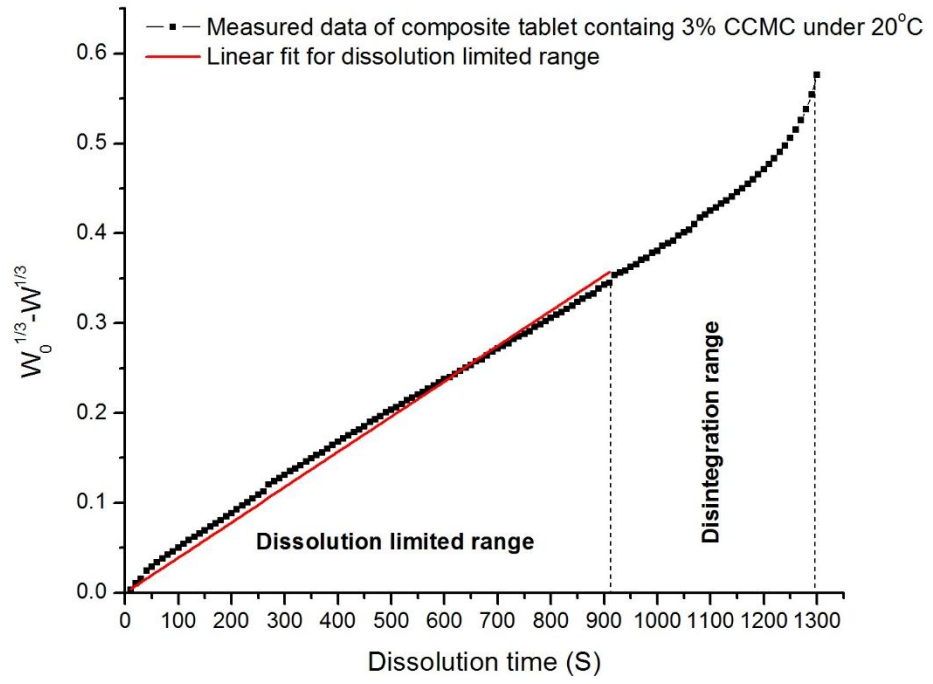
(e)

**Figure 5.19** Ratio of dissolved amount of sodium carbonate under (a) 20°C; (b) 30°C; (c) 40°C; (d) 50°C; (e) 60°C

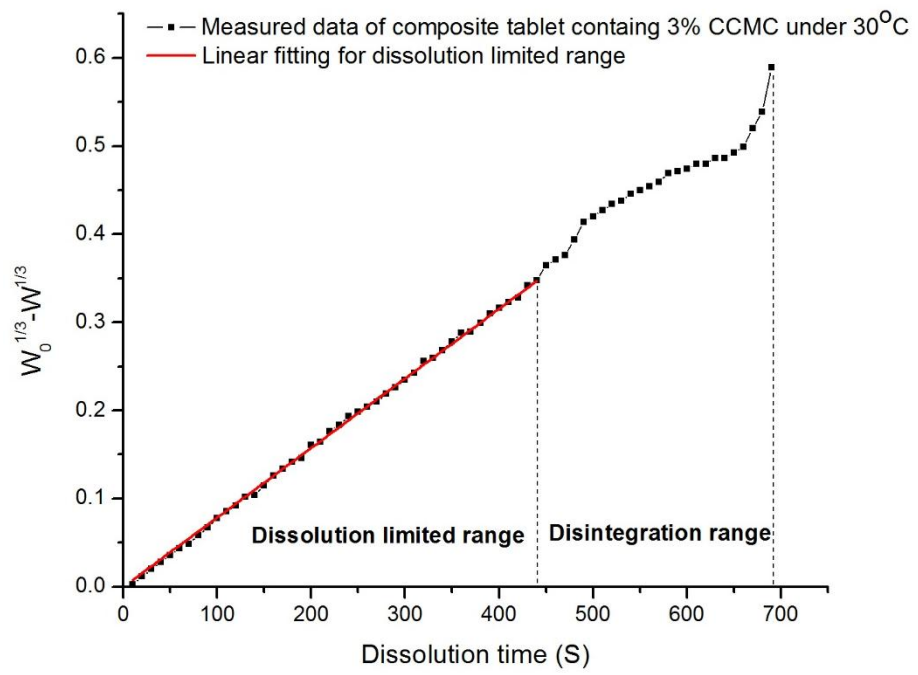
Through the results in Figure 5.19, it is obviously shown that croscarmellose sodium has the effect to prolong the dissolution time comparing with the dissolution

of pure sodium carbonate tablets. Furthermore, the dissolution time of composite tablet containing 5% croscarmellose sodium is longer than the composite tablet containing 3% croscarmellose sodium. Therefore, it can be determined that dissolution time can be prolonged by adding croscarmellose sodium, and higher amount of croscarmellose sodium means longer dissolution time. According to the results shown in Figure 5.19, the highest dissolution rate for every kind of tablet is at the starting dissolution time, and then decreases through the dissolution process till almost 0. For the overall evaluation of dissolution rate of every kind of tablet, croscarmellose sodium has the effect to weaken the dissolution rate comparing with pure sodium carbonate tablet, and more amount of croscarmellose sodium shows a slower dissolution rate. The effect of adding croscarmellose sodium is generally depending on the overall evaluation of dissolution data. Therefore, the dissolution rate constant is needed to be quantified accurately by Hixson-Crowell model to show the effect of croscarmellose sodium on dissolution rate constant.

Hixson-Crowell model is applied to quantify the dissolution rate constant in this case following the same method which is discussed previously. The fitting with Hixson-Crowell model for each case is suitable for dissolution limited range because of the phenomenon of tablet disintegration when the remaining tablet is lower than a possible certain amount. Therefore, the fitting with Hixson-Crowell model of dissolution limited range is applied in this work. In this way, a linear in dissolution limited range is fitted and the gradient of this linear is regarded as the dissolution rate constant for corresponding dissolution experiment. The fitting results for each case are shown in Figure 5.20 and Figure 5.21.

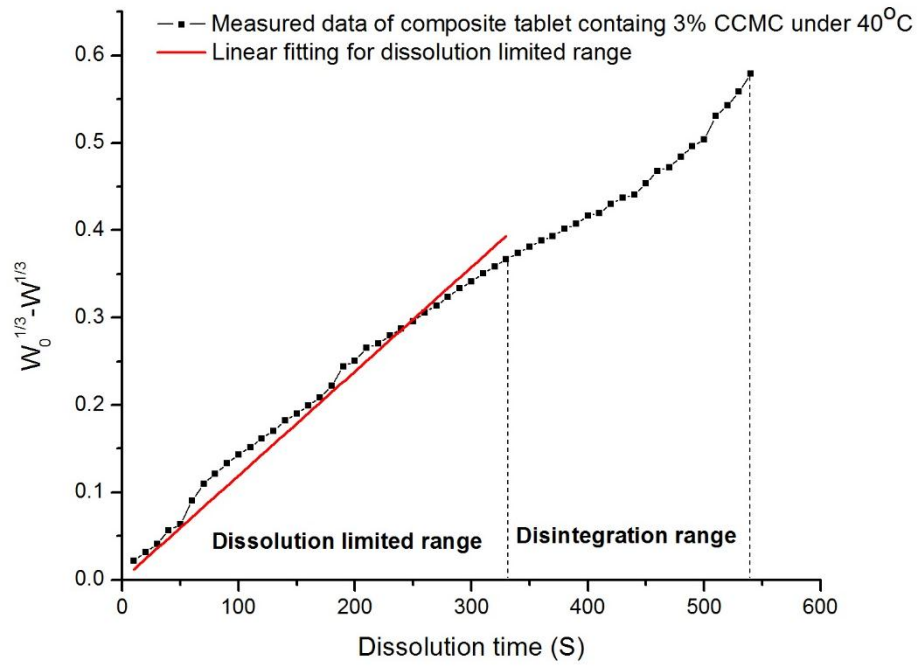


(a)

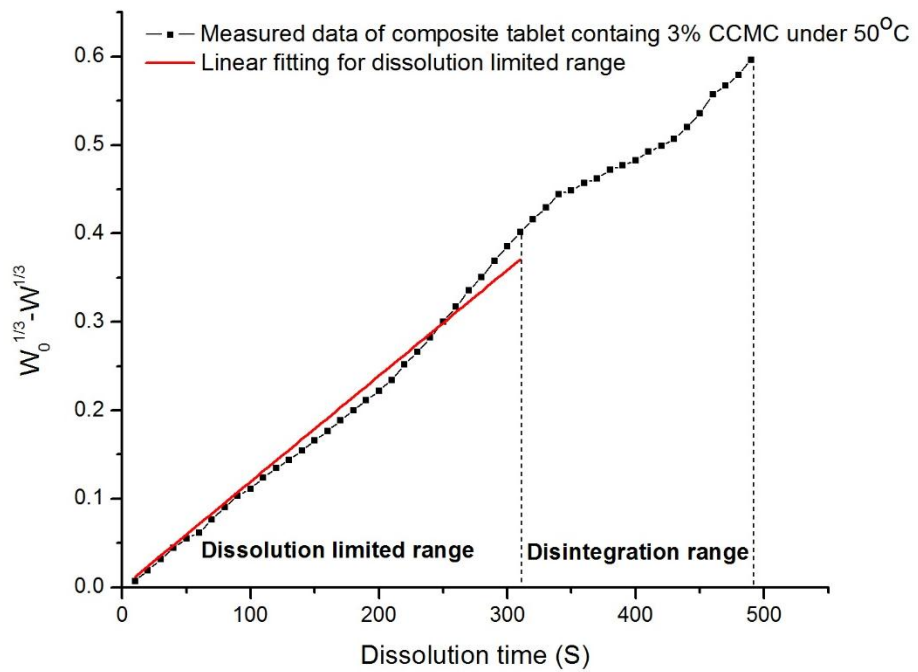


(b)

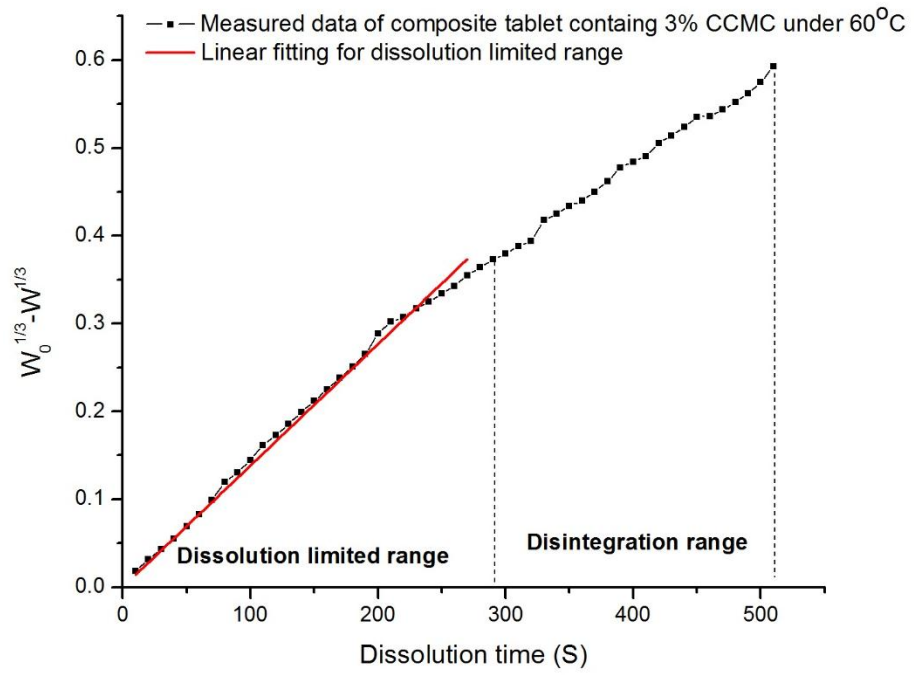




(c)

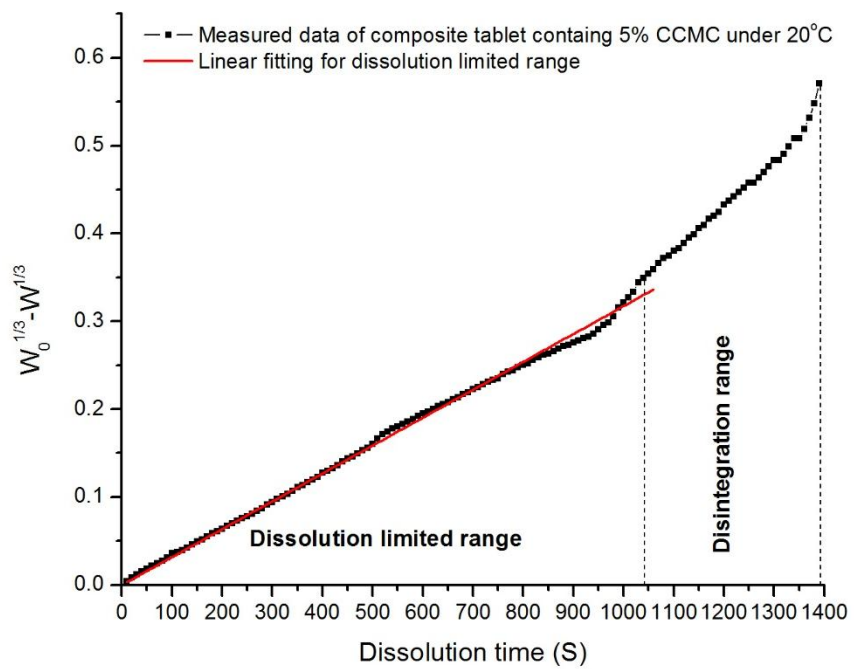


(d)

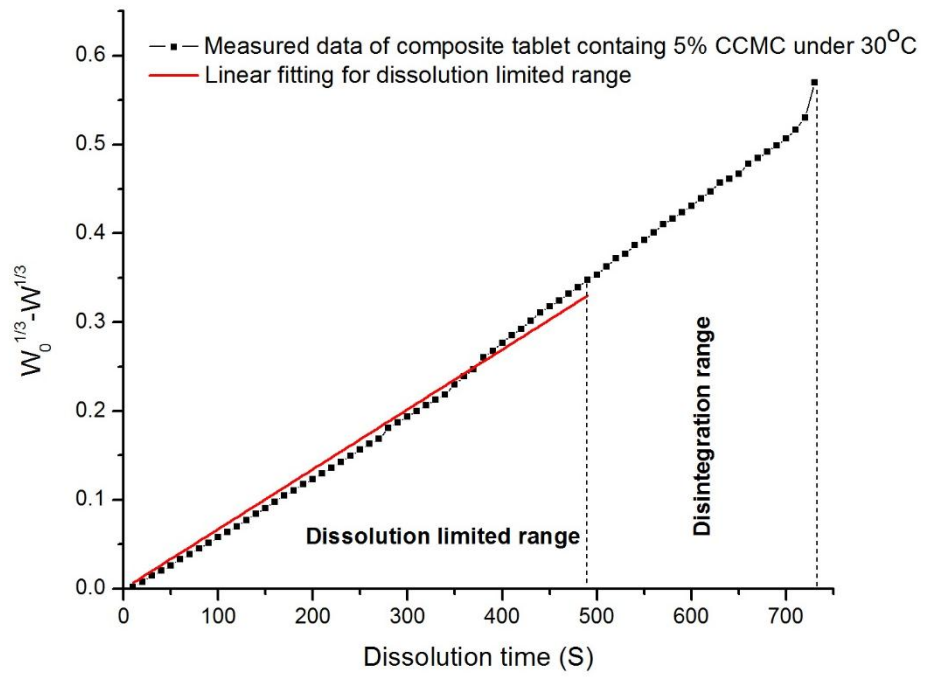


(e)

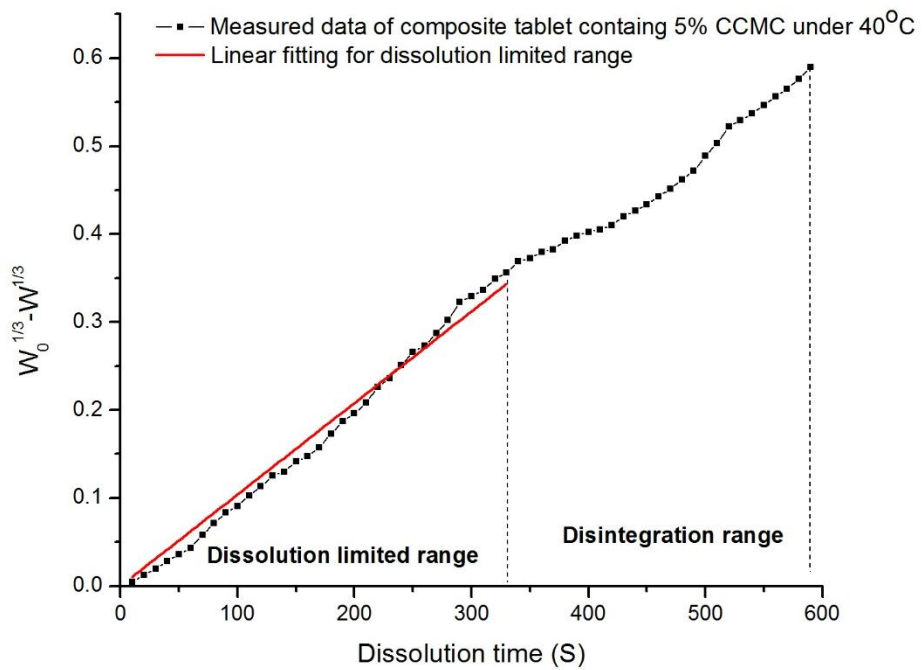
**Figure 5.20** Linear fitting of dissolution limited range with Hixson-Crowell model for composite tablet containing 3% CCMC under (a) 20°C; (b) 30°C; (c) 40°C; (d) 50°C; (e) 60°C



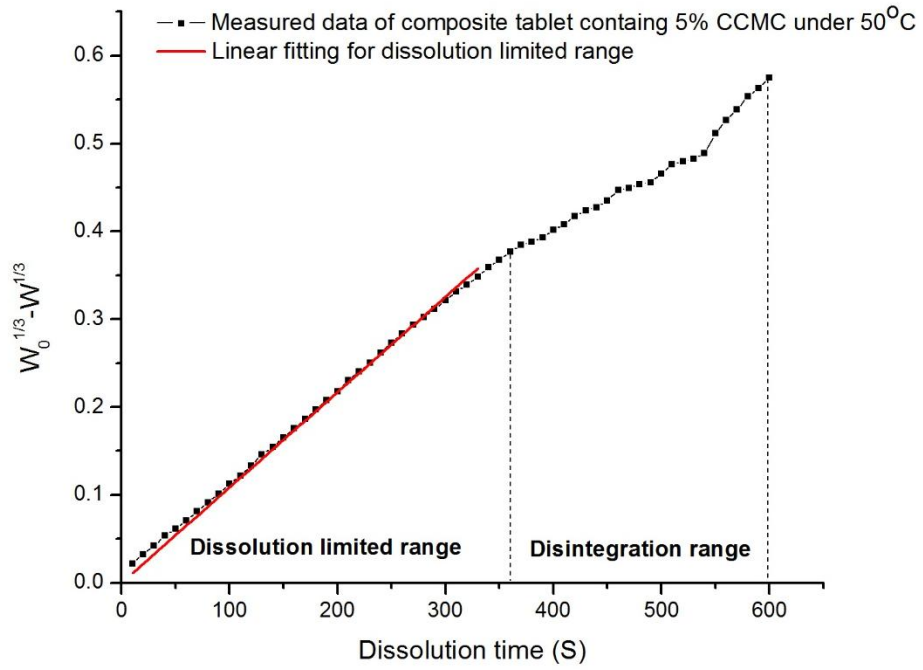
(a)



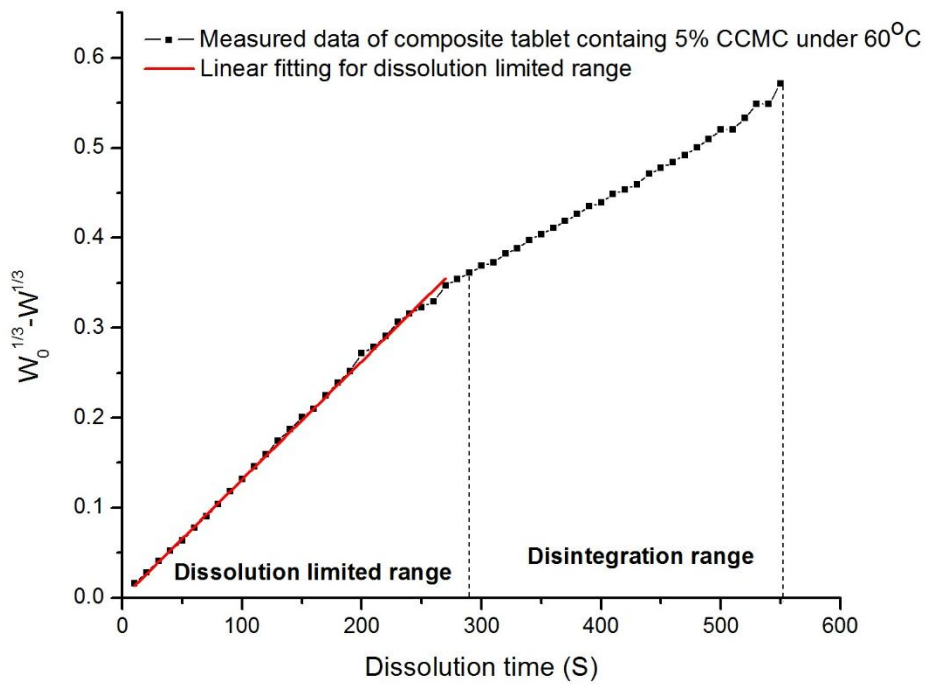
(b)



(c)



(d)



(e)

**Figure 5.21** Linear fitting of dissolution limited range with Hixson-Crowell model for composite tablet containing 5% CMCC under (a) 20°C; (b) 30°C; (c) 40°C; (d) 50°C; (e) 60°C

According to the fitting results for dissolution limited range with Hixson-Crowell model of each case shown in Figure 5.20 and Figure 5.21, the dissolution rate

constant of every kind of tablet including pure sodium carbonate tablet, composite tablet containing 3% croscarmellose sodium and 5% croscarmellose sodium is quantified and represented in Figure 5.22.

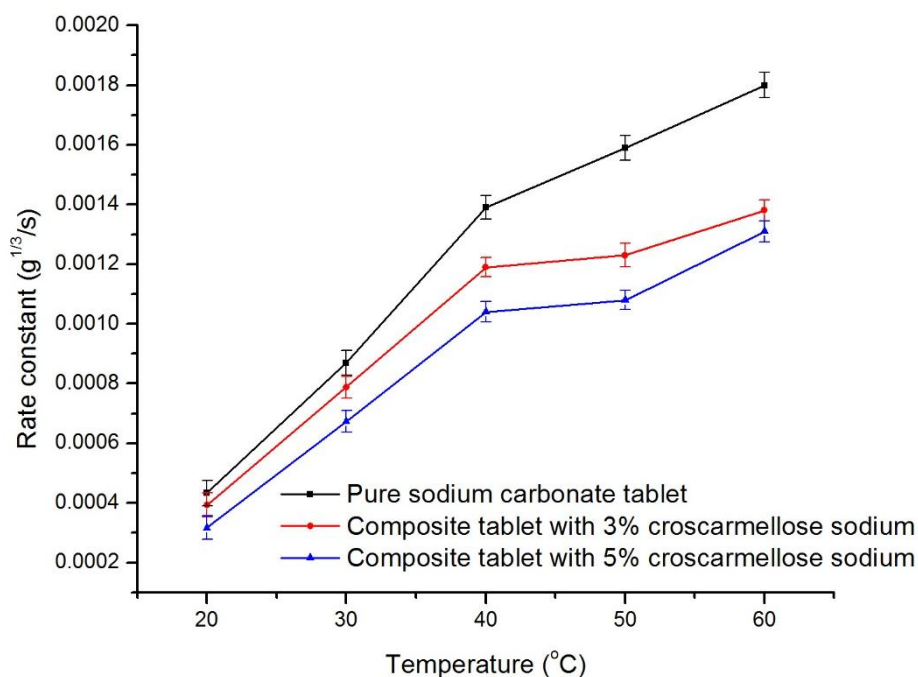


**Figure 5.22** Dissolution rate constant for pure sodium carbonate tablet, composite tablet with 3% croscarmellose sodium and 5% croscarmellose sodium

According to the results of dissolution rate constant shown in Figure 5.22, adding croscarmellose sodium is significantly weakening the dissolution rate constant at every temperature. And more amount of croscarmellose sodium results into a lower dissolution rate constant. Because of the special chemical structure of croscarmellose sodium that contains cross-linked sodium carboxymethylcellulose, croscarmellose sodium is essentially water-insoluble. That means the effect of croscarmellose sodium is greatly related to its physical behaviors and changes in water. Depending on the expected functions on dissolution behaviors of tablet in water, croscarmellose sodium particle should swell many times than its weight by absorbing water. And this swelling of particle should leads to the improvement on disintegrate of tablet. However, the results show the special conclusion that adding

croscarmellose sodium into tablet will weaken the dissolution rate constant inversely. The possible conjectures of this conclusion may be thought from the imbalanced functions of croscarmellose sodium in water. It is possible that the swelling properties of croscarmellose sodium is greatly weakened after placing for a long period that might lead to invalid of swelling its properties. This conjecture can be proved according to the observation of tablet dissolving experiment in water that there is no apparent disintegration happens during the dissolution process. Also at the same time, because croscarmellose sodium is insoluble in water, the dispersed croscarmellose sodium suspensions are very likely to be wrapped around the sodium carbonate particles. Under this situation, the contacting of sodium carbonate with water is obstructed and the dissolution process is inhibited. Therefore, the dissolution rate and rate constant is weakened due to the croscarmellose sodium's water-insoluble property and minimized swelling and integration functions. And more croscarmellose sodium aggravates these functions.

### **5.5.3 Dissolution Kinetics of Sodium Carbonate-Crospovidone Composite**

#### **Tablet**

The composite tablets used in this work are sodium carbonate-crospovidone composite tablets containing 3% and 5% crospovidone respectively. As the dissolution experimental method and measured data analysis method have been detailed expressed in Chapter 5.5.1 and 5.5.2 of composite tablet, and the dissolution experiments and data analysis used in this work are the same method as other sections in this Chapter. Therefore, the measured data analysis from dissolution experiments of this work will be expressed directly.

The sodium carbonate-crospovidone composite tablets used in this work are tested

with SEM at first shown in Figure 5.23. According to Figure 5.23, the sodium carbonate-crospovidone composite tablet after compression show a relative similar surface as pure sodium carbonate tablet shown in Chapter 4. That means the adding of crospovidone has not shown apparent impact on SEM to change the surface of tablet.

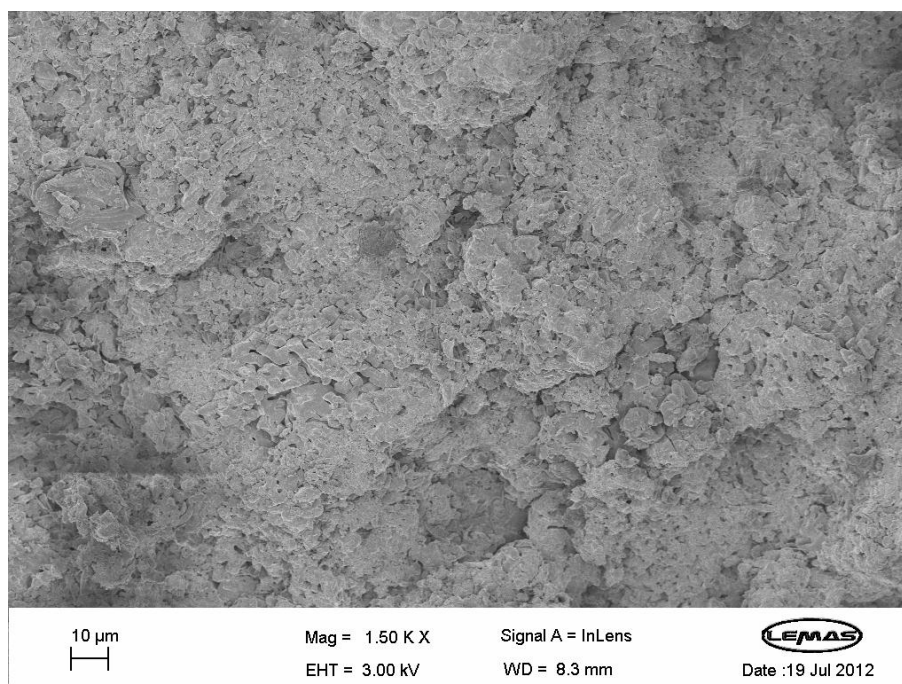


**Figure 5.23.** SEM image of sodium carbonate-crospovidone composite tablet

Then the sodium carbonate-crospovidone composite tablets used in this work are tested with XRD to show the crystalline forms of each kind of composite tablet that are shown in Figure 5.24 and Figure 5.25. The measurement equipment and method of XRD is the same as shown in Chapter 4 for pure sodium carbonate tablet. According to Figure 5.24, it is shown sodium carbonate-crospovidone composite tablet containing 3% crospovidone shows almost the same result as pure sodium carbonate tablet. However, sodium carbonate-crospovidone composite tablet containing 5% crospovidone has the higher intensity of peak and shows slightly leftward panning than pure sodium carbonate tablet according to Figure 5.25.

According to the basic theoretical model of XRD, Bragg Law, the results shown in Figure 5.24 and Figure 5.25 prove that after compression with adding 5% crospovidone, the crystal size and the layer distance of diffraction surface of sodium carbonate likely becomes larger. These results provide useful information to discuss that to make the dissolution happening after compression with 5% crospovidone, the energy that breaks the bond between sodium atom, carbon atom and oxygen atom from sodium carbonate-crospovidone composite tablet containing 5% crospovidone might be slightly smaller than the breaking energy that for pure sodium carbonate tablet.

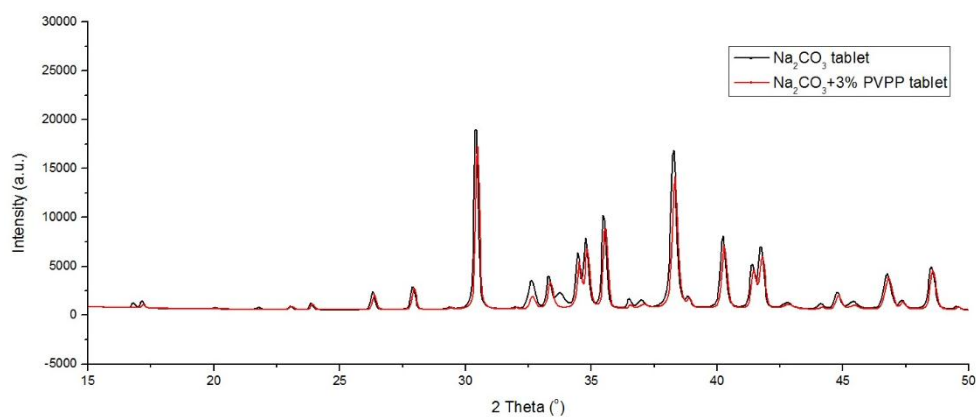


**Figure 5.24** XRD of sodium carbonate-crospovidone composite tablet containing 3% crospovidone comparing with pure sodium carbonate tablet

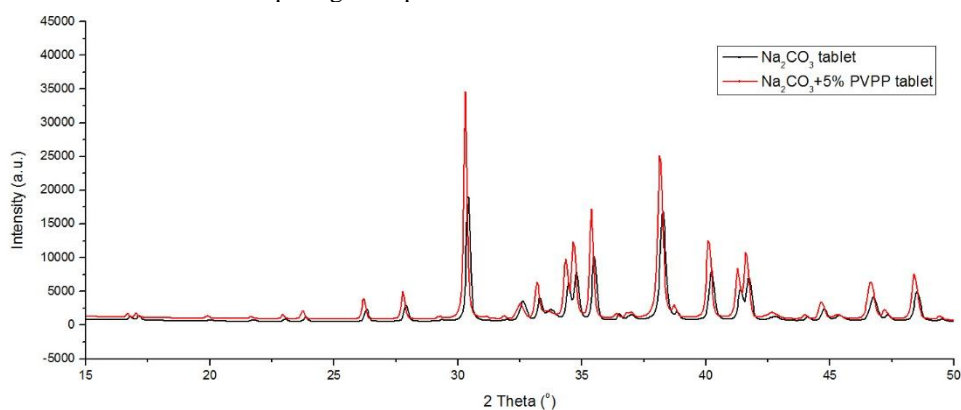


**Figure 5.25** XRD of sodium carbonate-crospovidone composite tablet containing 5% crospovidone comparing with pure sodium carbonate tablet

An example of dissolution experimental data of sodium carbonate-crospovidone



composite tablets containing 3% crospovidone under 30°C are shown as the measured dissolution data analysis method. In this way, the conductivity values measured from dissolution experiment under 30°C are shown in Table 5.7.

**Table 5.7** Conductivity values of composite tablet containing 3% crospovidone under 30°C

Time (S)	Conductivity (mS)	Time (S)	Conductivity (mS)
10	0.203	240	3.88
20	0.45	250	3.96
30	0.697	260	4.03
40	0.9	270	4.11
50	1.103	280	4.18
60	1.355	290	4.24
70	1.555	300	4.31
80	1.766	310	4.37
90	1.946	320	4.44
100	2.15	330	4.5
110	2.29	340	4.57
120	2.44	350	4.6
130	2.58	360	4.65
140	2.72	370	4.71
150	2.87	380	4.77
160	2.97	390	4.81
170	3.11	400	4.84
180	3.21	410	4.87
190	3.34	420	4.92
200	3.46	430	4.94
210	3.56	440	4.96
220	3.66	450	4.97
230	3.77		

With measured conductivity values shown in Table 5.7, the amount of dissolved sodium carbonate can be calculated with the calibration relation shown in Figure 4.7 as  $COND_t = 18.91M_t$ . With this calibration relation, the dissolved amount of sodium carbonate from composite tablet are shown in Table 5.8.

**Table 5.8** Dissolved amount of sodium carbonate from composite tablet containing 3% crospovidone under 30°C

Time (S)	Dissolved amount (g)	Time (S)	Dissolved amount (g)
10	0.0107	240	0.2052
20	0.0238	250	0.2094
30	0.0369	260	0.2131
40	0.0476	270	0.2173
50	0.0583	280	0.221
60	0.0717	290	0.2242
70	0.0822	300	0.2279
80	0.0934	310	0.2311
90	0.1029	320	0.2348

100	0.1137	330	0.238
110	0.1211	340	0.2417
120	0.129	350	0.2433
130	0.1364	360	0.2459
140	0.1438	370	0.2491
150	0.1518	380	0.2522
160	0.1571	390	0.2544
170	0.1645	400	0.2559
180	0.1698	410	0.2575
190	0.1766	420	0.2602
200	0.183	430	0.2612
210	0.1883	440	0.2623
220	0.1935	450	0.2628
230	0.1994		

Because composite tablet used in this work is dissolved into 100ml distilled water, the concentration of sodium carbonate from dissolved composite tablet containing 3% crospovidone under 30°C in solution is determined and shown in Table 5.9. And the ratio of dissolved amount of sodium carbonate from dissolved composite tablet containing 3% crospovidone as function of time is shown in Figure 5.26.

**Table 5.9** Concentration of sodium carbonate from composite tablet containing 3% crospovidone in solution under 30°C

Time (S)	Concentration (g/ml)	Time (S)	Concentration (g/ml)
10	0.000107	240	0.002052
20	0.000238	250	0.002094
30	0.000369	260	0.002131
40	0.000476	270	0.002173
50	0.000583	280	0.00221
60	0.000717	290	0.002242
70	0.000822	300	0.002279
80	0.000934	310	0.002311
90	0.001029	320	0.002348
100	0.001137	330	0.00238
110	0.001211	340	0.002417
120	0.00129	350	0.002433
130	0.001364	360	0.002459
140	0.001438	370	0.002491
150	0.001518	380	0.002522
160	0.001571	390	0.002544
170	0.001645	400	0.002559
180	0.001698	410	0.002575
190	0.001766	420	0.002602
200	0.00183	430	0.002612
210	0.001883	440	0.002623
220	0.001935	450	0.002628
230	0.001994		

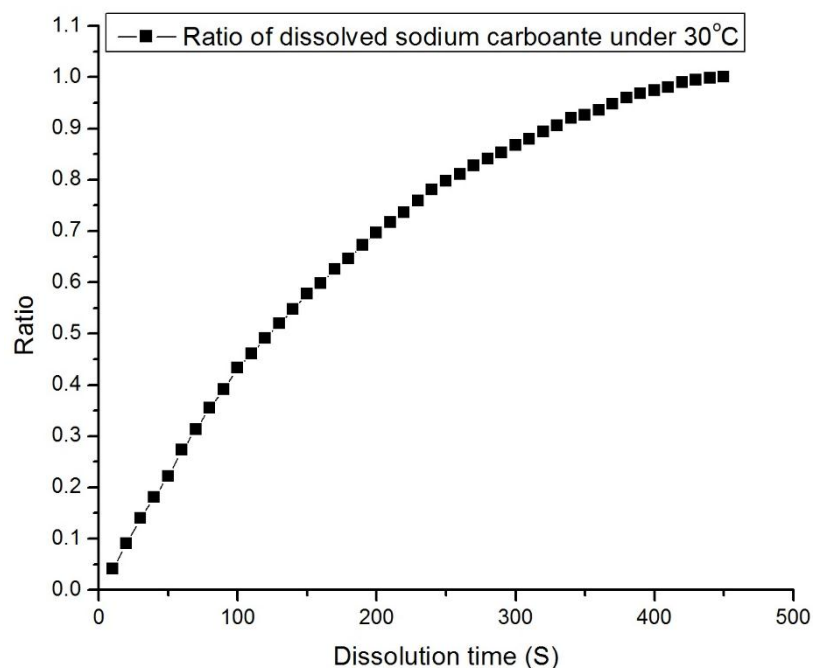


**Figure 5.26** Ratio of dissolved sodium carbonate from composite tablet containing 3% crospovidone under 30°C

As it has been discussed in Chapter 4 for the fitting of dissolution experiment data of pure sodium carbonate tablet, a linear should be obtained for the experimental data if the dissolution process is matching the assumptions of mathematical model during the whole dissolution process that the shape factor of dissolved tablet should keep as a constant and only the diminishing of size of tablet happens during dissolution process. However, according to the observation of dissolution experiment of composite tablet, the tablet dissolution process is not following the assumption of Hixson-Crowell model for the whole dissolution process when the undissolved composite tablet is thinner and smaller enough as it is very unlikely to keep as a whole tablet. That means once the remaining sodium carbonate tablet is lower than a possible amount, the tablet will be disintegrated into pieces due to the external stirring force from solution. The disintegration is not only from the effect of external stirring condition, but also comes from the effect of polymers used in this work. As adding crospovidone, the important super swelling functions of

crospovidone leading to the disintegration of composite tablet becomes more likely. Therefore, the practical dissolution of sodium carbonate-crospovidone composite tablet in this work can be said has two ranges that the tablet will dissolve with dissolution limited process as a whole, and once the tablet starts to disintegrate, the dissolution steps into disintegration process. In this way, the fitting of measured experimental data with Hixson-Crowell model should be carried out for two ranges. One is the dissolution limited range, and another is disintegration range. Therefore, the linear fitting with Hixson-Crowell model for dissolution limited range is the appropriate method to quantify the dissolution rate constant for dissolution of experiment with Hixson-Crowell model. In this way, based on the measured dissolution data, the fitting with equation (5.1) for dissolution limited range is shown in Figure 5.27.

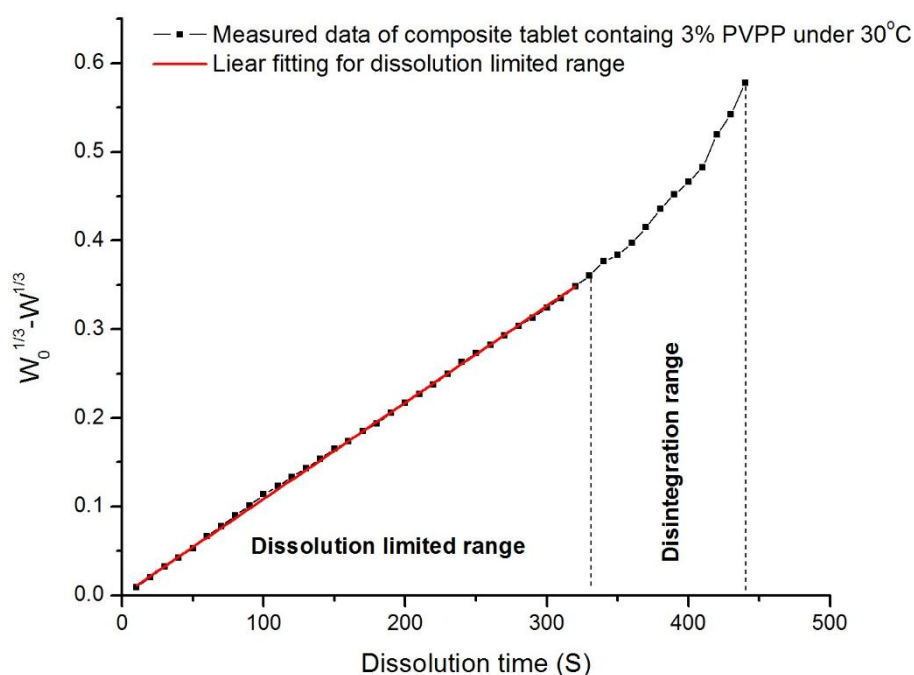
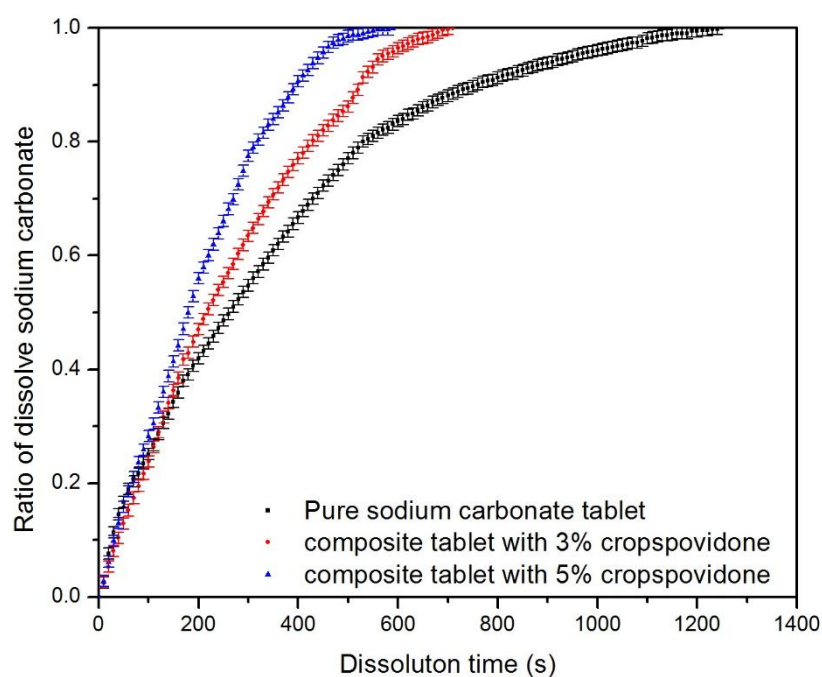


**Figure 5.27** Fitting of dissolution experiment for composite tablet containing 3% crospovidone under 30°C

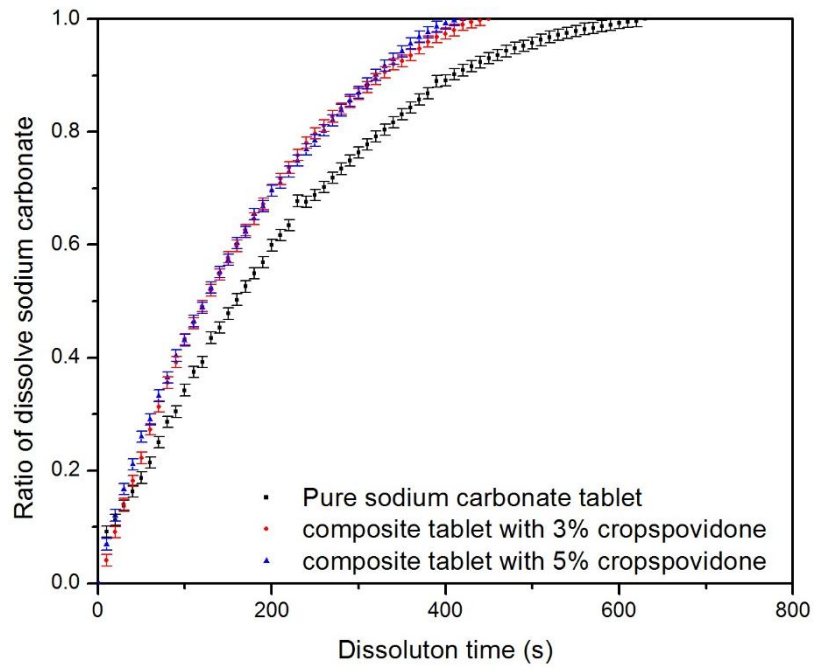
Based on the analysis for quantifying tablet dissolution rate constant, the fitting result in dissolution limited range is the dissolution rate constant of measured

composite tablet with Hixson-Crowell model. According to Figure 5.27, the dissolution rate constant for composite tablet containing 3% crospovidone under 30°C is **0.00109** (g<sup>1/3</sup>/S).

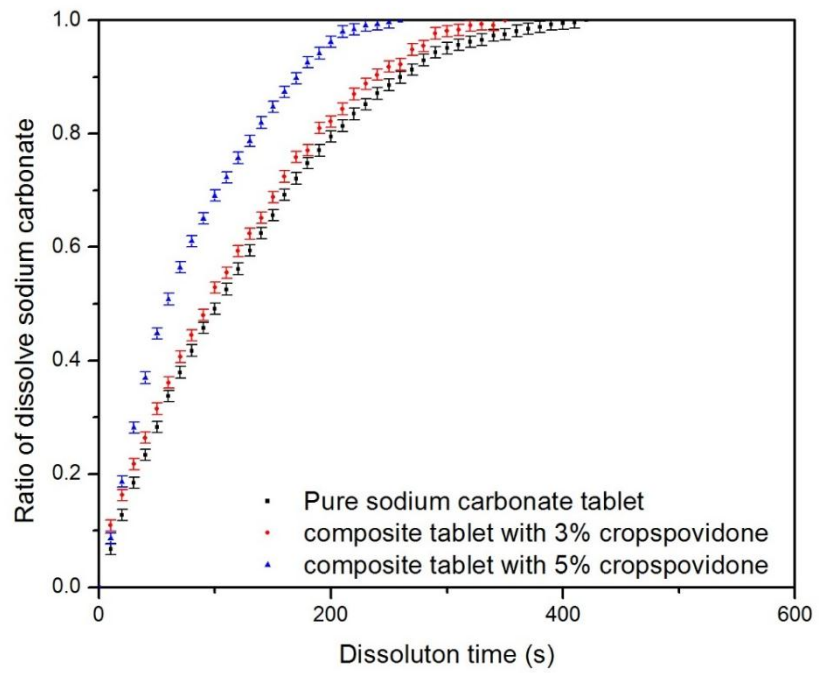
Following the same analysis method and step shown above of the example of composite tablet containing 3% crospovidone under 30°C, the measured dissolution data for each case in this work are shown below. The ratio of dissolved amount of sodium carbonate for each case are shown in Figure 5.28.



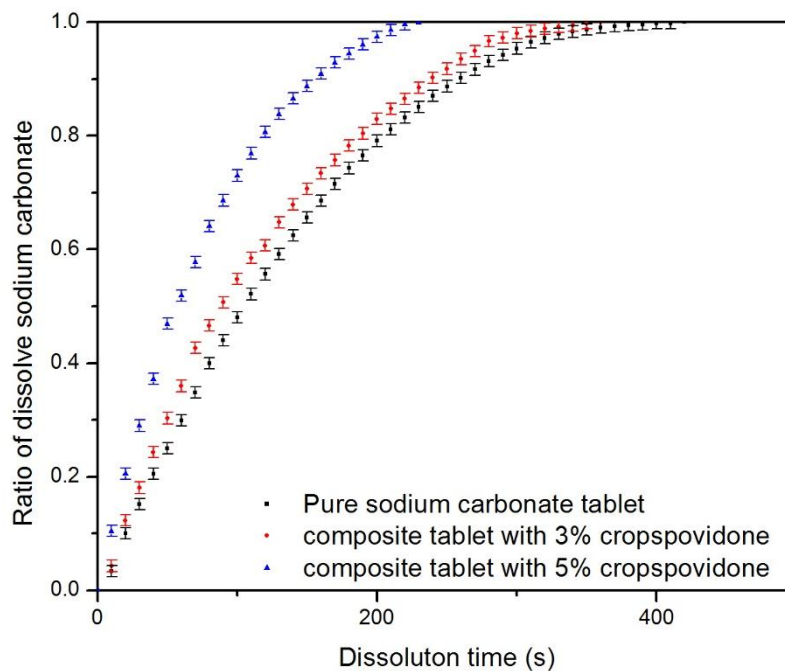
(a)



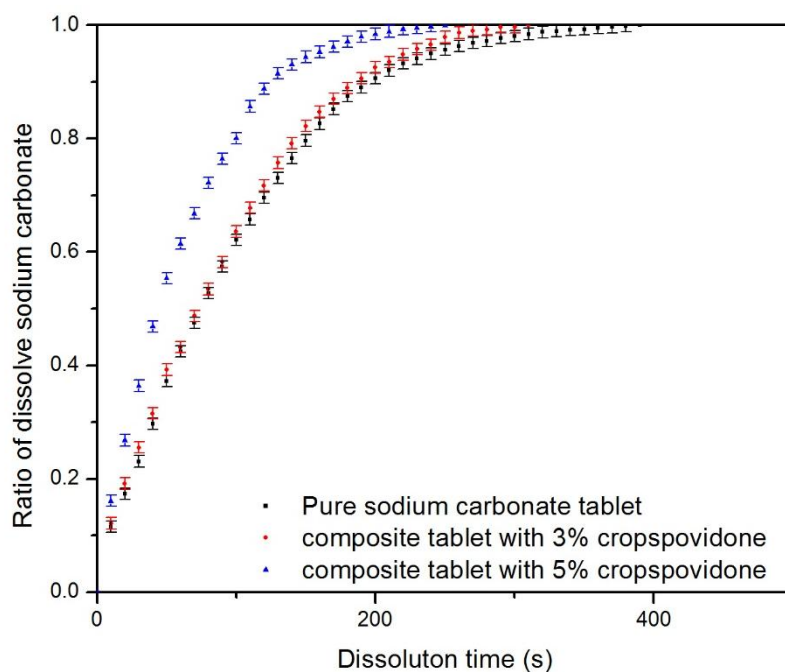
(b)



(c)



(d)



(e)

**Figure 5.28** Ratio of dissolved sodium carbonate from pure sodium carbonate, composite tablet containing with 3% croscopolvidone and 5% croscopolvidone under (a) 20°C; (b) 30°C; (c) 40°C; (d) 50°C; (e) 60°C.

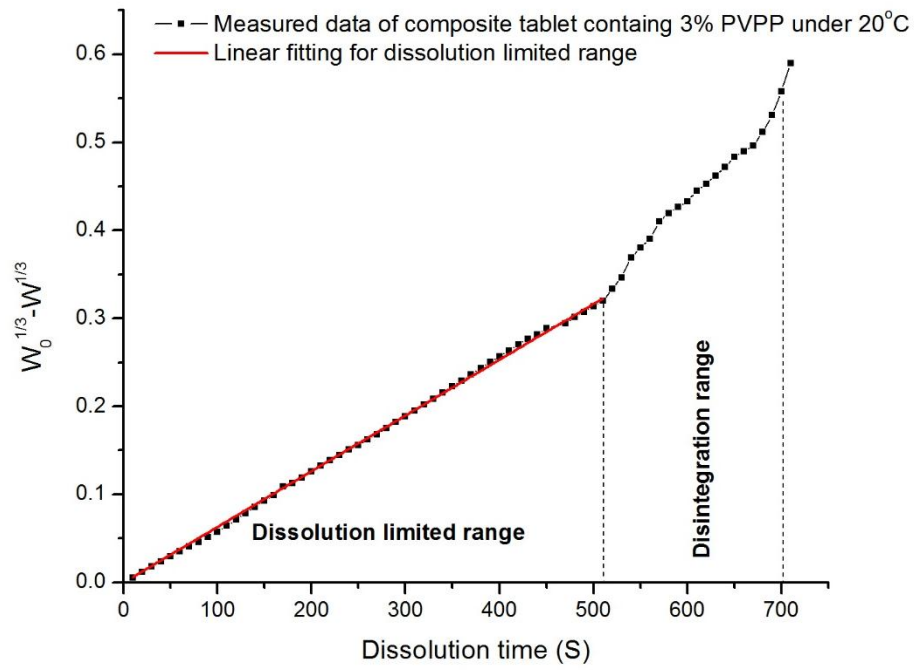
Following the same quantification method, the dissolution rate is regarded as the gradient of each time point and it is changing with the function of dissolution time.

Therefore, the evaluation of effect of crospovidone is also suggested to be viewed from the overall effect through the whole dissolution process.

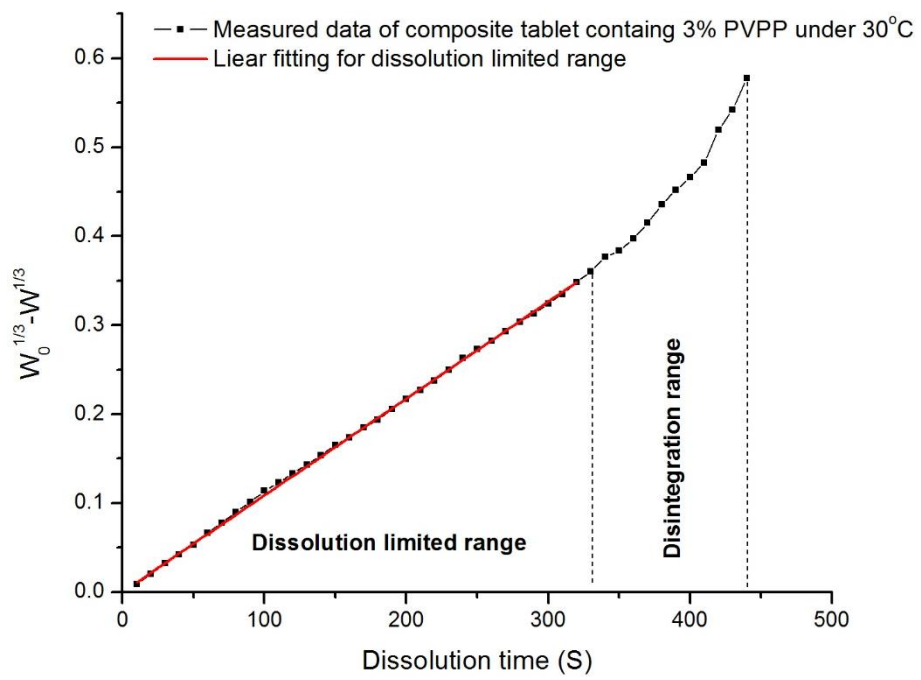
According to the results shown in Figure 5.28, the highest dissolution rate is at the starting point of dissolution time, and then decreases through the dissolution process till almost 0. For the overall evaluation of dissolution rate, adding crospovidone has the positive effect to enhance the dissolution rate and more amount of crospovidone shows a better enhancement. This conclusion is based on the overall evaluation of dissolution curve, therefore the dissolution rate constant in this case is needed to be quantified by Hixson-Crowell model to show the effect of crospovidone on dissolution rate constant accurately.

Hixson-Crowell model is applied to quantify the dissolution rate constant in this case following the same method which is shown previously. The fitting with Hixson-Crowell model for each case is suitable for dissolution limited range because of the phenomenon of tablet disintegration when the remaining tablet is lower than a possible amount. Therefore, the fitting with Hixson-Crowell model of dissolution limited range is applied in this work. In this way, a linear in dissolution limited range is fitted and the gradient of this linear is regarded as the dissolution rate constant for corresponding dissolution experiment. The fitting results for each case are shown in Figure 5.29 and Figure 5.30.

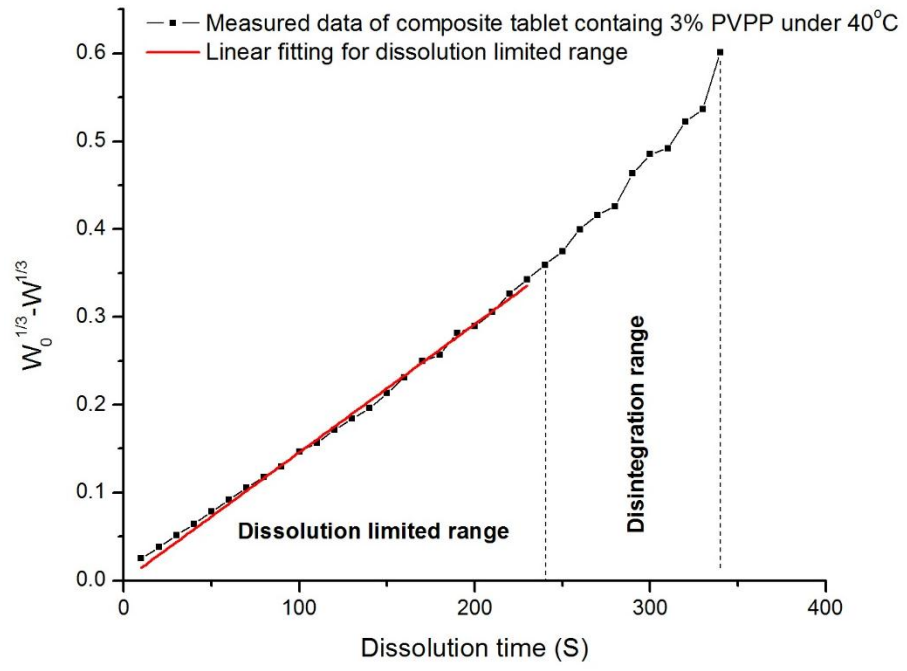




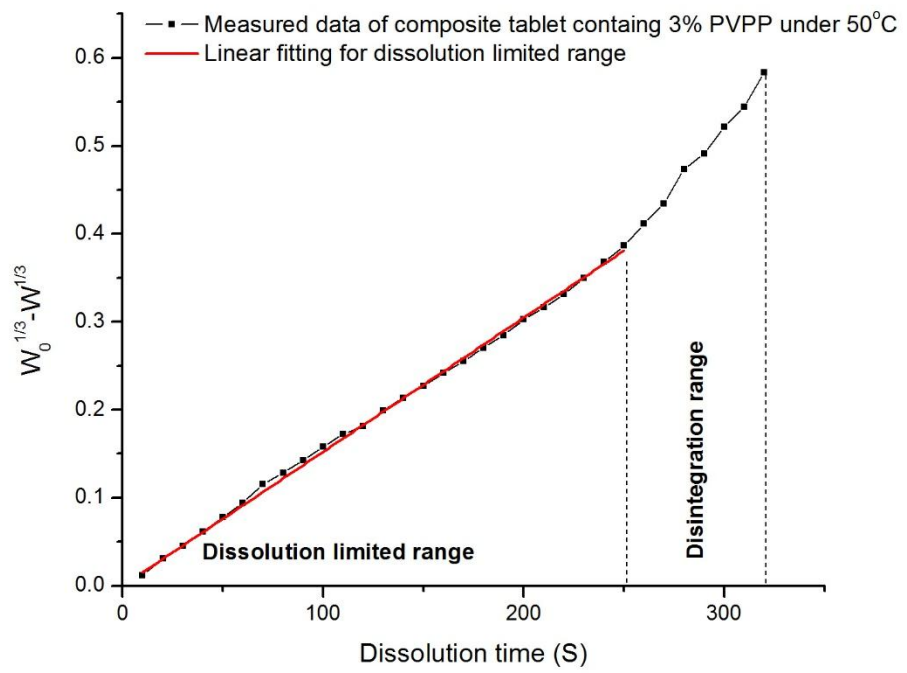
(a)



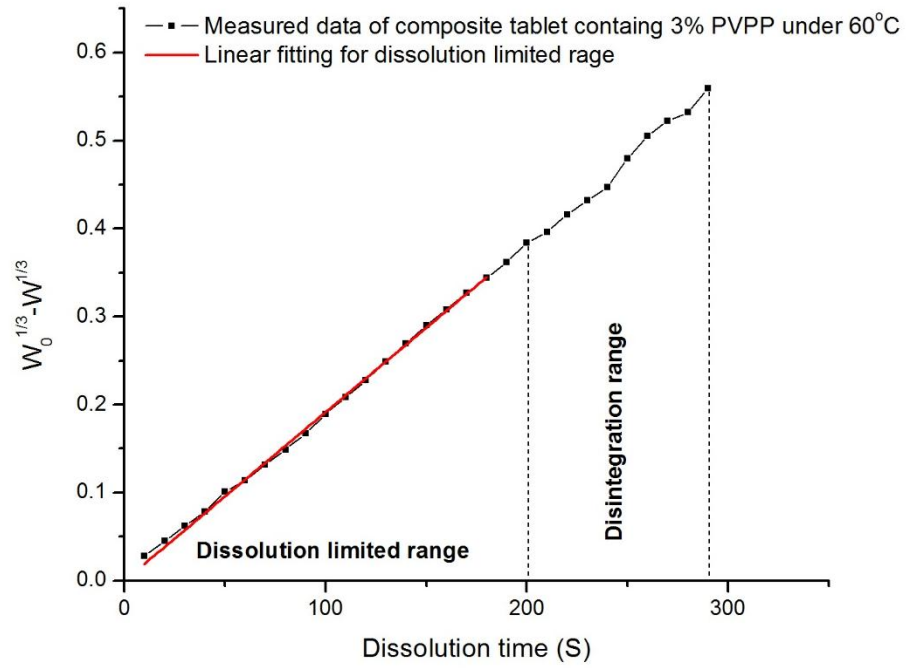
(b)



(c)

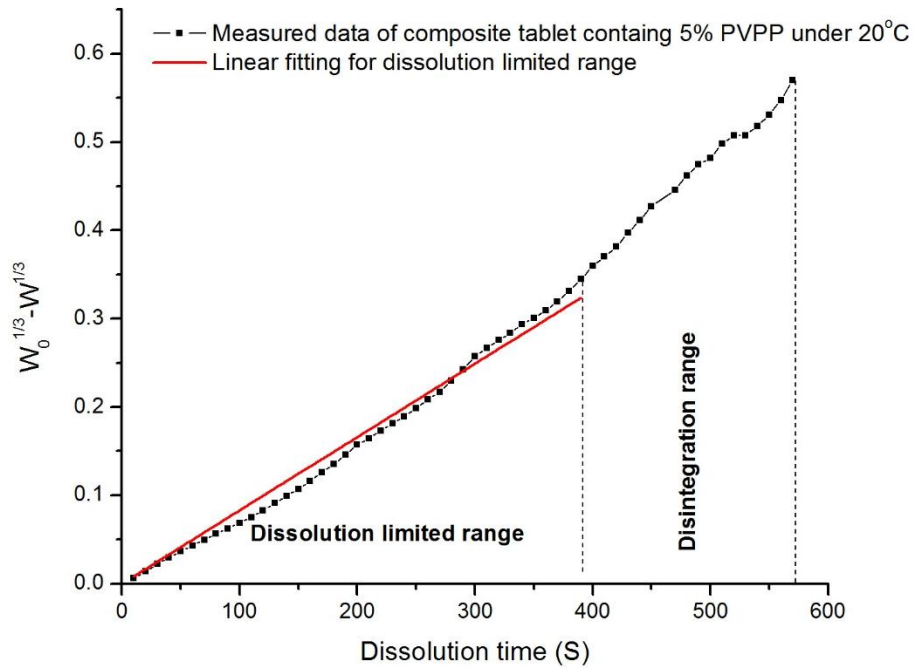


(d)

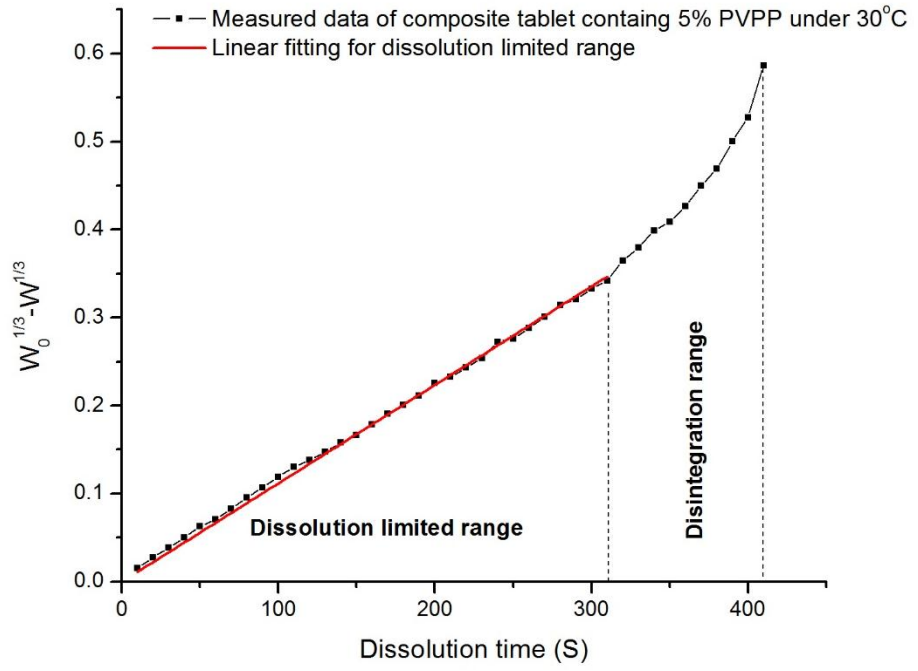


(e)

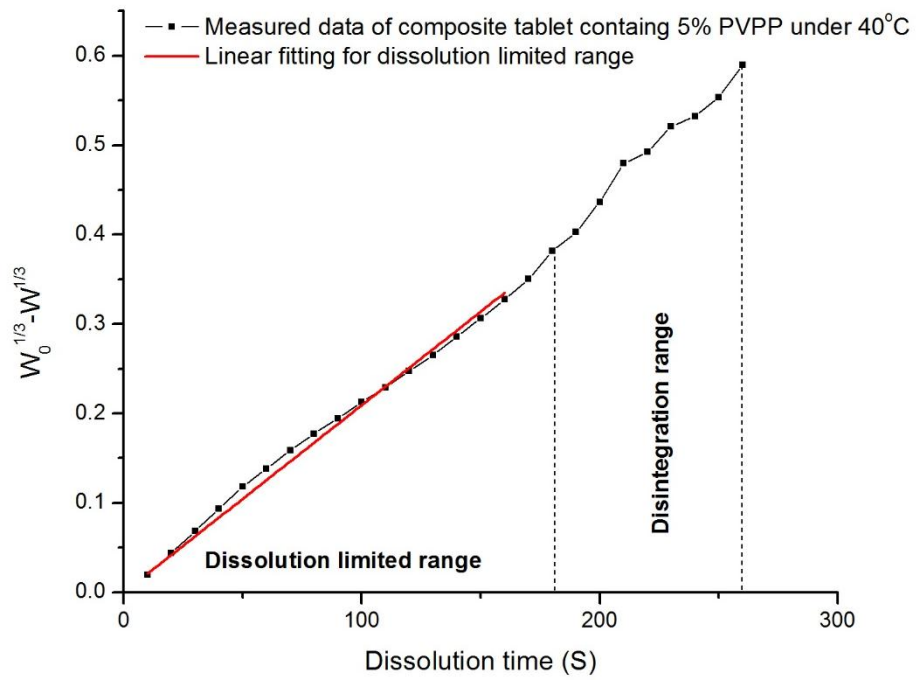
**Figure 5.29** Linear fitting of dissolution limited range with Hixson-Crowell model for composite tablet containing 3% PVPP under (a) 20°C; (b) 30°C; (c) 40°C; (d) 50°C; (e) 60°C



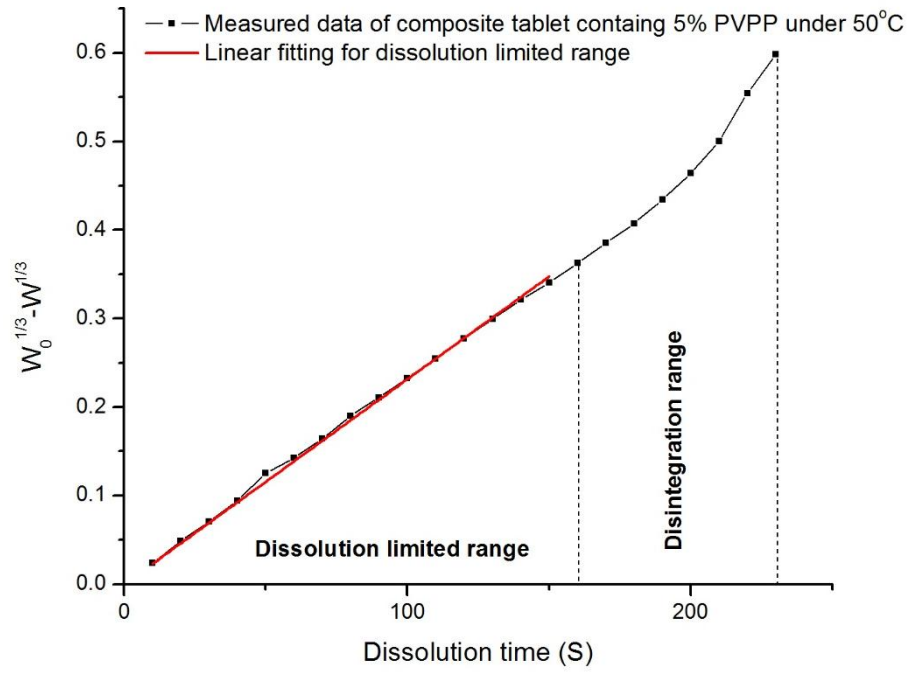
(a)



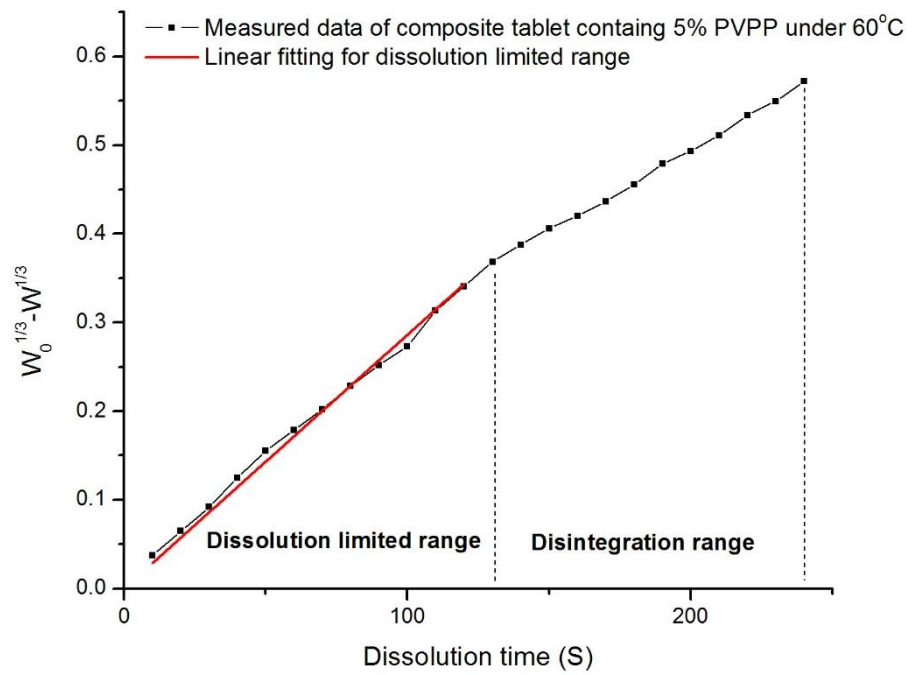
(b)



(c)



(d)



(e)

**Figure 5.30** Linear fitting of dissolution limited range with Hixson-Crowell model for composite tablet containing 5% PVPP under (a) 20°C; (b) 30°C; (c) 40°C; (d) 50°C; (e) 60°C

According to the fitting results for dissolution limited range with Hixson-Crowell model of each case shown in Figure 5.29 and Figure 5.30, the dissolution rate

constant of every kind of tablet including pure sodium carbonate tablet, composite tablet containing 3% crospovidone and 5% crospovidone is quantified and represented in Figure 5.31.

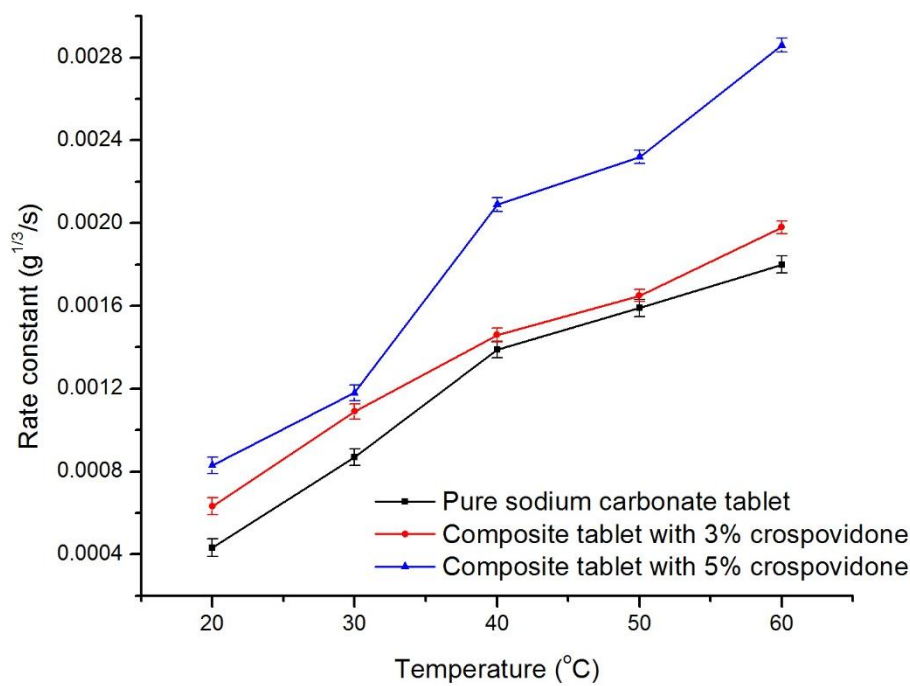


**Figure 5.31** Dissolution rate constant for pure sodium carbonate tablet, composite tablet with 3% crospovidone and 5% crospovidone

Through the results shown in Figure 5.31, the effect of crospovidone shows a clear enhancement on dissolution rate constant at every temperature. And more amount of crospovidone leads to a greater dissolution rate constant. According to the chemical structure of crospovidone, this cross-link bounded to polyvinylpyrrolidone leads to a function of super disintegrate. This function of super disintegrate not only accelerates the dissolution process of tablet, but also improve the bioavailability of tablet with its power. Coordination with the function of high soluble and absorption, crospovidone has the great performance on dissolution of tablet. That is the reason that dissolution kinetics are enhanced by adding crospovidone.

#### 5.5.4 Comparison of Dissolution Rate Constant of Sodium carbonate-Polymer Composite Tablet

Through the investigation and analysis of dissolution experiments of composite tablets containing carboxymethyl cellulose, croscarmellose sodium and crospovidone respectively, the dissolution rate constant of each case is quantified, discussed and explained respectively. Combing the quantified results of dissolution rate constant of each kind of composite tablet, it is clearly shown to compare the effects of different polymer on dissolution process and kinetics. The comparison of dissolution rate constant of each kind of composite tablet is shown in Figure 5.32 and Figure 5.33.

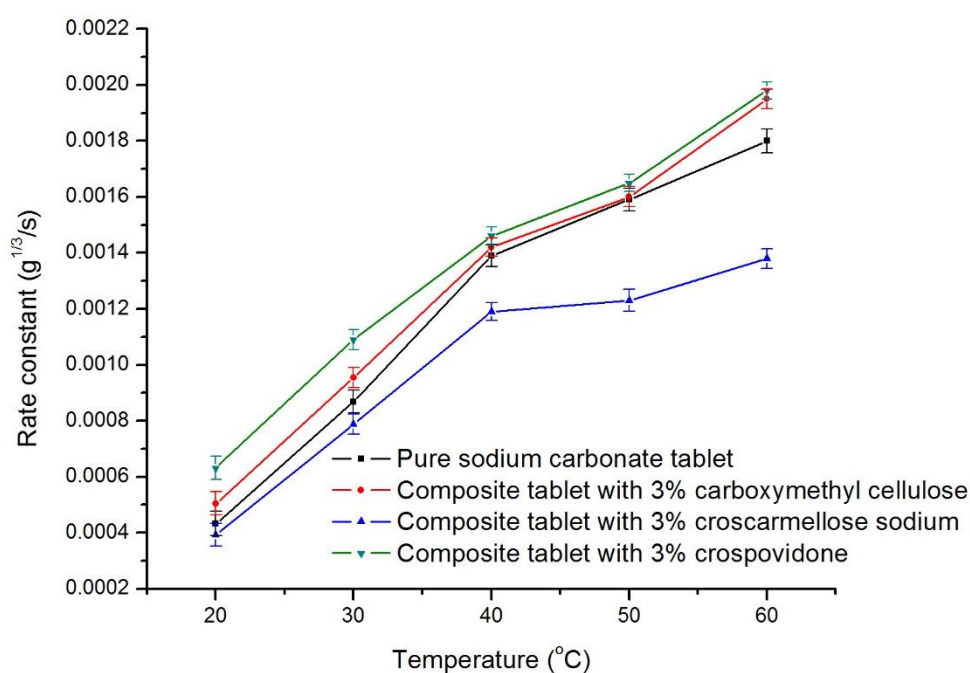


**Figure 5.32.** Dissolution rate constants of pure sodium carbonate tablet; composite tablet containing 3% carboxymethyl cellulose, 3% croscarmellose sodium and 3% crospovidone respectively.

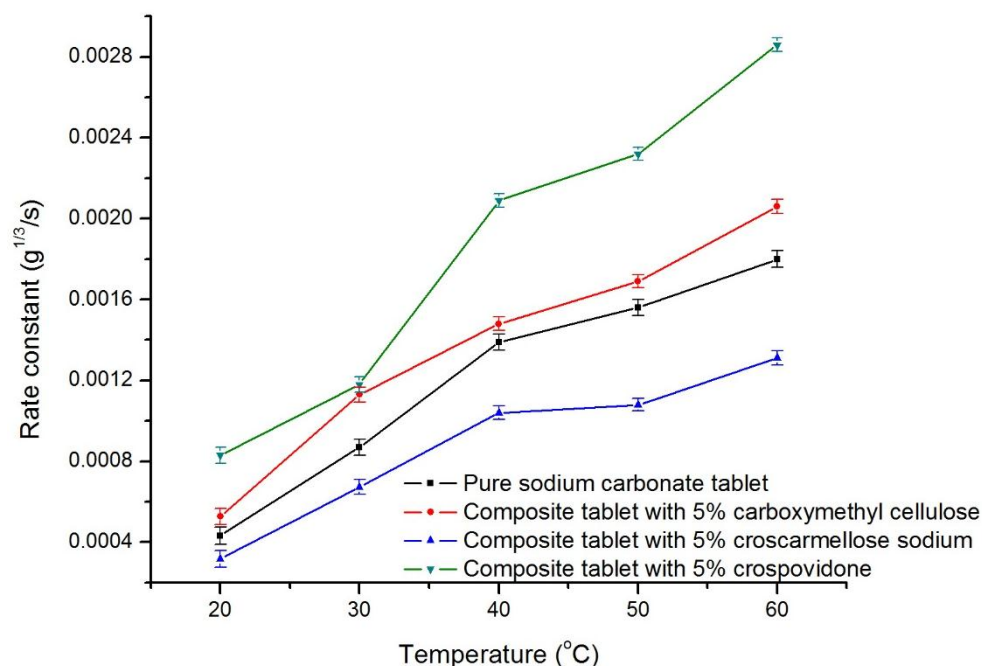


**Figure 5.33.** Dissolution rate constants of pure sodium carbonate tablet; composite tablet containing 5% carboxymethyl cellulose, 5% croscarmellose sodium and 5% crospovidone respectively.

According to Figure 5.32 and 5.33, it is clearly determined that the dissolution rate constant is enhanced by adding crospovidone and carboxymethyl cellulose, and crospovidone shows a stronger enhancement than carboxymethyl cellulose. However, adding croscarmellose sodium leads to the reduction of dissolution rate constant. That means croscarmellose sodium is not preferred to be used as the expectation of accelerating the dissolution process in this work. In this way, combining with the analysis on dissolution rate constant for these 3 kinds of polymer, it can be determined that crospovidone has the best performance and effect on enhancing the dissolution kinetics of composite tablet.

## 5.6 Conclusions

In this Chapter, several dissolution experiments are undertaken to investigate and quantify the dissolution and kinetics of composite tablets containing carboxymethyl cellulose, croscarmellose sodium and crospovidone respectively. The effect of



polymers on dissolution kinetics of composite tablets are further quantified with Hixson-Crowell model for dissolution limited range. The dissolution experiments with different kinds of tablets are carried out at different temperatures. Through the works in this Chapter, the effects of carboxymethyl cellulose, croscarmellose sodium and crospovidone on dissolution kinetics are quantified accurately, and the results and conclusions are clearly discussed and determined. The conclusions of the effects of polymers on dissolution kinetics can be summarized as that carboxymethyl cellulose and crospovidone both have the positive effect to enhance the dissolution kinetics of composite tablet, and more amount of these two kinds of polymers show a greater dissolution kinetics. Also crospovidone has stronger effect than carboxymethyl cellulose to enhance dissolution kinetics of composite tablet. However, croscarmellose sodium shows the effect to reduce the dissolution kinetics of composite tablet. These results and conclusions are expected to provide necessary information and suggestions to the practical production use of detergent products.

## **CHAPTER 6. CONCLUSIONS OF RESEARCH WORK AND SCOPE FOR FUTURE WORK**

### **6.1 Conclusions of Research**

Through my research, the dissolution behaviours of structured particles including sodium carbonate particle, sodium carbonate tablet and 2-component tablet is studied and investigated accurately by the experimental methods and quantified by appropriate mathematical models. The experimental methods used in this thesis are well applied to the dissolution research on different kinds of particles. The dissolution kinetics are well quantified with the effect of the conditions including temperature, stirring speed and pH, and the relationship between the dissolution kinetics and conditions is further quantified and discussed accurately. Simply speaking, the dissolution kinetics increase with temperature and stirring speed due to the effect on diffusion properties according to the diffusion layer theory and mathematical models based on Noyes-Whitney equation, but decrease with pH due to the effect of pH on the process of hydrolysis reactions of sodium carbonate in water.

Furthermore, the work in Chapter 5 about the dissolution of 2-component tablet provides useful information and a new idea to research on multi-component particles that are expected expanded into the research related to detergent dissolution. Based on the results and conclusions in Chapter 3, 4 and 5, the research in this thesis can be said to have achieved the aims and expects expressed at the start of this thesis. And the works are expected to contribute the improvement of manufacturing of detergent products.

## **6.2 Scope of future research**

As the most difficulty area of dissolution research, multi-component and multi-particles are the main scope of future research. The works that have done in this thesis provide useful information to test 2-component particles, therefore the research is expected to be expanded into the area of particles containing 3 or more components. Due to the complex conditions and interactions between each component, the future work is recommended to be done cooperated with method by simulation.

## REFERENCES

- [1] Gee, G. W., Bauder, J. W., & Klute, A. (1986). Particle-size analysis. *Methods of soil analysis. Part 1. Physical and mineralogical methods*, 383-411.
- [2] Black, C. A. (1965). Particle fractionation and particle-size analysis. *Methods of Soil Analysis Part 1, Physical and Mineralogical Properties Including Statistics of Measurement and Sampling*, 550-551.
- [3] Allen, T. (1997). *Particle Size Measurement: Volume 2: Surface Area and Pore Size Determination* (Vol. 2). Springer.
- [4] Chantrell, R. W., Popplewell, J., & Charles, S. (1978). Measurements of particle size distribution parameters in ferrofluids. *Magnetics, IEEE Transactions on*, 14(5), 975-977.
- [5] Uchino, K., Sadanaga, E., & Hirose, T. (1989). Dependence of the crystal structure on particle size in barium titanate. *Journal of the American Ceramic Society*, 72(8), 1555-1558.
- [6] Zhang, Z., Wang, C. C., Zakaria, R., & Ying, J. Y. (1998). Role of particle size in nanocrystalline TiO<sub>2</sub>-based photocatalysts. *The Journal of Physical Chemistry B*, 102(52), 10871-10878.
- [7] Jillavenkatesa, A., Dapkunas, S. J., & Lum, L. S. H. (2001). Particle size characterization. *NIST Special publication*.
- [8] Sneed, E. D., & Folk, R. L. (1958). Pebbles in the lower Colorado River, Texas a study in particle morphogenesis. *The Journal of Geology*, 114-150.
- [9] Wentworth, C. K. (1922). *The shapes of beach pebbles*. US Government Printing

Office.

[10] Zingg, T. (1935). *Beitrag zur schotteranalyse* (Doctoral dissertation, Die Eidgenossische Technische Hochschule in Zurich.).

[11] Krumbein, W. C., & Pettijohn, F. J. (1938). Manual of sedimentary petrography.

[12] Krumbein, W. C. (1941). Measurement and geological significance of shape and roundness of sedimentary particles. *Journal of Sedimentary Research*, 11(2).

[13] Wentworth, C. K. (1919). A laboratory and field study of cobble abrasion. *The Journal of Geology*, 507-521.

[14] Wentworth, C. K. (1923). *Method of Measuring and Plotting the Shapes of Pebbles*. US Government Printing Office.

[15] Wadell, H. (1935). Volume, shape, and roundness of quartz particles. *The Journal of Geology*, 250-280.

[16] Kuenen, P. H. (1956). Experimental abrasion of pebbles: 2. rolling by current. *The Journal of Geology*, 336-368.

[17] Dobkins Jr, J. E., & Folk, R. L. (1970). Shape development on Tahiti-nui. *Journal of Sedimentary Research*, 40(4).

[18] Cox, E. P. (1927). A method of assigning numerical and percentage values to the degree of roundness of sand grains. *Journal of Paleontology*, 1(3), 179-183.

[19] Rittenhouse, G. (1943). A visual method of estimating two-dimensional sphericity. *Journal of Sedimentary Research*, 13(2).

[20] Riley, N. A. (1941). Projection sphericity. *Journal of Sedimentary Research*, 11(2), 94-95.

- [21] Winterbottom, W. L. (1967). Equilibrium shape of a small particle in contact with a foreign substrate. *Acta Metallurgica*, 15(2), 303-310.
- [22] Champion, J. A., Katare, Y. K., & Mitragotri, S. (2007). Particle shape: a new design parameter for micro-and nano-scale drug delivery carriers. *Journal of Controlled Release*, 121(1), 3-9.
- [23] Cleary, P. W., & Sawley, M. L. (2002). DEM modelling of industrial granular flows: 3D case studies and the effect of particle shape on hopper discharge. *Applied Mathematical Modelling*, 26(2), 89-111.
- [24] Mosharraf, M., & Nyström, C. (1995). The effect of particle size and shape on the surface specific dissolution rate of micronized practically insoluble drugs. *International Journal of Pharmaceutics*, 122(1), 35-47.
- [25] Cho, G. C., Dodds, J., & Santamarina, J. C. (2006). Particle shape effects on packing density, stiffness, and strength: natural and crushed sands. *Journal of Geotechnical and Geoenvironmental Engineering*, 132(5), 591-602.
- [26] Kourosch Kalantar-zadeh, B.F. (2007), Nanotechnology-Enabled Sensor, 1<sup>st</sup> Edition. Springer.
- [27] Brunauer, S., Emmett, P. H., & Teller, E. (1938). Adsorption of gases in multimolecular layers. *Journal of the American Chemical Society*, 60(2), 309-319.
- [28] Sing, K. S. (1998). Adsorption methods for the characterization of porous materials. *Advances in Colloid and Interface Science*, 76, 3-11.
- [29] Rouquerol, J., Rouquerol, F., Llewellyn, P., Maurin, G., & Sing, K. S. (2013). *Adsorption by powders and porous solids: principles, methodology and applications*. Academic press.

- [30] Barrett, E. P., Joyner, L. G., & Halenda, P. P. (1951). The determination of pore volume and area distributions in porous substances. I. Computations from nitrogen isotherms. *Journal of the American Chemical Society*, 73(1), 373-380.
- [31] Lu, G. Q., Zhao, X. S., & Wei, T. K. (2004). *Nanoporous materials: science and engineering* (Vol. 4). Imperial College Press.
- [32] Dubois, L. H., & Nuzzo, R. G. (1992). Synthesis, structure, and properties of model organic surfaces. *Annual Review of Physical Chemistry*, 43(1), 437-463.
- [33] Cole, H. (1970). Bragg's law and energy sensitive detectors. *Journal of Applied Crystallography*, 3(5), 405-406.
- [34] X-ray Diffraction. (2014). Available at:  
[web.pdx.edu/~pmoeck/phy381/Topic5a-XRD.pdf](http://web.pdx.edu/~pmoeck/phy381/Topic5a-XRD.pdf)
- [35] Sparagana, M., & Mason, W. B. (1962). Infrared Microspectrophotometry Using Reflecting-Type 6X Beam Condensing Optics in Reference and Sample Beams. *Analytical Chemistry*, 34(2), 242-247.
- [36] Nguyen, T. T., Janik, L. J., & Raupach, M. (1991). Diffuse reflectance infrared Fourier transform (DRIFT) spectroscopy in soil studies. *Soil Research*, 29(1), 49-67.
- [37] Carlson, J. (1988). Alpha particle structure. *Physical Review C*, 38(4), 1879
- [38] Flagan, R. C., & Lunden, M. M. (1995). Particle structure control in nanoparticle synthesis from the vapor phase. *Materials Science and Engineering: A*, 204(1), 113-124.
- [39] Lemb, M. T. H. H. B., Oei, T. H., Eifert, H., & Günther, B. (1993). Technegas: a study of particle structure, size and distribution. *European journal of nuclear*

*medicine*, 20(7), 576-579.

[40] Pavlović, M. G., Pavlović, L. J., Ivanović, E. R., Radmilović, V., & Popov, K. I. (2001). The effect of particle structure on apparent density of electrolytic copper powder. *Journal of the Serbian Chemical Society*, 66(11-12), 923-933.

[41] Han, B. C., Miranda, C. R., & Ceder, G. (2008). Effect of particle size and surface structure on adsorption of O and OH on platinum nanoparticles: A first-principles study. *Physical Review B*, 77(7), 75410.

[42] Bown, R. (1998). Particle size, shape and structure of paper fillers and their effect on paper properties. *Paper technology*, 39(2), 44-48.

[43] Dark, G. (2004). *On-line medical dictionary*. University of Newcastle upon Tyne. Department of Medical Oncology.

[44] Williamson, K., & Masters, K. (2010). *Macroscale and microscale organic experiments*. Cengage Learning.

[45] Fredrickson, G. H., Liu, A. J., & Bates, F. S. (1994). Entropic corrections to the Flory-Huggins theory of polymer blends: architectural and conformational effects. *Macromolecules*, 27(9), 2503-2511.

[46] Hansen, C. M. (2012). *Hansen solubility parameters: a user's handbook*. CRC press.

[47] Martin, A., Newburger, J., & Adjei, A. (1980). Extended Hildebrand solubility approach: Solubility of theophylline in polar binary solvents. *Journal of pharmaceutical sciences*, 69(5), 487-491.

[48] Philibert, J. (2005). One and a half century of diffusion: Fick, Einstein, before



and beyond. *Diffusion Fundamentals*, 2(1), 1-10.

[49] Hida, T. (1980). *Brownian motion* (pp. 44-113). Springer US.

[50] Einstein, A. (1905). Über die von der molekularkinetischen Theorie der Wärme geforderte Bewegung von in ruhenden Flüssigkeiten suspendierten Teilchen. *Annalen der physik*, 322(8), 549-560.

[51] Palmes, E. D., & Lindenboom, R. H. (1979). Ohm's law, Fick's law, and diffusion samplers for gases. *Analytical Chemistry*, 51(14), 2400-2401.

[52] Lavery, P. S., Oldham, C. E., & Ghisalberti, M. (2001). The use of Fick's First Law for predicting porewater nutrient fluxes under diffusive conditions. *Hydrological Processes*, 15(13), 2435-2451.

[53] Denny Kamaruddin, H., & Koros, W. J. (1997). Some observations about the application of Fick's first law for membrane separation of multicomponent mixtures. *Journal of membrane science*, 135(2), 147-159.

[54] Dill, K. A., & Bromberg, S. (2003). *Molecular driving forces: statistical thermodynamics in chemistry and biology*. Garland Science.

[55] Van Zeghbroeck, B. (2004). Principles of semiconductor devices. *Colorado University*.

[56] AZUARA, E., CORTÉS, R., GARCIA, H. S., & BERISTAIN, C. I. (1992). Kinetic model for osmotic dehydration and its relationship with Fick's second law. *International journal of food science & technology*, 27(4), 409-418.

[57] Ding, S., & Petuskey, W. T. (1998). Solutions to Fick's second law of diffusion with a sinusoidal excitation. *Solid state Ionics*, 109(1), 101-110.

- [58] Ben-Avraham, D., & Havlin, S. (2000). *Diffusion and reactions in fractals and disordered systems*. Cambridge University Press.
- [59] Weiss, G. (2005). *Aspects and Applications of the Random Walk (Random Materials & Processes S.)*.
- [60] Higuchi, W. I. (1967). Diffusional models useful in bio pharmaceuticals. Drug release rate processes. *Journal of Pharmaceutical Sciences*, 56(3), 315-324.
- [61] Nernst, W. (1904). Theory of reaction velocity in heterogenous systems. *Zeit. physikal. Chem*, 47, 52-55.
- [62] Higuchi, T. (1961). Rate of release of medicaments from ointment bases containing drugs in suspension. *Journal of pharmaceutical sciences*, 50(10), 874-875.
- [63] Danckwerts, P. V. (1951). Absorption by simultaneous diffusion and chemical reaction into particles of various shapes and into falling drops. *Transactions of the faraday society*, 47, 1014-1023.
- [64] Noyes, A. A., & Whitney, W. R. (1897). The rate of solution of solid substances in their own solutions. *Journal of the American Chemical Society*, 19(12), 930-934.
- [65] Brauer, I. H. (1986). Reaktionstechnik, Bindeglied zwischen Chemie und Verfahrenstechnik. *Wärme-und Stoffübertragung*, 20(4), 329-345.
- [66] O'hara, T., Dunne, A., Butler, J., & Devane, J. (1998). A review of methods used to compare dissolution profile data. *Pharmaceutical Science & Technology Today*, 1(5), 214-223.
- [67] Costa, P., & Sousa Lobo, J. M. (2001). Modeling and comparison of dissolution

profiles. *European journal of pharmaceutical sciences*, 13(2), 123-133.

[68] Yang, L., & Fassihi, R. (1996). Zero - order release kinetics from a self - correcting floatable asymmetric configuration drug delivery system. *Journal of pharmaceutical sciences*, 85(2), 170-173.

[69] Bhattachar, S. N., Wesley, J. A., Fioritto, A., Martin, P. J., & Babu, S. R. (2002). Dissolution testing of a poorly soluble compound using the flow-through cell dissolution apparatus. *International journal of pharmaceutics*, 236(1), 135-143.

[70] Bravo, S. A., Lamas, M. C., & Salomon, C. J. (2002). In-vitro studies of diclofenac sodium controlled-release from bio polymeric hydrophilic matrices. *Journal of Pharmacy Science*, 5(3), 213-219.

[71] Dash, S., Murthy, P. N., Nath, L., & Chowdhury, P. (2010). Kinetic modeling on drug release from controlled drug delivery systems. *Acta Poloniae Pharmaceutica*, 67(3), 217-223.

[72] Grassi, M., & Grassi, G. (2005). Mathematical modelling and controlled drug delivery: matrix systems. *Current drug delivery*, 2(1), 97-116.

[73] Kravtchenko, T. P., Renoir, J., Parker, A., & Brigand, G. (1999). A novel method for determining the dissolution kinetics of hydrocolloid powders. *Food Hydrocolloids*, 13(3), 219-225.

[74] Hixson, A. W., & Crowell, J. H. (1931). Dependence of reaction velocity upon surface and agitation. *Industrial & Engineering Chemistry*, 23(10), 1160-1168.

[75] Korsmeyer, R. W., Gurny, R., Doelker, E., Buri, P., & Peppas, N. A. (1983). Mechanisms of solute release from porous hydrophilic polymers. *International*

*Journal of Pharmaceutics*, 15(1), 25-35.

[76] Ritger, P. L., & Peppas, N. A. (1987). A simple equation for description of solute release II. Fickian and anomalous release from swellable devices. *Journal of Controlled Release*, 5(1), 37-42.

[77] Siepmann, J., & Peppas, N. A. (2001). Modeling of drug release from delivery systems based on hydroxypropyl methylcellulose (HPMC). *Advanced drug delivery reviews*, 48(2), 139-157.

[78] van Boekel, M. A. (2002). On the use of the Weibull model to describe thermal inactivation of microbial vegetative cells. *International journal of food microbiology*, 74(1), 139-159.

[79] Costa, P. (2001). An alternative method to the evaluation of similarity factor in dissolution testing. *International journal of pharmaceutics*, 220(1), 77-83.

[80] Moore, J. W., & Flanner, H. H. (1996). Mathematical comparison of dissolution profiles. *Pharmaceutical Technology*, 20(6), 64-74.

[81] Koester, L. S., Ortega, G. G., Mayorga, P., & Bassani, V. L. (2004).

Mathematical evaluation of in vitro release profiles of hydroxypropylmethylcellulose matrix tablets containing carbamazepine associated to  $\beta$ -cyclodextrin. *European journal of pharmaceutics and bio pharmaceutics*, 58 (1), 177-179.

[82] Bruner, L., Tolloczko, S., (1900). Ueber die Aufloesungsgeschwindigkeit Fester Koerper. *Journal of Physical Chemistry*, 35, 283-290.

[83] Nernst, W. (1904). Theorie der Reaktionsgeschwindigkeit in heterogenic

Systemen. *Journal of Physical Chemistry*, 47, 52-55.

[84] Wurster, D. E., & Polli, G. P. (1961). Investigation of drug release from solids IV. Influence of adsorption on the dissolution rate. *Journal of pharmaceutical sciences*, 50(5), 403-406.

[85] Levy, G. (1963). Effect of particle size on dissolution and gastrointestinal absorption rates of pharmaceuticals. *American journal of pharmacy and the sciences supporting public health*, 135, 78.

[86] Swarbrick, J., & Ma, D. (1981). In vitro dissolution of dapsone. *Journal of Pharmacy and Pharmacology*, 33(1), 787-789.

[87] Wurster, D. E., & Taylor, P. W. (1965). Dissolution rates. *Journal of pharmaceutical sciences*, 54(2), 169-175.

[88] Mosharraf, M., & Nyström, C. (1999). The effect of dry mixing on the apparent solubility of hydrophobic, sparingly soluble drugs. *European journal of pharmaceutical sciences*, 9(2), 145-156.

[89] Hintz, R. J., & Johnson, K. C. (1989). The effect of particle size distribution on dissolution rate and oral absorption. *International Journal of Pharmaceutics*, 51(1), 9-17.

[90] Haverkamp, R. G., & Welch, B. J. (1998). Modelling the dissolution of alumina powder in cryolite. *Chemical Engineering and Processing: Process Intensification*, 37(2), 177-187.

[91] Niebergall, P. J., Milosovich, G., & Goyan, J. E. (1963). Dissolution rate studies II. Dissolution of particles under conditions of rapid agitation. *Journal of*

*pharmaceutical sciences*, 52(3), 236-241.

[92] Dali, M. (1999). Determination of mass transfer dissolution rate constants from critical time of dissolution of a powder sample. *Pharmaceutical development and technology*, 4(1), 1-8.

[93] Haverkamp, R. G., & Welch, B. J. (1998). Modelling the dissolution of alumina powder in cryolite. *Chemical Engineering and Processing: Process Intensification*, 37(2), 177-187.

[94] Sing, K. S. (1985). Reporting physisorption data for gas/solid systems with special reference to the determination of surface area and porosity (Recommendations 1984). *Pure and applied chemistry*, 57(4), 603-619.

[95] Korson, L., Drost-Hansen, W., & Millero, F. J. (1969). Viscosity of water at various temperatures. *The Journal of Physical Chemistry*, 73(1), 34-39.

[96] "Sodium Carbonate" CAS No: 497-19-8.

[97] Levich, V. G. (1962). *Physicochemical hydrodynamics* (Vol. 689). Englewood Cliffs, NJ: Prentice-Hall.

[98] McNaught, A. D., & McNaught, A. D. (1997). *Compendium of chemical terminology* (Vol. 1669). Oxford: Blackwell Science.

[99] Bellini, D., Pavesio, A., & Terrasan, M. (2006). *U.S. Patent Application 11/989,224*.

[100] Li, J., Lewis, R. B., & Dahn, J. R. (2007). Sodium carboxymethyl cellulose a potential binder for Si negative electrodes for Li-ion batteries. *Electrochemical and Solid-State Letters*, 10(2), A17-A20.

- [101] He, F., & Zhao, D. (2007). Manipulating the size and dispersibility of zerovalent iron nanoparticles by use of carboxymethyl cellulose stabilizers. *Environmental science & technology*, 41(17), 6216-6221.
- [102] Rossi, S., Bonferoni, M. C., Ferrari, F., & Caramella, C. (1999). Drug release and wash ability of mucoadhesive gels based on sodium carboxymethylcellulose and polyacrylic acid. *Pharmaceutical development and technology*, 4(1), 55-63.
- [103] Bodmeier, R. A., Swarbrick, J., & Boylan, J. C. (1998). Encyclopedia of pharmaceutical technology.
- [104] Ferrero, C., Munoz, N., Velasco, M. V., Muñoz-Ruiz, A., & Jiménez-Castellanos, R. (1997). Disintegrating efficiency of croscarmellose sodium in a direct compression formulation. *International journal of pharmaceutics*, 147(1), 11-21.
- [105] Zhao, N., & Augsburger, L. L. (2006). The influence of product brand-to-brand variability on super disintegrate performance a case study with croscarmellose sodium. *Pharmaceutical development and technology*, 11(2), 179-185.
- [106] Gordon, M. S., Chatterjee, B., & Chowhan, Z. T. (1990). Effect of the mode of croscarmellose sodium incorporation on tablet dissolution and friability. *Journal of pharmaceutical sciences*, 79(1), 43-47.
- [107] Haaf, F., Sanner, A., & Straub, F. (1985). Polymers of N-vinylpyrrolidone: synthesis, characterization and uses. *Polymer Journal*, 17(1), 143-152.
- [108] Shu, T., Suzuki, H., Hironaka, K., & Ito, K. (2002). Studies of rapidly disintegrating tablets in the oral cavity using co-ground mixtures of mannitol with crospovidone. *Chemical and pharmaceutical bulletin*, 50(2), 193-198.

[109] Shin, S. C., Oh, I. J., Lee, Y. B., Choi, H. K., & Choi, J. S. (1998). Enhanced dissolution of furosemide by coprecipitating or cogrinding with crospovidone.

*International journal of pharmaceutics*, 175(1), 17-24.

[110] Fujii, M., Okada, H., Shibata, Y., Teramachi, H., Kondoh, M., & Watanabe, Y. (2005). Preparation, characterization, and tableting of a solid dispersion of

indomethacin with crospovidone. *International journal of pharmaceutics*, 293(1), 145-153.